Sediment Ripening with Biochar

Assessing the effect of biochar content and particle size on the biophysicochemical ripening processes of sediments

Tjasa du Val d'Eprémesnil

Delft University of Technology

TU Delft

Sediment Ripening with Biochar

Assessing the effect of biochar content and particle size on the biophysicochemical ripening processes of sediments

by

Tjasa du Val d'Eprémesnil

Student number:	6059120	
Project duration:	February, 2025 – August, 2025	
Thesis committee:	Dr. J. Gebert,	TU Delft (Chair)
	Dr. L. L. Cutz,	TU Delft
	Prof. Dr. H. M. Jonkers,	TU Delft
	PhD. Candidate N. Elnaker,	TU Delft

Cover: Robèrt Kroonen
Style: TU Delft Report Style, with modifications by Daan Zwaneveld

Preface

This project has been an invaluable learning experience that was only possible thanks to the support I received. I would first like to extend my gratitude to my supervisors, Julia Gebert, Luis Cutz, and Nazeir Elnaker, who offered their expertise and guidance throughout this project. Their advice helped me overcome the many challenges of laboratory and field work. I would also like to thank Cristina Cavero Panez, along with the Geoscience laboratory staff, who have helped me find my way through the equipment and were always available to lend a helping hand whenever I encountered a problem.

It was a pleasure working with Bio Energy Netherlands and Inge Nieuwoudt, and I hope this project is only the start of a long collaboration with TU Delft.

I would also like to thank the people who have shaped my experience during this Master's program. To my Delft friends, housemates and fellow board members of the Dispuut, thank you for making this place feel like home these past two years. To my family, thank you for always supporting me and encouraging me. Finally, Gabriel, thank you for being an amazing soil lab mate, especially on COLE extrusion days.

Tjasa du Val d'Eprémesnil
Delft, August 2025

Summary

The growing demand for sustainable construction materials has prompted interest in reusing dredged sediments as an alternative to traditional raw materials in dike construction. Before they can be reused, sediments must undergo the lengthy ripening process, during which they are transformed into stable soil. Accelerating this transformation could significantly improve the feasibility of sediment reuse. This study investigates whether biochar amendment can enhance the biophysicochemical ripening of dredged sediments, focusing on the influence of biochar application rate and particle size.

Dredged material from the port of Hamburg, Germany, that was dewatered and processed at the METHA plant, was mixed with biochar produced by Bio Energy Netherlands from the gasification of wood waste at 800-1000°C for 90-120 minutes. The mixtures contained biochar with varying application rates (2%, 4%, 6%) and particle sizes (<2 mm, 2-5 mm, >5 mm). Over the course of 15 weeks of field ripening, the sediment-biochar mixtures were exposed to natural weather conditions and turned weekly. Biochar amendment introduced additional porosity which increased water holding capacity by 33-72% compared to the control after 15 weeks of ripening, resulting in values of 24-72% DW. The oven-dried COLE, ranged from of 2.2 to 5.4% which represents a decrease of up to 54% relative to the unamended sediments. This improvement can be attributed to the non-plastic behavior of biochar and explains the decreasing shrinkage observed with an increasing application rate. Increasing particle size was correlated to decreasing shrinkage ($p < 0.05$) which could be due to the interrupting effect of coarse biochar particles on tensile load propagation in the rods. A qualitative assessment of the structure development of the experimental variants suggests an acceleration of structure formation with higher biochar application rate and larger particle size when combined with weekly turning. This resulted in a faster breakdown of the dense and platy METHA material into smaller and more aerated aggregates. Overall, the physical ripening of the dredged material was improved with the addition of biochar at increasing application rates and particle size, which promoted a faster stabilization of sediment aggregates and enhanced physical properties beneficial for construction applications.

The occurrence of sulfur oxidation, the main chemical ripening reaction, was evidenced by a loss in the total sulfur content of samples and an increasing electrical conductivity during dry periods. The pH was expected to decrease as a result of the release of protons from this reaction, however this was not observed. Instead, increasing biochar application rates was correlated to a higher pH ($p < 0.05$) and was evidence of the material's buffering capacity which can be attributed to its high functional group and mineral content. The total sulfur content reduced on average by 5% and 22% in the amended samples and the control, and this smaller decrease compared to the control could be explained either by a slower chemical ripening in amended sediments or by measurement limitations. Furthermore, the evolution of electrical conductivity over the 15 weeks of field ripening evidenced the accumulation of chemical reaction products in dry periods.

The influence of biochar on sediment physical and chemical properties, including the increased pore structure, water holding capacity, aeration and buffering capacity, all contributed to creating conditions favorable to microbial activity. A priming effect of biochar application could be observed in the first six weeks of ripening, with high respiration rates, high decomposition rates, and decreasing stabilization of organic matter. In this period, total organic carbon content decreased on average by 30% in amended samples, compared to only 6% in the control. At the same time, nitrogen content decreased on average by 13% in the samples with biochar, further confirming the high microbial activity. This was followed by a period of decreasing microbial activity until the end of the experiment, which was marked by 14-32% lower respiratory carbon release of the amended samples compared to the control, decreasing decomposition rates and increasing stabilization of organic matter. Thus, biochar application accelerated the decomposition of labile carbon and enhanced the biological stabilization of organic matter in sediments.

These findings suggest that biochar amendment can significantly improve sediment ripening processes and can result in a material with properties desirable for dike construction.

Contents

List of Figures

List of Tables

Nomenclature

Abbreviations

Abbreviation	Definition
TU Delft	Technical University of Delft
IPCC	Intergovernmental Panel on Climate Change
S2S	Sediment to Soil
EBC	European Biochar Certification
GHG	Greenhouse Gas
SSA	Specific Surface Area
EC	Electrical Conductivity
WHC	Water Holding Capacity
COLE	Coefficient of Linear Extensibility
DW	Dry weight

Abbreviation	Biochar Content
A1	2%-fine
A2	2%-medium
A3	2%-coarse
B1	4%-fine
B2	4%-medium
B3	4%-coarse
C1	6%-fine
C2	6%-medium
C3	6%-coarse
Control	N/A

1

Introduction

1.1. Problem Definition

In the Netherlands, nearly one third of the land is below sea level and floods constitute a major threat to this low-lying system [127]. This vulnerable land has been historically protected with the construction of dikes, which form a physical barrier between water surges and land. Dikes are traditionally made with a sand core covered with an impermeable clay layer [36], however the extraction of these raw materials comes with an environmental cost as they are associated with habitat and biodiversity loss, and emissions from machinery use and transportation [117].

The Koninklijk Nederlands Meteorologisch Instituut (KNMI) is signaling the risk of higher flood peaks and longer dry periods in Dutch rivers, including the Rhine River, a vital trading route for the Dutch economy [42]. As the frequency and intensity of extreme weather events are predicted to increase in the future due to climate change, the construction of more flood defense infrastructures such as dikes and embankments may be necessary. However, meeting the growing demand for primary earthen construction materials requires innovative and sustainable solutions, as the Netherlands has pledged to reduce greenhouse gas (GHG) emissions in the construction sector—which currently accounts for 35% of national emissions—in pursuit of full material circularity by 2050 [41].

In response to the growing demand for more circular construction materials, specifically for dike construction, the use of alternative materials such as ripened sediments is starting to gain popularity. Sediment ripening is the combination of the physical, chemical and biological transformations of sediments into aerated, aggregated and stable soil that is functionally equivalent to soil [99, 128, 35]. Transforming dredged sediments could be an adequate solution given the growing volume dredged each year. In 2020, nearly 120 million tonnes of dredged material were recorded for waterway maintenance purposes by the OSPAR Convention, which regulates marine activities in the North-East Atlantic [21]. This material is for the most part clean enough for relocation at sea or reuse, while a small portion must be treated or placed in confined disposal due to high concentrations of pollutants such as heavy metals [29, 120]. Furthermore, the volume of dredged material is likely to grow as ports lower their channel entrance depth to accommodate large ships with drafts now reaching up to 16-16.5 m capable of carrying 24,000 containers [111].

Research into the potential applications of dredged sediments has explored several areas relevant to this study. Examples of beneficial reuse applications of dredged sediments vary in technique (on land, in water) and in function (raw material, remediation, reclamation, restoration, resiliency) [15]. Several dikes have been built using sediments, including the Maade River dike in Friesland, Germany, constructed with marsh sediments in 2001 which demonstrated the physical and geochemical suitability of this material [88]. The Norddeich CT 4 is a dike spanning over 900 m constructed in Bremerhaven, Germany, which further confirmed that the properties of processed dredged material could match or even exceed that of marsh sediments traditionally used for such applications [110]. The construction of the Brede Groene Dijk (Broad Green Dike) near Delftzijl, in the Netherlands, is another prime example of the beneficial use of the large amount of locally dredged sediments for the reinforcement of dikes.

Dredged sediments from the Ems-Dollar estuary were ripened locally to form clay that could be used to reinforce the 750 meter long dike [126]. The ripening parameters were further investigated as part of the Clay Ripening Pilot, which highlighted the importance of thin ripening layers and frequent plowing to accelerate the ripening process [27].

Ripening of dredged sediment is considered complete when chemical, physical, and biological transformations have stabilized the material, including the complete degradation of labile organic matter, the oxidation of reduced compounds, and the formation of structured soil aggregates [130]. However, this natural process can take many years, which results in high operation costs and makes it difficult for this resource to compete with primary material [9]. Thus, bridging the gap between this growing sediment supply and the pressing demand for circular construction materials has the potential to significantly increase the circularity of the Dutch construction industry, and enhancing the ripening process to make it faster may be the key to making this material the new standard in dike construction.

One particular way in which sediment ripening could be enhanced is with the addition of biochar. The European Biochar Certification (EBC) defines biochar as the thermochemical conversion of biomass between 350°C and 1000°C [28]. At these high temperatures and in the absence of oxygen, organic substances break down and form syngas, which is mainly composed of carbon monoxide and hydrogen; biochar, a highly stable carbonaceous material; and depending on the process, oil. The use of biochar in agricultural soils is well established due to the many benefits of this material. With its high specific surface area (SSA), exceeding 150 m^2/g in many cases [112, 123], biochar can efficiently adsorb pollutants [51, 139, 102]. A more recalcitrant biochar is able to resist abiotic and biotic degradation and is ideal for carbon fixation [19, 144, 31]. Finally, soil amendment applications benefit from biochar rich in nutrients and minerals and a high water holding capacity [143, 104].

Biochar may have the capacity to enhance the ripening process by creating physical, chemical and biological conditions enabling a faster stabilization of the dredged material. Some examples of studies conducted on sediments and biochar include the work of Fang, Zhao, Rong, Chen, Xu, Qiu, and Cao [30], who successfully converted coastal silt into soil with biochar from varying feedstocks (peanut shells, cow dung, sewage sludge) and production temperatures (300°C, 500°C, 700°C) and cement application, which resulted in a material with enhanced compressive strength and increased CO_2 absorption. Furthermore, Ojeda, Patrício, Mattana, and Sobral [90] amended estuarine sediments with biochar from the gasification of pine biomass at 600-900°C at different application rates and demonstrated an increase in water content, a decrease of CO_2 emissions only noticeable at the highest application rate of 14%, a higher pH and lower electrical conductivity with the application of biochar. This study highlighted the role of aromatic carbons and increased water holding capacity in reducing CO_2 emissions. This lack of scientific studies assessing the impact of biochar application rate and particle size on the main physical, chemical and biological sediment ripening processes highlights an important research gap.

Gathering a better understanding of sediment ripening with such an approach is the motivation for the Sediment-to-Soil (S2S) project, which aims to extensively analyze different ripening strategies and identify the parameters that will consistently and efficiently deliver stable soil [35]. The effect of a range of ripening strategies, including the turning frequency, moisture content, vegetation cover and layer thickness, will be investigated throughout the ripening process as part of the S2S research project. In association with the S2S experiments, the proposed thesis will focus on the impact of biochar amendment on sediment ripening and answer the following research question: ***"How does biochar application rate and particle size affect biophysicochemical sediment ripening processes?"***

Thus, the investigation of the impact of biochar application on sediment ripening could contribute to answering the broader problem of increasing material circularity in a changing climate. The Intergovernmental Panel on Climate Change (IPCC) sounded the alarm in its most recent report, projecting a global mean sea level rise relative to 1995-2014 of 0.28 to 0.55 meters under the most optimistic emission scenario, and up to 0.63 to 1.01 meters under the most pessimistic emissions scenario by 2100 [46]. As global warming accelerates, the threat of rising relative sea levels can be felt in coastal cities across the world, as is the urgency to erect resilient flood defense infrastructure. At the same time, the high environmental impact of primary construction material extraction further motivates the development of more sustainable alternatives such as ripened dredged sediments with biochar.

1.2. Research Questions

This research was conducted by combining an outdoor ripening experiment and laboratory tests. In the outdoor experiment setup, buckets were filled with sediments and biochar in varying amounts and particle sizes and the same weekly turning frequency was applied to all samples. With the laboratory testing, biological and chemical and physical parameters were measured under controlled conditions to evaluate the impact of the ripening strategies. A series of sub-questions will contribute to answering the research question.

a. How does biochar amendment change the shrinkage potential and the water holding capacity of ripening sediment? The porous structure of biochar in combination with its large specific surface area and microporosity [34] can decrease sediment bulk density which in turn can improve the sediment mechanical properties[147] and increase soil water holding capacity [141]. It was therefore hypothesized that biochar amendment could increase the water holding capacity and reduce swell-shrinkage behavior.

b. Does biochar amendment accelerate the stabilization of organic matter? Biochar is rich in minerals, with a high C content, large SSA, high pH, which makes it ideal for increasing soil organic matter[19]. Previous research has shown that biochar amendment resulted in a rapid increase in C mineralization, which was explained by the protecting effect of biochar against the decomposition of OM by microbes [52]. Thus, the organic matter in the sediments may stabilize faster with the addition of biochar.

c. How does the microbial decomposer community respond to biochar amendment? The addition of biochar may create a favorable environment for microbial activity by increasing soil pH and water retention, by providing habitats for microbes with the macropores on the biochar particle surfaces and by introducing large amounts of C and nutrients[131, 108, 95]. A short term response may be observed with an increase of the decomposition rate and a decrease of the stabilization factor, which corresponds to the proportion of non-decomposed hydrolysable labile fraction [24].

d. How does biochar amendment change principal chemical sediment properties? The pH is expected to increase due to the alkalinity of biochar: the oxides (calcium, magnesium, potassium) it contains dissolve in water and neutralize soil activity [119]. The electrical conductivity should also increase with the addition of biochar as previous research relates EC to soluble ash content [119, 114]. The total organic carbon (TOC) should increase due to biochar's high C content, its complex aromatized structure and inherent chemical inertness [119]. The addition of biochar may modify sediment chemical properties during the ripening process by increasing EC, TOC and pH.

e. What is the effect of the biochar-to-sediment ratio and of the biochar particle size on the processes above? Small biochar particles have a higher specific surface area, a highly porous structure and microporosity, lower C content (more completely pyrolyzed) and more functional groups than large particles [34, 23]. It is therefore expected that a more noticeable increase in OM stabilization will be observed with smaller biochar particles [19]. The higher porosity and specific surface area of fine biochar particles may provide habitats for microbial communities, thus favoring the decomposition process [48]. Smaller biochar particles may result in greater water holding capacity increases because of their effect on soil texture and have been observed to have more functional groups than larger particles, but smaller SSA and C content [34, 23]. It is possible that the smallest size fraction will show no significant improvement compared to the intermediate fraction as it was the case in a study of the effect of biochar particle size on WHC [2]. The application of larger amounts of biochar relative to the sediment content of each bucket may result in improved OM stabilization, microbial activity, WHC and reduced shrinkage [34].

2

Literature Review

2.1. Biochar amendment background

The European Biochar Certificate (EBC) defines biochar as the carbonaceous and porous product of the thermochemical conversion of biomass at temperatures between 350°C and 1000°C in a low-oxygen environment [28]. The EBC emphasizes on the sustainable application of this material which must either act as a long-term carbon sink or replace fossil fuels. The term ”biochar” was only coined in 1998 to designate the solid byproduct of the pyrolysis of biomass [118], however it can be argued that the anthropogenic use of this carbonaceous material, albeit produced with evolving methods, has been present since the start of civilization [118]. Biochar application to soils can be traced as far back as 2,500 years ago in the Amazon Basin where areas of arable land patches, Terra Preta and Terra Mulata, stand out from the otherwise infertile soil [45]. Other examples of intentional biochar application can be found around the world, such as in Japan in the 17th century, China and Korea [87]. The use of biochar has evolved over time, shifting from primarily agricultural applications, to energy production and since the 1980s, carbon sequestration [39, 59].

The beneficial use of biochar gained scientific traction due to its carbon sequestration potential. When biochar is applied to soils, organic matter which would have otherwise decomposed and emitted CO_2 is perennially stored in soils, and the gas formed during its production can be used as a fossil fuel alternative [65]. These elements constitute a strong case for the mitigating effect of biochar application and production can have in climate change.

Research in the field of biochar amendment for sediment ripening is sparse, however, a review of the scientific literature pertaining to sediment ripening and biochar-amended soil provides a solid knowledge base for this topic.

2.2. Sediment ripening

Soil ripening is a well defined process by which sediments are transformed into soil suitable for agricultural or earthen construction use [35, 99]. This irreversible process is preceded by sedimentation and consolidation, which occur in a short time frame when the sediments are extracted from the original environment, fluvial or marine [130]. After this stage, the ripening begins and can take several years to complete. It can be characterized into three interconnected sub-processes: physical, chemical and biological ripening.

The ripening process begins with the physical transformation of the sediments. During the physical ripening of the sediments, the material loses a major part of its water mass as it is exposed to atmospheric weather conditions. This results in the formation of a more compact, aerated and permeable material [105]. Thus, as initially high moisture content of sediments reduces, they shrink and form aggregates with a friable consistency [130].

The formation of aggregates, macropores and cracks allows air to seep into the material and kick-starts the chemical ripening process [130]. This next stage changes pore water composition as oxidation

reactions and cation exchange occur, thus altering mineral formation and nutrient availability. Chemical ripening is defined as the changes in the chemical composition of sediments as a result of oxidation reactions and the leaching of soluble substances [128]. The fluvial sediments undergo a change in their ionic composition and concentration, the less stable minerals are weathered while new minerals and precipitates form [128]. As a result of the oxidation process, pH decreases due to the formation of sulfuric acid and the production of acid from the biological oxidation of soil organic matter (SOM) [115]. These chemical changes, most notably soil pH, have an effect on biological ripening and can alter microbial activity and growth rate [92].

Finally, in the biological ripening process, microbes decompose organic matter (OM) and plants enhance structure formation. Aerobic mineralization of OM is the main biochemical ripening process [130]. The aerobic microorganisms can degrade OM from 100 to 1000 times faster than their anaerobic counterpart found in unripe sediments [106]. Furthermore, their population increases throughout the ripening period, from 1×10^6 per gram soil at the start of the process to 6.5×10^7 per gram soil after 4 years [128].

2.2.1. Effect of sediment ripening on physical parameters

Water retention capacity changes over the course of the ripening process because of the nature of water-soil bonds. In coarse grains, water is bound by capillary forces, whereas is fine grains the adhesive and osmotic forces dominate [92]. Consequently, the fine fraction can release more water than the coarse fraction. Organic compounds in soils usually retain more water and as biological ripening reduces the amount of OM, the water holding capacity decreases [92]. Inversely, a high water retention capacity would hinder the ripening process by reducing the number of air-filled pores, which in turn decreases oxygen diffusion and OM oxidation [92].

During physical ripening, the clay platelets reorient face-to-face, and in this process the contacts between the platelets are destroyed, resulting in irreversible shrinkage [129]. However, clay content is not the only factor at play in shrink-swell behaviour. A study focusing on the effect of ripening of METHA sediments on shrinkage showed that total inorganic carbon (TOC) was also an important factor, as a higher TOC contents enable more water absorption and increased swelling [89]. As ripening progressed, shrinkage of METHA sediments measured with the coefficient of linear extensibility ($COLE_{rod}$) can drop by 20-80% relative to unripe materials [89].

2.2.2. Effect of sediment ripening on chemical parameters

The principal chemical ripening reaction is oxidation of sulfur into sulfate, which releases protons and decreases sediment pH [130, 98, 93]. The pH of ripening sediments decreases due to the oxidation process: organic matter decomposes and produces carbon dioxide and organic acids [98]. This means that chemical ripening requires aerobic conditions and OM [63].

Few studies quantify the evolution of sediment electrical conductivity (EC) during the ripening process despite it's highly informative value on the dissolvable ion load of a material. A linear correlation between sediment conductivity and buffering capacity was observed in a study monitoring the heavy metal release of ripening contaminated sediments, such that EC can be used as an indication of the chemical reactivity of the sediments Cappuyns, Swennen, and Devivier [14]. Additionally, an increase of EC values of ripening sediments from 5.48 mS/cm to 6.04 mS/cm over 14 weeks was observed, which could be explained by the oxidation of sulfides which releases soluble ions such as SO_4^{2-}. A later study confirmed the proportional relation of EC and SO_4^{2-} concentrations [13] and observed an overall increase of this value over the course of 150 days of ripening, from around 500 μS/cm up to 2000 μS/cm.

2.2.3. Effect of sediment ripening on biological parameters

Moisture plays an important role in aerobic microbial activity. Microbial activity is inhibited when matric pressures are below -16,000 hPa [106] but this is unlikely to happen in the Netherlands due to the temperate weather conditions [10]. The decomposition rate of SOM depends mainly on the amount of carbon, nitrogen and phosphorus (C, N, P) it contains: C gives the microorganisms the necessary energy to function whilst N and P provide them with nutrients [128]. The carbon rich substrates, carbohydrates, are the first to degrade according the chemical Equation 2.1 [130], thus releasing CO_2 into the atmosphere. After this initial breakdown, the remaining SOM is more recalcitrant and takes

longer to degrade [49]. The respiratory quotient relates the amount of CO_2 released to the amount of O_2 consumed and gives information on the evolution of the microbial population [130]. A growing microbial population that is assimilating C would have a respiratory quotient greater than 1, whereas a decaying population that is releasing C would have a quotient less than 1.

$$C(H_2O)n + nO_2 \rightarrow nCO_2 + nH_2O + energy \tag{2.1}$$

The total organic carbon (TOC) content sediments is a key parameter of the chemical and biological ripening processes. Microbial organisms feed off of TOC which enables OM mineralization and oxidation and contributes to structure formation [146]. Organic carbon can be found in soils both in dissolved and in particulate forms. Vermeulen, Van Gool, Dorleijn, Joziasse, Bruning, Rulkens, and Grotenhuis [130] analyzed the biochemical ripening of sediments and could not identify a clear change in dissolved organic carbon content over a 160 day period. Two hypotheses were developed to explain this phenomenon: either the organic matter in the sediments is highly recalcitrant or the its mineralization rate is the same as the rate at which new dissolved organic carbon is formed.

2.3. Biochar amendment

2.3.1. Biochar characterization

Biochar is the carbonaceous product of the thermochemical conversion of biomass under anoxic conditions [136, 30]. Biochar can be used for a range of projects depending on its properties. With its high specific surface area (SSA), it can efficiently adsorb pollutants [51, 102, 31]. A more recalcitrant biochar is able to resist abiotic and biotic degradation and is ideal for carbon fixation [19]. Finally, soil amendment applications benefit from biochars rich in nutrients and minerals and a high water holding capacity (WHC) [143]. These properties are primarily determined by the feedstock type and the pyrolysis temperature. Wood-based feedstocks produce biochar with a high carbon (C) content, high SSA and low plant-available nutrients; grass-based biochars have a high cation exchange capacity (CEC) and are rich in potassium and calcium; Crop waste biochars lie in between the wood and grass feedstocks [47]. Pyrolysis temperature is a key parameter influencing biochar properties: higher temperatures result in more stable material with increased SSA and porosity, higher C content, pH and ash content [47].

Biochar may have the capacity to drastically enhance the sediment ripening process by creating biological and chemical soil properties desirable for construction applications. This potential was demonstrated in numerous studies, some focusing on the biochar amendment to marine sediments [30, 38], and others on biochar addition to soils [131, 34].

2.3.2. Effect of biochar on soil physical properties

The relationship between biochar application and moisture content varies depending on its production method. Biochar produced at low temperatures (<450°C) tends to be hydrophobic and to reduce soil moisture content [137]. Biochar produced at a high temperature has the opposite effect and can significantly increase moisture content. This is due to the removal of organic compounds from biochar surfaces at high pyrolysis temperatures, which reduces hydrophobicity [43].

Omondi, Xia, Nahayo, Liu, Korai, and Pan [94] demonstrated that biochar amendment to soil could increase soil porosity by 8.4% and water holding capacity by 15.1%. Biochar has a high internal porosity which holds water and increases water holding capacity. However it can have the adverse effect of decreasing air permeability [60].

Studies show a positive effect of biochar application on reducing soil shrinkage. In a study of the effect of rice husk biochar and coal fly ash on the physical properties of a clay rich soil, Lu, Sun, and Zong [74] measured a decrease of the COLE from 0.63 (control) to 0.56 for a 6% biochar application rate. In a similar study, Zong, Chen, and Lu [147] found a reduction of the COLE from a 6% application rate of woodchip biochar on a clayey soil from 6.3% (control) to 3.4%. This drop in COLE could be explained by the modification of shrink-swell behaviour of clay minerals in contact with carbon particles, which form complexes and alter micro-structure and reduce shrinkage [147]. Another explanation for this COLE decrease could be that biochar particles cover clay mineral phase surfaces which would inhibit their shrink-swell behaviour [147].

2.3.3. Effect of biochar on soil chemical properties

A correlation between biochar application rate and increased soil pH has been demonstrated by Vijay, Shreedhar, Adlak, Payyanad, Sreedharan, Gopi, and Aravind [131] in a review of the effect of biochar amendment on agricultural soils. It was also observed that the effect on biochar on soil pH decreases over time, as no significant difference could be observed after 12 months. Biochar contains base ions in the form of oxides and soluble carbonates (calcium, potassium, sodium) which dissolve in water and neutralize soil acidity [121].

The effect of biochar amendment on soil electrical conductivity is convoluted, as some sources show a clear increase of EC with application rate [131], whereas others show the opposite trend [3] or no correlation [1]. This can be explained by the increased soil porosity due to biochar application, which leads to the leaching of nutrient ions and a reduction of soil EC [131].

Biochar application appears to increase soil organic carbon (SOC) [131]. This can be explained by its high carbon content, chemical inertness and complex aromatized structure which changes the composition of soil organic matter to increase SOC [131]. Furthermore, biochar with a high C/N ratio leads to microbial nitrogen immobilization and carbon substrate input in soil, which in turn decreases microbial activities and increases SOC [57].

2.3.4. Effect of biochar on soil biological properties

Several scientific studies point towards the positive effect of biochar amendment on microbial communities in soils. Liu, Zheng, Zhang, Cheng, Zhou, Zhang, Li, Chen, Joseph, and Pan [73] demonstrated that biochar could increase microbial habitats and access to microbial food. In acid soils, it can serve as an alkaline buffer and enhance microbial activity. This study also outlines the impact of C/N ratios on microbial activity: in high biochar application rates, microbial activity is reduced as the high C/N ratio immobilizes soil microbial nitrogen which hinders microbial activity. A review of the effects of biochar on soil biota concludes that biochar amendment may improve resource use in soils [66]. Furthermore, it identified biochar's sorption of growth-inhibiting substances as a potential cause for the increased abundance of soil microorganisms.

The application of biochar as a soil amendment strategy is of major scientific interest because of its carbon sequestration potential. Firstly, if the biochar comes from the pyrolysis of a waste material and beneficially used, it can be accounted as sequestered carbon which would have otherwise been emitted into the atmosphere (see Section 2.3.1). Additionally, biochar's direct impact on reducing soil CO_2 emissions may also contribute to the material's overall carbon sequestration. Fang, Zhao, Rong, Chen, Xu, Qiu, and Cao [30] estimated that 36-94 kg CO_2 could be sequestered per tonne of coastal silt converted to sub-grade soil.

Smith, Collins, and Bailey [116] analyzed the effect of young biochar on soil respiration and measured an initial increase of soil CO_2 production which decreased after 6 days. These findings suggest that biochar is not totally inert, and a small labile C pool contributes to the soil CO_2 flux on the short term. This labile C may originate from a portion of the condensates from the bio-oil formation during the pyrolysis process being absorbed by the biochar [122]. However, on a longer time-scale respiration rates decrease which validates the hypothesis that biochar can reduce GHG emissions. The findings of a field study of the application of biochar on agricultural land confirmed the presence of this initial CO_2 flush and observed a decrease in CO_2 emissions with an increase in biochar application rate [91]. However, these trends are not unanimous, as some studies observe an increased soil respiration after biochar amendment [145, 86], and others observe no significant difference [73, 133].

2.3.5. Effect of biochar particle size on soil properties

The influence of particle size on the physical, chemical and biological impact of biochar should also be considered in soil amendments. Smaller biochar particles may result in greater WHC increase because of their effect on soil texture: Garg, Wani, Zhu, and Kushvaha [34] conducted a study assessing the role of biochar particle size on soil water retention capacity and observed a correlation between the soil physical properties and biochar particle size: porous and irregularly shaped particles can result in a higher increase of soil water retention capacity [73]. Jesus Duarte, Glaser, and Pellegrino Cerri [50] tested the impact of biochar amendment on agricultural soil with three different particle size ranges: 2 mm, 2-0.15 mm, and <0.15 mm. This study revealed that the smallest particle size resulted in the most

significant increase of soil water retention capacity. Alghamdi, Alkhasha, and Ibrahim [2] assessed the effect of four different biochar particle size fractions (2–1 mm,1–0.5 mm, 0.5–0.1 mm,and <0.1mm) with a 4% application rate on soil water retention and availability. Whilst no significant impact of biochar particle size on pH and EC were observed, strong variations of the physical properties could be noted. The finest fraction (<0.1 mm) proved to have the strongest effect on increasing water content and available water, most likely due to the increased surface area, the micro-porosity and highly porous structure of the finest fraction.

A study investigating the influence of biochar pH and particle size (<0.5 mm, 0.5-1 mm, 1-2 mm, 2-5 mm, >5 mm) conducted by Cybulak, Sokołowska, Boguta, and Tomczyk [23] found no correlation between these two parameters, but identified a decrease in the total carbon content of the smallest particle size fraction. The latter was explained by the facilitated conversion of smaller biomass particles into gas during the pyrolysis process. This study also highlighted certain characteristics of the fine biochar particles, such as their higher adsorption energy, bulk density and functional group content. An increasing C/N ratio in biochar amended soil was observed with decreasing biochar particle, with the highest C/N ratios measured with the application of 2 - 0.15 mm biochar particles [50].

Jaafar, Clode, and Abbott [48] tested the hypothesis that biochar could enhance microbial activity by providing protection for soil microorganisms with its highly porous structure, in particular smaller biochar particles because of their higher porosity. The study included three different biochar particle size fractions (0.5–1.0, 1.0–2.0 and 2.0–4.0 mm), but found no significant long term impact of particle size on soil respiration, pH and microbial community. On the short term (less than 56 days), the microbial population appeared to increase with increasing particle size. This could be due to soil entering and blocking the smaller biochar pores, diminishing the benefits of applying smaller biochar particles in the long term. Liang, Gascó, Fu, Méndez, and Paz-Ferreiro [69] studied the impact of two biochar particle sizes (<2 mm and >2 mm) on mineralization rate and stability. The results revealed increased microbial respiration rates with the fine biochar particle size fraction, as smaller particle size could enhance degradation rates and OM mineralization [113]

Biochar specific surface area plays a significant role in improving soil aggregate stability by enabling the adsorption of more minerals and organic matter and increasing the amount of binding agents (hyphae and mucilage) in the biochar–soil mixtures [32]. Furthermore, the overall SSA of biochar amended increases for an increasing application rate [32], resulting in an increased soil water content, field capacity, permanent welting point, available water content and soil water holding capacity and confirmed previous findings Jesus Duarte, Glaser, and Pellegrino Cerri [50]. Cybulak, Sokołowska, Boguta, and Tomczyk [23] measured the SSA of biochar obtained from wood waste pyrolysis and found that the highest SSA was measured in the largest particle size fraction (>5 mm, 109.9 m²/g). Another study measured the SSA of three wood-based biochars and three particle size fractions (0.5-1 mm, 1-2 mm, 2-4 mm) Jaafar, Clode, and Abbott [48]. Whilst no trend could be identified between SSA and particle size, the highest SSA values were recorded in the finest particle size fraction for two types of feedstock (Jarrah wood and a mix of Jarrah and Wandoo wood), and in the medium fraction for one feedstock (australian wattle branches). Alghamdi, Alkhasha, and Ibrahim [2] corroborates these findings with the observation of a clear increase in soil SSA amended with smaller biochar particles, reaching up to 197.2 m²/g when mixed with <0.1 mm biochar particles.

2.3.6. Effect of biochar application rate on soil properties

Understanding the impact of biochar application rate in soil amendments is in the best interest of stakeholders in order to maximize the benefits of this amendments while minimizing the biochar material use.

The influence of biochar application rate on soil physical properties has been the focus of multiple studies outlined below, and gave insights into the effect of this parameter on soil physical and chemical properties. Chen, Liu, Yang, Xu, Shen, and Chen [20] investigated the effects of biochar application rate (0%, 1%, 2.5%, 5%, 10%) on the remediation of saline-alkali soil with the aim of enhancing crop growth. This study demonstrated the highest biochar content (10%) resulted in the highest increase of soil water content, SOC and the highest reduction of salt content, EC and Na^+, Cl^- and SO_4^{-2}. Higher biochar application rates were also proven to correlate with a reduced particle density, bulk density and porosity [38]. Biochar application may reduce shrinkage behaviour: a fraction of the water which would

have normally been absorbed by the clay minerals and produced swelling is absorbed by the biochar, reducing overall swelling [134]. Biochar was applied at four different rates (0, 50, 100, 150 g/kg dry soil weight) to lime concretion black soil soil and a significant shrinkage reduction was observed from 23% in the control experiment, to 14% and 13% for the 100 and 150 g/kg application rates [134]. This drastic difference can be explained by the lower clay content of samples with biochar.

Sun, Hu, Shi, Li, Pang, Liu, and Jia [119] observed that a higher biochar application rate results in a higher soil pH increase, which is related to biochar's high alkalinity. Furthermore, electrical conductivity was initially increased with biochar amendment in this same study and was linked to the introduction of ash into the soil mix. On the long term, the increase in soil porosity due to the addition of biochar facilitates the leaching of water soluble ions and reduced EC. An increase of soil organic carbon following the amendment was also observed, which was linked to the high porosity of biochar. Soil organic carbon finds itself protected in the biochar's expansive pore structure, which prevents its degradation.

Increased biochar application rate may result in lower soil CO_2 emissions [91]. In field study where three different biochar application rates (5, 15 and 25 t/h) were tested, it was observed that CO_2 emissions increased with increasing biochar application rates yet the percentage of biochar-C mineralized decreased. The latter trend could be explained by the increased biochar biotoxicity which could have an inhibiting effect on microbial degradation activities. This could also be due to the higher protection of soil and biochar-C from biochar surface adsorption or occlusion.

3

Materials and Methods

3.1. Materials

3.1.1. Biochar

The biochar is supplied by Bio Energy Netherlands, a research and design focused company located in Amsterdam whose goal is to produce energy in a more sustainable way. Local non-recyclable woodchips are fed into the gasification reactor. The biochar comes from the gasification of local non-recyclable woodchips which are fed into a reactor at 800 - 1000°C at rate of 7.7 m^3/hour. The biochar spends 90 to 120 minutes in the reactor and is removed at a rate of 0.5 m^3/hour. The biochar comes from a batch registered with the European Biochar Organisation (EBC) (BA-NL-538-1-1), produced in 2024 and stored outside in atmospheric conditions to limit the risk of spontaneous combustion. The basic characteristics of the biochar are available in Table 3.1, as defined by Bio Energy Netherlands.

Table 3.1: Biochar Characteristics [85]

Parameter	Value	Parameter	Value
Ash 550°C	0.76 % DW	Bulk Density	107 kg/m^3
Carbon (C)	15.61 % DW	Electrical Conductivity	217.0 $\mu S/cm$
Organic Carbon (Corg)	15.57 % DW	Salt Content	1.146 g/kg
Hydrogen	0.04 % DW	pH	7.20
Nitrogen (N)	0.09 % DW	H/Corg	0.03
Sulphur (S)	0.01 % DW	O/Corg	0.03
Oxygen (O)	0.71 % DW	C/N	173.44

The three different particle size fractions were obtained by successively sieving the biochar. First, a 5 mm sieve was used to collect the coarse fraction with particles > 5 mm in size. Then a 2 mm sieve retained the particles in the $2<x \leq 5$ mm particle range for the medium fraction. Finally, the remaining biochar was used in the fine fraction with a particle size smaller than 2 mm. The biochar was saturated with water due to its storage conditions, so it was air dried until its mass stabilized before being applied to the sediments.

3.1.2. METHA material

The sediment used in this experiment was dredged in the port of Hamburg, Northern Germany, then dewatered and processed in the METHA plant (Mechanical Treatment of Harbour-Sediment).

First, hydrocyclones and upstream current classifiers separate the 63 μm fraction. The fine fraction (< 63 μm) used in this experiment was dewatered in the High Intensity Press (HIP) with a vacuum belt up to approximately 50% moisture content [16]. This fraction is usually further treated, dewatered, and landfilled in the absence of a specific use for this material. The sediments used are a mix of samples processed between December 2nd 2025 and January 1st 2025. The average particle size distribution

of this material is represented in Figure 3.1. The sediments are composed on 46.7% clay (< 20 μm), 33.7 % silt (20-63 μm), 18.1 % fine and very fine sand (63-200 μm) and 1.7% medium sand or coarser (> 200 μm). Once on site, the original material was mixed together and distributed into each bucket, then the biochar was added, marking the start of the experimental phase.

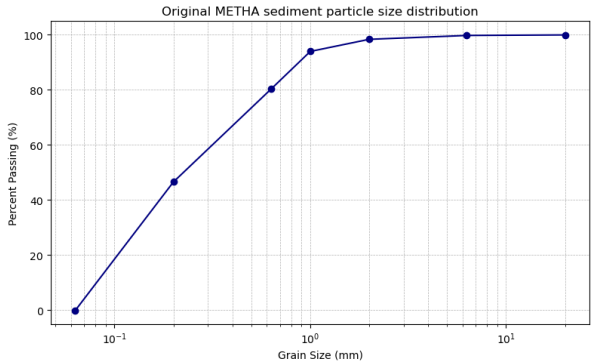

Figure 3.1: Particle size distribution of original METHA sediments

The sediments used in this project were collected at the METHA plants from batches processed December 2nd 2025 and January 1st 2025. The original total organic carbon content of this material is of 3.0 wt/ % TS and its pH of 7.3.

3.2. Experimental approach and setup

The biochar experiment was setup in an outdoor experimental space located on the Flood Proof Holland site, 2 km away from the TU Delft Civil Engineering Faculty (see Figure 3.2a. At this location, the ten experiment variants each containing a different sediment-to-biochar ratio were exposed to natural atmospheric conditions over the course of 15 weeks. Small holes drilled at the bottom of the buckets let excess water drain onto layer of sand, preventing the accumulation of water at the bottom during intense precipitation events. Samples were regularly taken from the buckets and brought to the TU Delft Geoscience and Engineering Laboratory for analysis.

(a) Biochar experiment in Flood Proof Holland (photograph by Robèrt Kroonen, 2025)

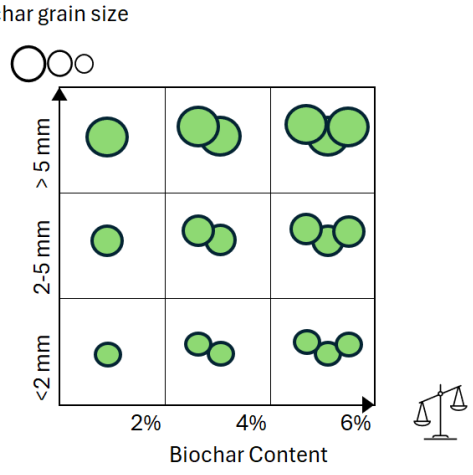

(b) Biochar Experiment Setup

Figure 3.2: Setup of outdoor sediment ripening experiment with biochar variants

Three biochar size fractions and three different application rates were tested to assess their respective impact on chemical, biological and physical properties. The biochar experiment consist of 10 different experiment variants. Each bucket contains 7 kg of fine-grained dredged sediments from the Port of

Hamburg already partially dewatered in the German soil treatment plant METHA.

The biochar experiment was designed such that each bucket tests a different biochar content and particle size combination defined according to published studies [23, 34, 2, 70] (see Figure 3.2b). This design of experiment aims to establish correlations between the measured biological, chemical and physical parameters and the biochar characteristics. The other parameters were kept the same in all experiments: the samples were turned weekly, the water content was uncontrolled (changed depending on natural precipitation and evaporation) and all vegetation was removed (see Table 3.2). The turning was done by hand, mixing all the material from top to bottom and redistributing it evenly in the bucket.

Several laboratory analyses were conducted on samples from each experiment variant throughout the experimental period. These analyses, described in Section 3.3, were conducted on the samples at gradually increasing time steps, from one to six weeks apart. The higher initial sampling frequency was selected to reflect the quick changes occurring at the start of the ripening process.

Table 3.2: Overview of particle size, biochar mixing ratios and boundary conditions of field experiment

Name	Turning	Water	Vegetetation Cover	Content	Particle Size	Biochar Mass
Control	Weekly	Natural	Removed	0%	N/A	0 kg
A1	Weekly	Natural	Removed	2%	<2 mm	0.42 kg
A2					2–5 mm	
A3					>5 mm	
B1	Weekly	Natural	Removed	4%	<2 mm	0.84 kg
B2					2–5 mm	
B3					>5 mm	
C1	Weekly	Natural	Removed	6%	<2 mm	1.26 kg
C2					2–5 mm	
C3					>5 mm	
					Total Mass	2.52 kg

3.3. Analyses

3.3.1. Soil biological properties

Respiration

The analysis of sediment respiration is essential for understanding the anaerobic and aerobic organic matter degradation processes and assess the impact of biochar may have on the ripening process.

The respiration bottles are prepared as follows:

1. 1 L glass bottles are filled with 50 g of sample and sealed with rubber stoppers;
2. 100 mL of ambient air is injected into the bottle;
3. The bottles are then kept away from direct light like a cupboard or a cardboard box in a horizontal position;
4. Using the gas chromatograph (see 3.3.1), the content of gaseous CO_2, CH_4, N_2 and O_2 in each bottle is measured at regular intervals.

Gas chromatograph

The gas chromatograph (GC) determines the concentration of CH_4, CO_2, O_2 and N_2 in gas samples. Measurements were made with the Agilent 490-PRO Micro Gas Chromatograph equipped with a thermal conductivity detector (TCD). The gas sample is injected into the device and is transported by the carrier gas (He) through a packed column designed to separate the sample compounds. The column configuration is comprised of the Molsieve 5A column, which separates permanent gases, and the PoraPLOT Q column which targets hydrocarbons. Thus the four different gases measured reach the

detector at different retention times and produce a signal that can then be analyzed to quantify the relative share of these gases in the sample. The procedure to follow to use the gas chromatograph are detailed in Appendix A.1.

The resulting gas concentrations are adjusted for their sum to reach 100%. Then the corrected CO_2 content is converted from a percentage to moles using the ideal gas law. A series of equations are applied to convert the CO_2 concentration to the amount of carbon respired in mg C/ g DW (see Appendix A.2).

Soil respiration can be influenced by soil structure, thus crushing the sample could lead to erroneous readings. Careful handling of the samples is primordial to minimize this error. Changing storage conditions (temperature and moisture) can also alter soil respiration rates, so it is important to keep the bottles in a stable environment such as a cardboard box or a cupboard in a temperature controlled room.

The results of these measurements were fitted to an exponential decay function when sufficient data was available according to Equation 3.1. The data was considered sufficient when it had been collected over a significant time span with numerous measurements (>50 days, > 4 measurements) to prevent erroneous fitting. In this equation, x is the date of the measurement relative to the start of the analysis, $y0$ is the asymptote value, $t1$ is the decay constant and $A1$ is the initial amplitude. The quality of the fit was assessed with the coefficient of determination, R^2, which ranges from 0 to 1, with 1 corresponding to a perfect fit. Once the curve fitting parameters determined, a carbon emission value could be estimated for any specific date within the analysis period. This enabled the comparison of the respiration rate of all samples at the same date, even if measurements had not been made on that date.

$$f(x) = A1 \times e^{-x/t_1} + y0 \tag{3.1}$$

Teabag index

The teabag index (TBI) is a standardized test to measure the decomposition and stabilization of organic matter in a soil, which can interpreted to assess the activity of the microbial community in the sample. Measuring the weight loss of the teabags over time enables the quantification of the litter stabilization factor S and the recalcitrant rate *k* of a specific sample and separates litter quality from external conditions. The tea used for this test must have non-biodegradable nylon bag and specific types are used according to the standard method [124]: the Japanese Sencha EAN 5 063270 101797 for green tea and the Lipton Infusion Rooibos: EAN 5 063270 101612 for rooibos tea. While the green tea decomposes quickly, the rooibos tea is more recalcitrant, meaning that the decomposition of the labile material continues in rooibos tea after it has been completely consumed in the green tea [56]. The TBI takes advantage of this difference in litter types to calculate both the green tea decomposable fraction and the rooibos rate constant with a single measurement.

The teabags are buried according the following protocol:

1. 200 g of soil are taken from each experiment variant;
2. 4 teabags, two of rooibos tea and two of green tea, are labeled and dried at 60°C overnight after which their mass is recorded;
3. In a jar, 100 g of sediments are poured and the water content is adjusted to 60% of the sample's water holding capacity;
4. The four teabags are laid flat over the sediment layer and the final 100 g of sample cover the top and are adjusted to 60% of the sample's water holding capacity;
5. The jar is then closed and placed in a cool dark place for a 21 day period during which is opened daily for 15 min to aerate the material and ensure that O_2 availability does not limit the microbial activity;
6. After the 21 day period, the teabags are taken out of the jar and any soil stuck to the bags is carefully removed with a brush;
7. The teabags are then dried at 70°C for 3 days after extraction and are weighed.

The litter stabilization factor S is computed with the green tea mass loss values according to Equation 3.2. This value represents the inhibiting effect of the sample on the decomposition of the labile fraction.

$$S = 1 - \frac{a_g}{H_g} \tag{3.2}$$

S : Stabilisation factor
a_g : Decomposable fraction of green tea (g/g_{DM})
H_g : Hydrolysable fraction of green tea (g/g_{DM})

The decomposable fraction of rooibos tea a_r can then be calculated with formula 3.3.

$$a_r = H_r(1 - S) \tag{3.3}$$

a_r : Decomposable fraction of rooibos tea (g/g_{DM})
S : Stabilisation factor
H_r : Hydrolysable fraction of rooibos tea

Finally, the rate constant k for both green and rooibos teas is estimated by fitting the mass loss to the exponential decay function 3.4 [56], assuming that in the span of the short 21-day incubation period, the mass loss of the recalcitrant fraction (rooibos tea) is negligible.

$$M(t) = ae^{-kt} + (1 - a) \tag{3.4}$$

$M(t)$: Mass of tea after burial time t (g)
t : Burial time (day)
a : Labile fraction
$1 - a$: Recalcitrant fraction of both teas
k : Rate constant fitted from the decomposition curve for teas(day^{-1})

3.3.2. Soil physical properties

Coefficient of linear extensibility

The coefficient of linear extensibility (COLE) test characterizes the shrink-swell behavior of a soil. When the soil is moist, the clay mineral swell and increase the volume. Quantifying this behavior gives valuable insights into the physical properties of a soil and was achieved using two different methods: the COLE rod extrusion method for experiments in the fine and medium biochar size fraction (A1, A2, B1, B2, C1, C2), and the shrinkage molds for the coarse size fraction (A3, B3, C3).

The COLE was analyzed following these steps:

1. Sample 100 g of unsieved soil from each experiment;
2. Add water and mix until a thick paste forms;
3. Let the soil mixture equilibrate for 24 hours and then adjust the moisture if necessary;
4. Extrude three 6 cm (L_m) rods for each sample onto an aluminum plate with a 1.2 cm diameter syringe hole, trimming them perpendicular to the plate surface with a spatula to the appropriate length if necessary;
5. After air drying the rods for 72 hours, measure the dried lengths L_d and calculate the $COLE_{rod}$ value according to Equation 3.5.

6. Complete the drying at 105°C overnight and calculate a new value for the $COLE_{rod,OD}$ according to Equation 3.6

The shrinkage mold method is based on the standard BS 1377-2:1990 and uses a half-cylinder metal mold, 14 cm in length and 1.25 cm in radius. The method applied is described below:

1. Prepare the samples in the same way as for the COLE rod method (steps 1-3);
2. Coat the shrinkage mold with a thin layer of petroleum jelly to prevent the sample from sticking to the mold;
3. Pour the mixture into the mold in a slight excess, and gently jar the mold to remove air bubbles;
4. Remove the excess with a palette knife and tidy the rims with a damp cloth;
5. Let the mold air dry from 4 days or until its mass has stabilized;
6. Continue the drying at 65°C overnight and measure the length of the soil bar L_d for the calculation of the $COLE$ value;
7. Finally, leave in the oven at 105°C overnight to measure the oven dried (OD) length L_{od} and calculate the $COLE_{OD}$.

$$COLE = [(L_m/L_d) - 1] \times 100 \tag{3.5}$$

$$COLE_{OD} = [(L_m/L_{OD}) - 1] \times 100 \tag{3.6}$$

Where L_m is the length of the moist sample and L_d is the length of the dry sample and L_{od} if the length of the oven dried sample in cm.

The biochar particles may hinder the rod extrusion and can be a source of error, which is why the linear shrinkage molds were used for the coarse fraction. With the material collected during the final sampling, both methods were applied to all samples. A larger syringe diameter of 2 cm was used for the biochar coarse fraction samples. To ensure the cohesion and comparability of the results from the two methods, a correction factor was applied to the results from the rod extrusion method.

Water holding capacity

The measurement of soil water holding capacity (WHC) is essential in understanding a sample's physical properties as it quantifies its ability to retain water which has an impact on processes such as solute gas transport and soil respiration. This measurement is necessary for the TBI and the respiration analyses as the moisture content of these samples is adjusted to 60% of WHC. The WHC test consists in saturating a sample with water, letting the excess drain freely, and measuring the amount of water that the soil was able to hold against gravity. This test was conducted for all ten experiment variants with a duplicate.

The procedure for WHC measurement is as follows:

1. Prepare the test by placing a funnel over an Erlenmeyer and lining it with a circular filter paper folded into a cone shape;
2. Place 20 g of the sample into the lined funnel;
3. Pour 100 mL of distilled water over the sample;
4. Cover the funnel with aluminum foil and let it drain for 48 hours to prevent evaporation
5. After the resting period, scrape the soil out of the filter paper, avoiding the parts adhered to the paper, and dry overnight at 105°C;
6. Calculate the gravimetric water content of the drained soil samples, also known as the the WHC, according to the Equation 3.7:

$$WC_{DM} = \frac{WM - DM}{DM} \times 100 \tag{3.7}$$

With:

WC_{DW} : Water content in proportion of the dry weight (%)
WM : Soil wet mass (g)
DM : Soil dry mass (g)

This test is associated with instrumental errors, as the scale could be miscalibrated and give an incorrect reading. Furthermore, the improper sealing of if the wet sediment mix could allow water to evaporate, thus under-representing the WHC.

Moisture Content

The moisture content is determined by weighting 50 g of the sample and drying it overnight at 105°C. The mass loss during the drying period is due to water evaporating and this value is used to calculated moisture content on the dry basis according to Equation 3.8

$$mc_{\%} = \frac{WM - DM}{DM} \tag{3.8}$$

With:

$mc_{\%}$: Moisture content in proportion of the dry mass (%)
WM : Soil wet mass (g)
DM : Soil dry mass (g)

3.3.3. Soil chemical properties

Elemental analysis: total carbon, hydrogen, nitrogen, sulfur

The elemental analysis of the samples gives important information about their chemical characteristics, in particular the total carbon (TC) which is necessary to calculate the total organic carbon (TOC). The samples are fully combusted in a furnace at high temperatures reaching 1200°C in the presence of an excess of oxygen. This results in the complete gasification of the samples into CO_2, H_2O, N_2 and SO_2. These gases are then isolated as they pass through gas-specific columns, using helium as a carrier gas. Finally, the thermal conductivity detector (TCD) quantifies each gas based on their thermal conductivity. This result is converted to a concentration of each element: carbon, hydrogen, nitrogen and sulfur. The analysis was conducted with the CHNS elemental analyzer Vario El Cube, produced by Elementar, Germany. The analysis is repeated with one duplicate for each sample and the protocol is as follows:

1. Prepare the sample by drying overnight at 105°C and finely grinding it with a pestle and mortar;
2. Deposit approximately 25 mg of the prepared sample in a tin foil sheet;
3. Encapsulate the sample in the sheet by first closing it with tweezers, then using the compression tool;
4. Place the sample in the elemental analyzer for measurement.

pH and electrical conductivity

pH is a key indicator of sediment ripening as it can be used to understand which chemical reactions may be occurring in a sample, the availability of nutrients and the rates of biological processes [82]. It is calculated by taking the negative logarithm of the hydronium (H_3O^+) concentration of a solution. It was measured in a soil-water suspensions at a 1:2.5 ratio of sample to water with a glass hydrogen electrode.

The electrical conductivity (EC) of a sample is a measure of its ability to transmit and electrical current, which depends on ionic concentrations, their size and charge. The EC value is measured based on Ohm's law: the voltage drop at a constant current is measured by the EC probe and inversely proportional to the ionic concentration of the soil solution [125].

These measurements are done on each sample with one duplicate according to the procedure below:

1. Weigh 10 g of each sample into a small container (50 mL centrifuge tube);
2. Add 25 mL of distilled water and stir;
3. Wait 1 hour, then stir again before making the measurements;
4. Calibrate the pH sensor with neutral buffer of pH 7 and acidic buffer of pH 4;
5. Before each measurement, the electrode must first be rinsed in distilled water and dried;
6. Place the electrode in the solution to measure, wait 1 minute and record the pH value measured;
7. Calibrate the EC sensor with the 1.412 mS/cm solution;
8. Repeat step 6 until all the solutions have been measured.

It is possible that the sensor does not stabilize to a value and continues to drift. For this reason, the measurements were systematically taken after 1 min.

Total inorganic carbon

The total inorganic carbon (TIC) content of a soil sample can be determined by converting the TIC to carbon dioxide (CO_2) and measuring it with gas chromatography. This value combined with the total carbon can be used to calculate the total organic carbon contained in a sample [138]. Inorganic carbon refers to carbon compounds without carbon-hydrogen bonds, such as CO_2, carbonates, and bicarbonates. These compounds are usually in ionic or covalent bonds. Thus, inorganically bound carbon must be released as CO_2 to be quantified. This is achieved by adding acid to the soil samples, which initiates the following reactions:

$$CaCO_3 + 2H^+ \rightarrow H_2CO_3 + Ca^{2+} \tag{3.9}$$

$$H_2CO_3 + Ca^{2+} \rightarrow H_2O + CO_2 + Ca^{2+} \tag{3.10}$$

The sample is prepared by first being dried and crushed. Then an acidic solution is added to facilitate the release of CO_2 and the gas produced is analyzed in a GC. The GC analyzes the gas released by the soil with a thermal conductivity detector (TCD). The TCD measures the thermal conductivity of CO_2, which is proportional to its concentration. The output of this measurement is a graph of the CO_2 signal in time. The CO_2 concentration can then be estimated by comparing the peak area or height of this signal to a calibration curve obtained with known standards of TIC.

This test is repeated for each biochar experiment at each sampling, with one duplicate, according to the following procedure:

1. Prepare the sample by drying it at 105°C overnight and finely grinding it with a pestle and mortar;
2. Place 0.50 g of the crushed sample into a 100 mL bottle and seal it;
3. Inject 5 mL of phosphoric acid (H_3PO 40%) into the sealed bottle;
4. Place in an oven at 80°C overnight;
5. Let the sample cool for 1 hour;
6. Measure the pressure in the container;
7. Extract 1-2 mL of air from the container with a syringe and inject into the gas chromatograph (GC) for analysis (see 3.3.1.

Once the results for CO_2 concentration are obtained from the GC reading, a value for the TIC can be calculated according to the calculation outlined in Appendix A.3. Then total organic carbon could be calculated as the difference of total carbon and and TIC.

3.3.4. Biochar characterization

The physical characteristics of each biochar size fraction (coarse: > 5 mm, medium: 2-5 mm, fine: <2 mm) were measured with the Quantachrome Autosorb-iQ2 BET Surface Analyzer with automated nitrogen absorption. This analysis was conducted in the TU Delft Process and Engineering Laboratory. The biochar samples were initially dried in an oven at 105°C overnight. Then a 100 mg sample of each particle size fraction was degassed at 150°C for 2 hours with a constant vacuum according to DIN ISO 9277 (2014). The analysis was conducted at a pressure in the 0.05-0.99 p/peq range, resulting

in a reading for the biochar specific surface area (SSA) in m^2/g, pore volume in m^3/g, and pore size distribution.

3.3.5. Field analyses

Weight monitoring

The weight of the each experimental variant was measured on site every week with a scale kept at Flood Proof Holland. In between weeks when samples are taken, this record can be used to estimate the moisture content of the variants.

Standardized photos

Photos of the experiment variants were taken at each sampling date before mixing to qualitatively monitor the changes in soil structure. A ruler was placed in each photo to provide a scale.

Field respiration measurement

The CO_2 efflux of each experiment variant was measured on site using the IAQ-Calc Indoor Air Quality Meters 7525. In order to create a sealed environment for the experiment, the material should be transferred into a small bucket with a lid with a known volume. The probe is placed inside and the cable connecting it to the device goes through a small hole in the lid that is covered with tape to maintain the seal. The CO_2 measurements are taken at a 15 second interval over the course of 15 minutes. The analyzer also records the temperature and atmospheric pressure throughout the measurement. The flux of carbon emitted is then calculated using the same equations as for the laboratory respiration analysis, available in Appendix A.2. A bottle volume of 22.68 L was used to account for the size of the bucket, and volume of the soil was recalculated for each experimental variant based on its mass to reflect the reduced gas volume of the fuller buckets.

Figure 3.3: Field respiration measurement setup

3.3.6. Statistical analysis

The statistical analysis of the results of this experiment was conducted using a response surface model and a central composite design in Stat.Ease 360. The biochar application rate and particle size were input as the two factors of the design, and the analysis results were input as system responses. The best fitting model was then automatically selected between linear, quadratic, cubic, 2FI according to the lowest p-value and highest coefficient of determination.

4

Results

4.1. Field weather conditions

The outdoor experiment started on March 5, 2025, with a first sampling a week later on March 12, and the final sampling taken on June 18, 2025, 15 weeks later. The weather conditions during this period are shown in Figure 4.1. The weather data was extracted from the Rotterdam KNMI weather station, and includes precipitation, potential evaporation, and average daily temperature [109].

Over the course of the experimental period, the temperatures rose from 4°C to 15°C. Heavy precipitation events were recorded in week 5 to 7, week 11 and week 13, resulting in 33.9 mm, 32.3 mm, and 29.2 mm of rain respectively. The potential evaporation also increased during the 15 weeks, from a mean of 1.56 mm in week 1 to 5.1 mm in week 15.

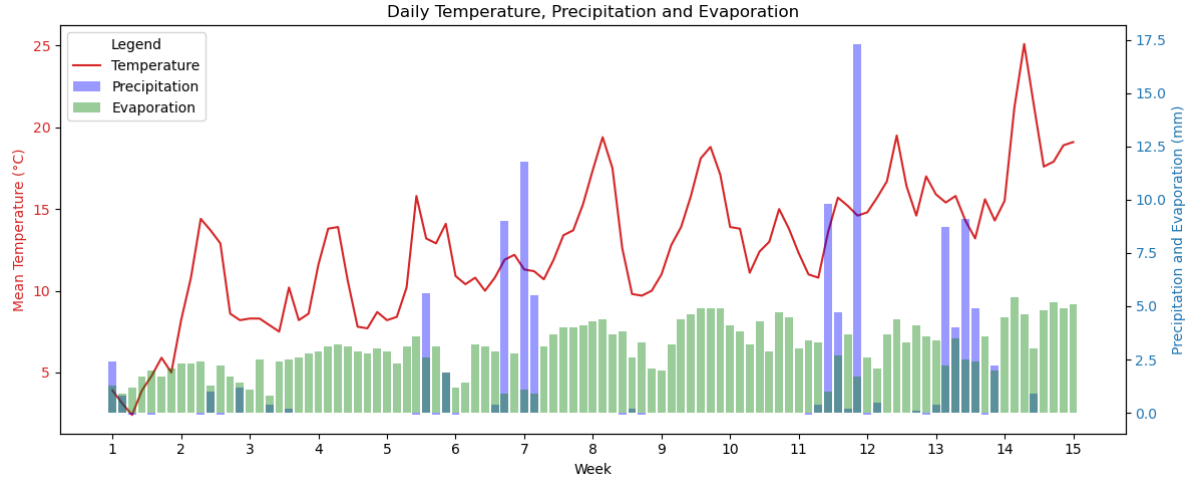

Figure 4.1: Weather conditions during ripening experiment [109]

4.2. Material characteristics

4.2.1. Biochar characteristics

The pH, electrical conductivity (EC), water holding capacity (WHC) and specific surface area (SSA) of each biochar particle size fraction measured in comparison to the specifications provided by Bio Energy Netherlands can be viewed in Table 4.1. The pH of the biochar is highest in the finest fraction, and slightly lower in the medium and coarse fractions. The pH values greatly surpass the values from the biochar specification of 7.2. The electrical conductivity of the sample appears to decrease with an increasing particle size, from 1.055 mS/cm for the fine fraction to 0.393 mS/cm for the coarse fraction. The electrical conductivity also exceed the specification value of 0.217 mS/cm. The water holding

capacity of the biochar increases significantly with a decreasing particle size, and reaches an average of 612% in the finest fraction. Whilst the Bio Energy Netherlands specifications do not include a general value for the biochar water holding capacity, it does contain the WHC of biochar particles <2 mm of 586.1 %. Finally the SSA showed similar results for the fine and medium fraction and the highest value was measured in the coarse fraction, at 541.39 m²/g, approximately 18% higher than the specified 457.06 m²/g measurement.

Table 4.1: Biochar characteristics

Biochar Sample	pH	EC (mS/cm)	WHC (% DW)	SSA (m²/g)	Pore volume (cm^3/g)
Fine (< 2 mm)	9.74	1.055	612	464.40	0.293
Medium (2-5 mm)	9.55	0.429	432	454.05	0.303
Coarse (> 5 mm)	9.60	0.393	350	541.39	0.304
Specification [85]	7.20	0.217	N/A	457.06	N/A

4.2.2. Sediment characteristics

The some characteristic of the original METHA sediments were determined are shown in Table 4.2. The results of this physical characterization show that the material has a high original moisture content of 51%, which amounts to approximately 44% of the water holding capacity. The shrinkage of the material, quantified with the coefficient of linear extensibility (COLE), is of 12.43% after air drying and 12.72% after oven drying.

Table 4.2: Original METHA sediments physical and biological characteristics

Physical Parameter	Value	Biological Parameter	Value
Moisture content (% DW)	51	Stabilization factor, S	0.397
Water holding capacity (% DW)	116	Decomposition rate, k	0.022
COLE air dried (%)	12.13		
COLE oven dried (%)	12.72		
Chemical Parameter	**Value**	**Chemical Parameter**	**Value**
Total carbon (% DW)	3.28	Total inorganic carbon (% DW)	0.924
Total hydrogen (% DW)	0.559	Total organic carbon (% DW)	2.357
Total nitrogen (% DW)	0.275	C/N ratio	11.766
Total sulfur (% DW)	0.409	pH	7.18
EC (μS/cm)	0.938		

The results of the material characterization conducted directly at the sediment treatment plant for batches sampled between November 11 and December 20, 2024, were averaged to estimate the properties of the initial material [81]. Furthermore, this analysis resulted in an average pH of 7.3, which is slightly above the value measured in the TU Delft laboratory of 7.18. The total organic carbon of this material amounted to an average of 3.0 % DW according to the METHA laboratory, which amounts to 0.643 % less than the value measured in the TU Delft laboratory.

4.3. Physical properties

4.3.1. Moisture content

The moisture content of the experimental variants was determined with two methods throughout the ripening period: in the laboratory and using mass measurement in the field. The laboratory measurements are more precise but limit the analysis to weeks when samples were collected. The moisture contents calculated from the wet mass of the samples in between those weeks may be less accurate, as

they assume a constant dry mass since the last sample collection, however they give valuable insights into the effects of field conditions on the samples.

The moisture content of each sample decreased significantly over the first weeks of ripening, from a mean of 34.29% DW in week 1 to a mean of 9.35% DW in week 6 (Figure 4.2). After the initial drop in moisture content, the biochar amended samples displayed a different behavior from the control sample: their moisture content increased again by 1-10% between week 6 and week 15 whereas the moisture of the control sample remained constant.

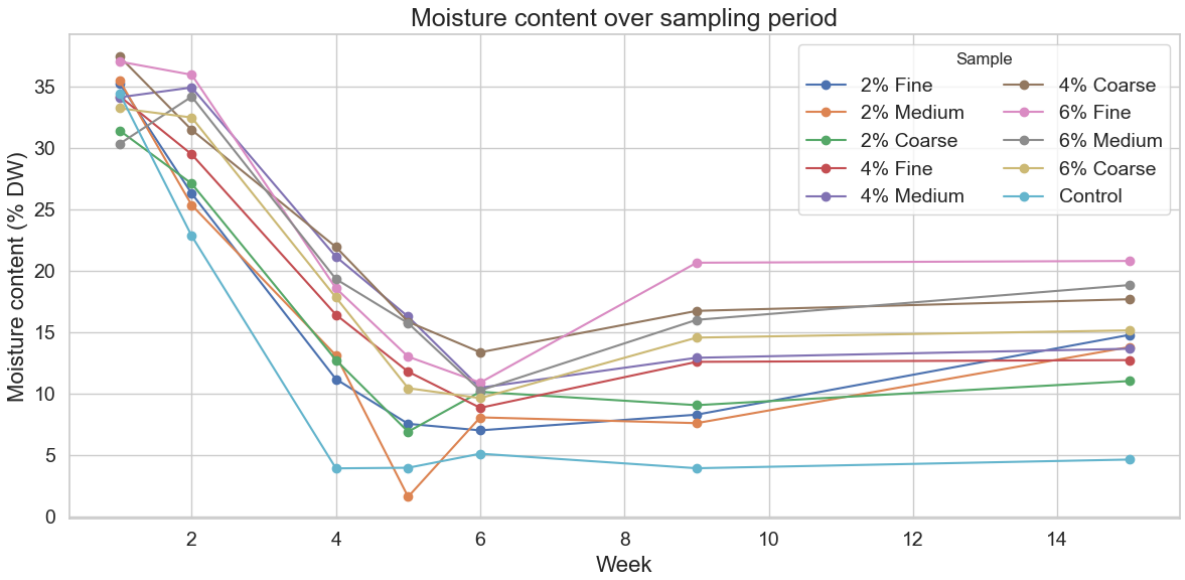

Figure 4.2: Moisture content of each experiment during the 15 week sampling period (laboratory results)

An increasing biochar application rate resulted in an increased average moisture content in the first 15 weeks of sediment ripening (see Table 4.4) . This correlation is statistically significant ($p < 0.05$) (details available in Appendix C). The moisture content of the control sample dropped by 87% during the ripening period, from 34% DW to a final value of 5% DW. Meanwhile the amended samples held more moisture which only dropped by 61%, 58% and 46% for the 2-4-6% application rates respectively. This represents a maximum average increase of 296% of the final moisture content of the 6% amended samples relative to the control sample.

Table 4.3: Average moisture content for each application rate during the 15 week field ripening period

Experiment Week	1	2	4	5	6	9	15
Moisture Content 2% Average (% DW)	34	26	12	5	8	8	13
Moisture Content 4% Average (% DW)	35	32	20	15	11	14	15
Moisture Content 6% Average (% DW)	34	34	19	13	10	17	18
Moisture Content Control (% DW)	34	23	4	4	5	4	5

The moisture content determined in the lab from samples taken in weeks 1, 2, 4, 5, 6, 9 and 15 were supplemented by values determined from the measurement of bucket mass in field. In between samplings, it was assumed that the dry mass remained constant which enabled the estimation of the moisture content of the experiment variants in weeks where samples were not collected. The results, presented in Figure 4.3, show the initial drying of the sample lasting until week 6, followed by three distinct wetting-drying cycles from week 6 to week 11, from week 11 to week 13 and finally from 13 to week 15. The peaks of each respective cycle took place in week 8, 12 and 14, reaching up to 37.4 % DW, 29.5 % DW, 93 % DW and 71.4 % DW respectively, from the 6%-fine or the 6%-medium sample.

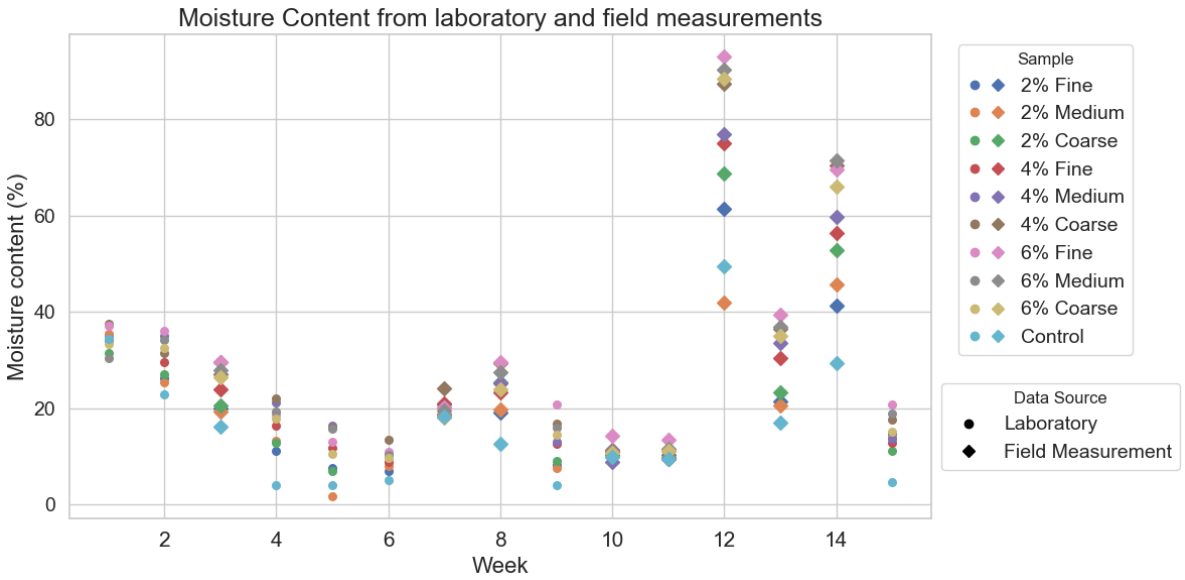

Figure 4.3: Development of sample moisture content over 15 weeks of field ripening combining results from laboratory and field measurements

4.3.2. Water holding capacity

Figure 4.4 describes the evolution of water holding capacity of the samples over the course of the 15 week experimental period. The values have a high initial spread, with a standard deviation of 21.27% DW, which decreases over time down to 10.96% DW, with the exception of a surge in week 6. The control sample presents the lowest WHC throughout the entire sampling period as it decreases from 82.68% DW to 48.22% DW, which represents a 42% decrease over 15 weeks of ripening. The water holding capacity of all samples appears to decrease rapidly in the first 5 weeks of ripening, after which they stabilized.

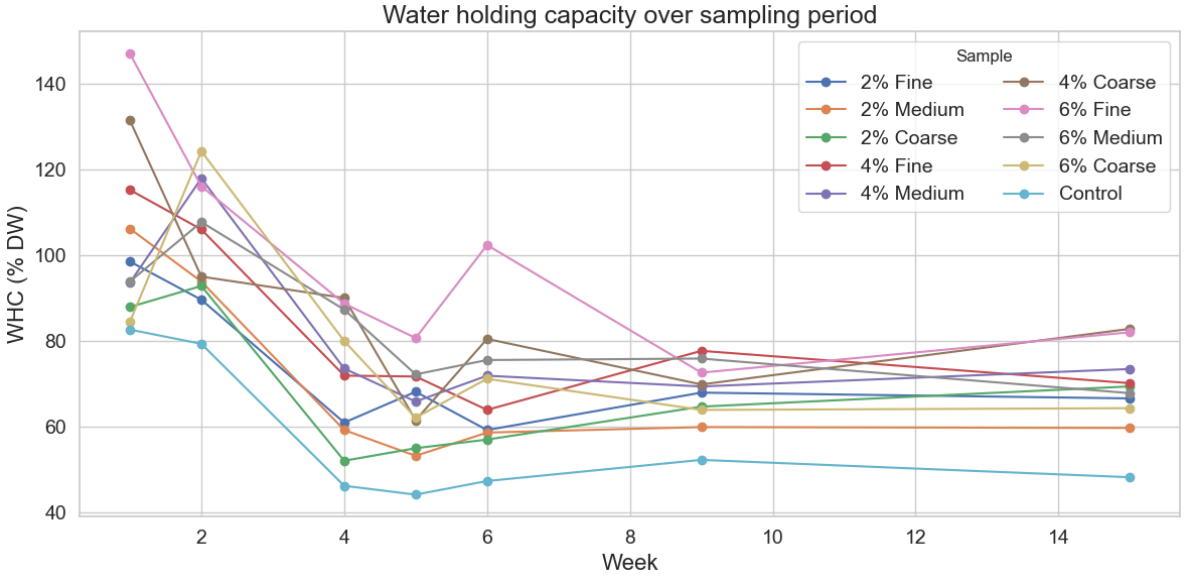

Figure 4.4: Water holding capacity of each experiment during the 15 week sampling period

The 4% biochar application rate results in the highest average WHC across the three particle size fractions, starting from 113% DW and ending with 76% DW after 15 weeks of ripening. Whilst samples from all three application rates start and end at different average water holding capacities, they experienced

a similar decrease of 33%, 33% and 34% for the 2-4-6% samples respectively.

Table 4.4: Average water holding capacity (WHC) for each application rate during the 15 week field ripening period

Experiment Week	1	2	4	5	6	9	15
WHC 2% Average (% DW)	98	92	57	59	58	64	65
WHC 4% Average (% DW)	113	106	79	66	72	72	76
WHC 6% Average (% DW)	109	116	85	72	83	71	71
WHC Control (% DW)	83	79	46	44	47	52	48

4.3.3. Coefficient of linear extensibility

The COLE was determined using two different methods: syringe extrusion for the samples amended with the fine and medium biochar particle size fractions, and linear shrinkage molds for the samples with the coarse biochar size fraction. In the last sampling, at week 15, both methods were applied to all samples with some modifications as the syringe opening was increased from 12 mm to 20 mm for the coarse fraction. Thus a correction factor could be estimated to adjust the shrinkage of the rods extruded with the syringe method to the results of the linear shrinkage molds. It was decided to correct the syringe values to match the linear shrinkage mold values because the exact same procedure could be applied to all samples with this method, contrary to the syringe method which required a different syringe diameter for the coarse fraction.

Table 4.5 shows the correction factors that should be used to adjust the COLE values obtained from the syringe method to the COLE values from the linear shrinkage mold method. As the COLE was calculated for both the air dried length and the oven dried length, a correction factor was calculated for both. A comparison of these two values shows more consistent results from the oven dried correction factors than the air dried correction factors. The air-dried correction factors lie in a much broader range than the oven-dried correction factors, 2.45-6.30% and 1.71-2.96% respectively. This difference reveals that oven drying the COLE rods may eliminate the uncertainty due to humidity that is present in the air dried samples. No correction factor was calculated for the coarse fraction of each application rate as the COLE values for these samples were obtained with the linear shrinkage molds in the previous weeks.

Table 4.5: COLE correction factors enabling the comparison between shrinkage mold and syringe methods

Sample	Air dried syringe to mold correction factor	Oven dried syringe to mold correction factor
2% Fine	2.78	2.64
2% Medium	3.00	2.37
4% Fine	6.30	2.96
4% Medium	2.51	1.71
6% Fine	2.84	2.68
6% Medium	5.58	2.49
Control	2.45	2.16

Oven-dried corrected COLE

The corrected oven dried coefficient of linear extensibility decreased after 15 weeks of ripening, from an average of 14.46% in week 1 to 3.90% in week 15 for the amended samples, and from 20.35% to 4.91% for the control 4.5. The data set is incomplete in weeks 1 and 2 due to method adjustment described earlier. The samples which were amended with coarse biochar (2% coarse, 4% coarse and 6% coarse) display a different behavior from the rest of the samples, as their COLE values are significantly lower than the rest of the samples. Furthermore, they appear to have reached a stable shrinkage behavior in week 9, when all the other samples still had a decreasing COLE. A statistical analysis of the samples after 15 weeks of ripening shows no significant correlation between application rate and COLE values.

However, the particle size of biochar may be an important factor, as a decrease of 39%, 55% and 35% of the COLE of the 2%-coarse, 4%-coarse and 6%-coarse samples compared to the control could be observed at the end of the ripening period. Thus, the application of coarse biochar particles is strongly correlated to a decrease in COLE values across of all application rates ($p < 0.05$) (details available in Appendix C).

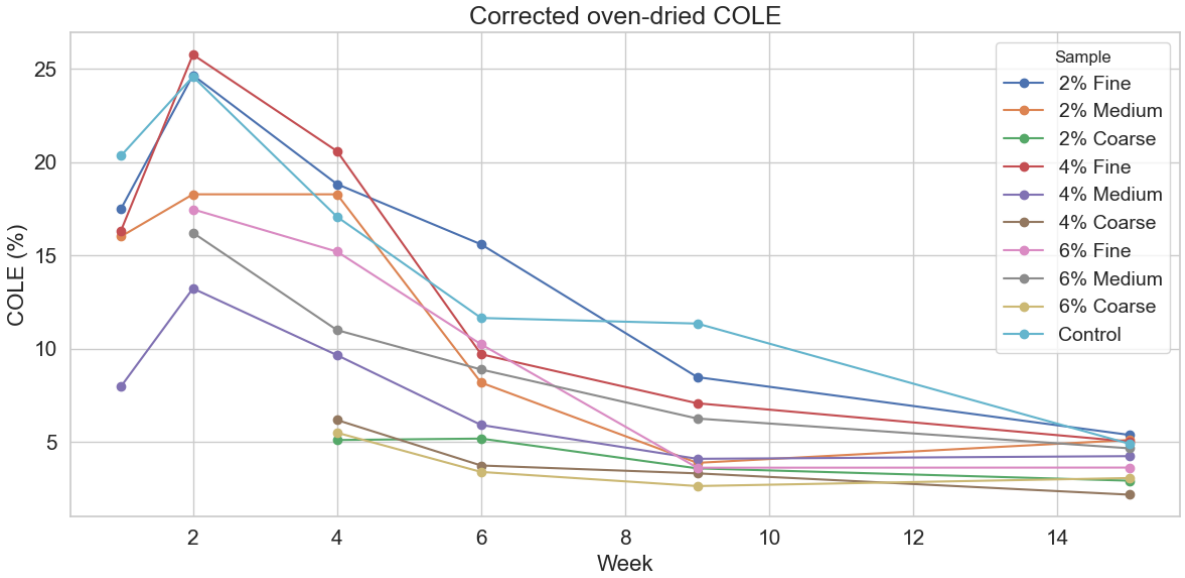

Figure 4.5: Corrected oven-dried COLE during 15 week field ripening period

Table 4.6: Average oven dried COLE (corrected) for each application rate during the 15 week field ripening period

Experiment Week	1	2	4	6	9	15
COLE 2% Average (%)	16.76	21.48	14.07	5.32	9.66	4.50
COLE 4% Average (%)	12.15	19.50	12.15	4.57	6.46	3.83
COLE 6% Average (%)	N/A	16.85	10.57	4.18	6.86	3.35
COLE Control (%)	20.35	24.59	17.08	11.35	11.65	4.91

Figure 4.6 shows the shrinkage potential of the week 15 samples from the mold method, which is the same as the corrected results. When comparing the oven-dried COLE of the amended samples to the control sample, biochar application rate and particle size both appear to play a role in reducing the shrinkage behavior of the material. The average shrinkage of the material from each application rate group decreases with an increasing application rate (see Table 4.6), from 4.50% to 3.35%. Furthermore, the coarse biochar appears to consistently deliver the lowest oven-dried COLE values.

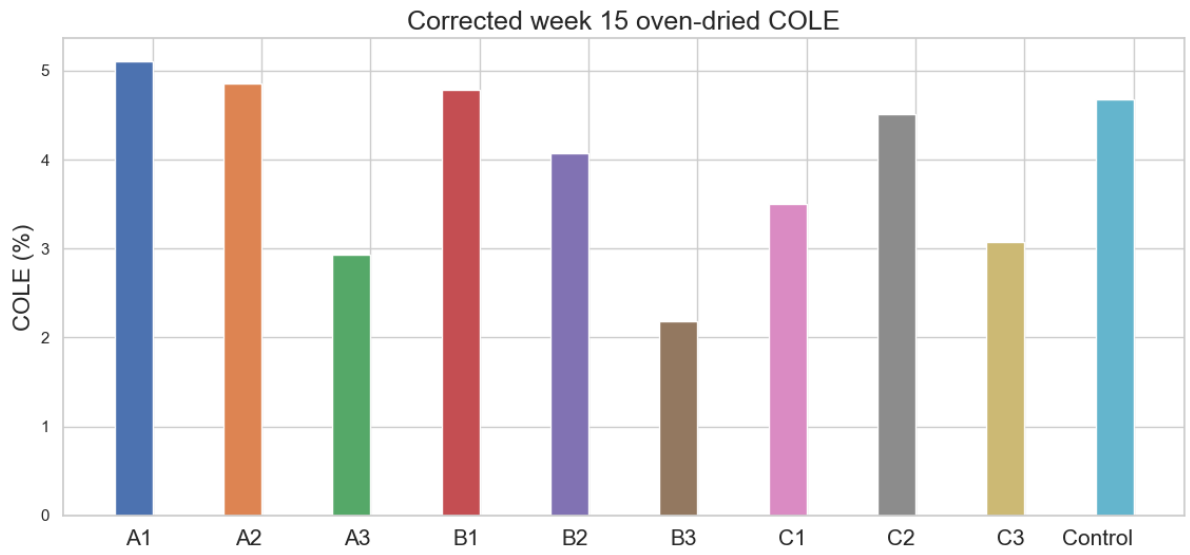

Figure 4.6: Week 15 oven dried COLE values obtained from mold method

4.3.4. Uncorrected air and oven dried COLE

The comparison of the uncorrected results of the COLE using the syringe method is presented in Figure 4.7. The samples amended with fine and medium biochar were extruded from a 12 mm syringe, and the samples with coarse biochar were extruded with a 20 mm syringe to accommodate the larger particle size.

The air-dried COLE results show lower values in all amended samples compared to the control except for the 2%-coarse and 4%-coarse. The amended samples (except 2%-coarse and 4%-coarse) achieved values 15-72% lower than the control, measured in the 2%-fine and 6%-medium samples respectively. The air dried values show no clear decreasing trend linked to biochar application rate, however the coarse particles appear to result in more shrinkage.

The COLE after oven drying increased in all samples as the rods lost their remaining moisture. However, this increase is relatively small in the samples amended with coarse biochar and in the control sample. The samples generally have an increasing oven dried COLE as biochar particle size increases. However, this effect is more noticeable in the 2% and 4% amended samples. The samples amended with 6% biochar seem to result in the smallest shrinkage in this analysis, as they achieved a 33-41% reduction compared to the control after oven drying, whereas the 2% and 4% amended generally have a similar or higher shrinkage than the control.

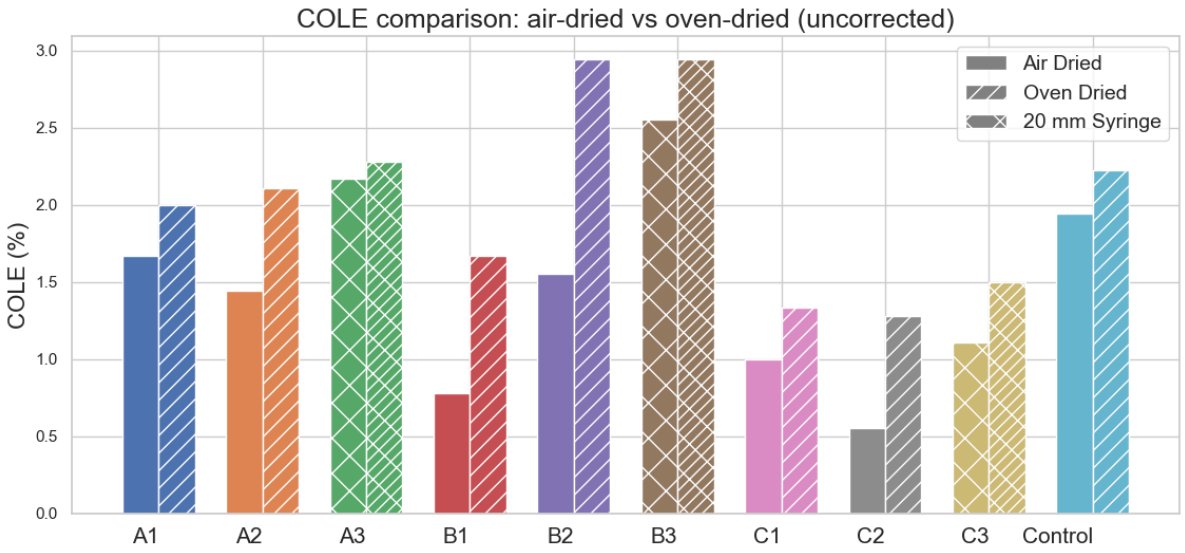

Figure 4.7: Comparison of week 15 air and oven dried COLE values obtained from the syringe method

4.3.5. Structure formation

Photos of each experiment variant in week 1, 5, 9 and 15 can be viewed in Appendix D. The photos were scaled to a 30 cm ruler to show the change in aggregate size over the course of the ripening period. A qualitative assessment of these photos shows a gradual breakdown of the aggregates from an initially platy structure to the formation of smaller aggregates. Over the course of the field ripening, the size of the biggest aggregates in the control dropped from approximately 5 cm to 2.5 cm. Furthermore, an increasing biochar application rate and decreasing particle size appears to have decreased aggregate size as shown in Figure 4.8

(a) Control week 1

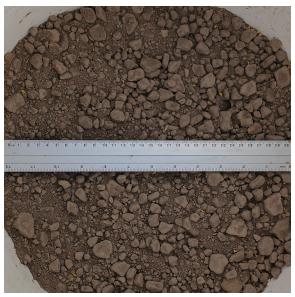

(b) Control week 15

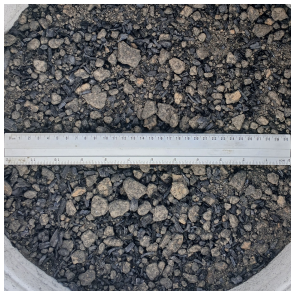

(c) 6%-Coarse week 1

(d) 6%-Coarse week 15

Figure 4.8: Soil structure formation of the control and 6%-coarse samples over the 15 weeks of field ripening

4.4. Chemical properties

4.4.1. pH

The change in pH over the course of the experiment can be seen in Figure 4.9, from an average value of 7.36 in week 1 to 7.71 in week 15. The original matter has a pH of 7.18 (Table **??**). The pH values measured in the first week of the experiment are very scattered in comparison to the following weeks, the standard deviation decreases from 0.21 in the first week to 0.12 in the last week. The pH reading of the control experiment increases over time, from 7.185 in week 1 to 7.635 in week 15, and most of the increase appears to take place between week 5 and week 9.

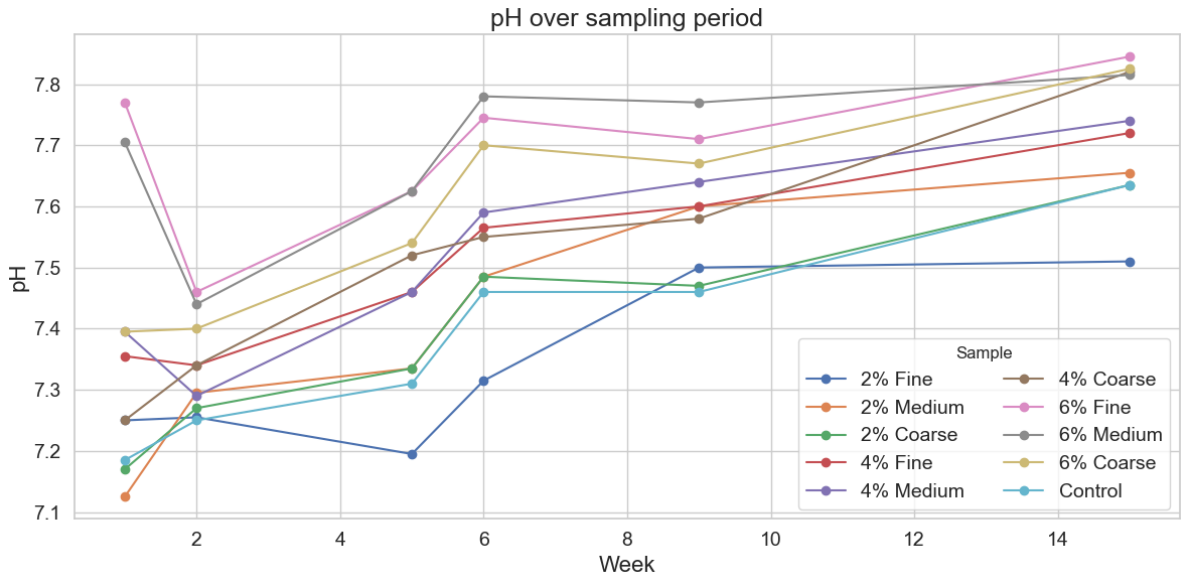

Figure 4.9: Development of pH over 15 weeks of field ripening

The experiments with the lowest application rate (2%) consistently present the lowest pH value of the three groups at each measurement, from an average of 7.18 in week 1 to 7.60 in week 15 (see Table 4.7). The highest biochar application rate (6%) led to the highest pH values during the full experimental period, from 7.62 to 7.83 over the same period. The measurements made of the buckets with an intermediate application rate (4%) placed themselves in between the two previous groups throughout the experiment duration with the exception of week 15, where the pH of sample 4%-coarse reached 7.82, thus neighboring the values of the 6% application rate group. A significant correlation between increasing biochar application rate and increasing pH can be noted ($p < 0.05$) in the last measurement (details available in Appendix C).

Table 4.7: Average pH for each application rate during the 15 week field ripening period

Experiment Week	1	2	5	6	9	15
2% Average	7.18	7.27	7.29	7.43	7.52	7.60
4% Average	7.33	7.32	7.48	7.57	7.61	7.76
6% Average	7.62	7.43	7.60	7.74	7.72	7.83
Control	7.19	7.25	7.31	7.46	7.46	7.64

A closer look at the influence of particle size on pH measurements in each application rate group can be seen in Appendix B, Figure **??**. At a 2% application rate, the lowest pH values are in majority recorded for the finest fraction, and the highest pH values are measured in the medium fraction. At a 4% application rate, the results are more varied as yet the coarse fraction gives predominantly the lowest pH reading and the medium fraction often gives the highest pH value. At the highest application

rate of 6%, the coarse fraction mostly has the lowest pH, whilst the medium and fine fractions share the same number of highest pH values. Despite these observations, no significant statistical correlation could be established between particle size and pH ($p > 0.05$) (details available in Appendix C).

4.4.2. Electrical conductivity

The electrical conductivity (EC) of the samples fluctuated significantly over the course of the ripening period (Figure 4.10. In the first two weeks of the experiment, the EC values remained close to each other and ranged between 0.98-1.42 mS/cm and 1.09-1.44 mS/cm respectively. In week 5, the range increased significantly, from 1.20 to 2.76 mS/cm, before decreasing in week 6 and increasing again in week 9 from 1.28 to 2.15 mS/cm. At each of those events, the 6%-coarse biochar application stands out for resulting in significantly higher values than the rest of the samples. Finally, the week 15 EC reading shows a difference separating the 6% amended samples from the rest of the sample with higher values in the 1.31-1.6 mS/cm range. A correlation between increasing biochar application rate and increasing electrical conductivity could be established ($p < 0.05$), however the particle size does not seem to have a significant effect on EC values (details available in Appendix C).

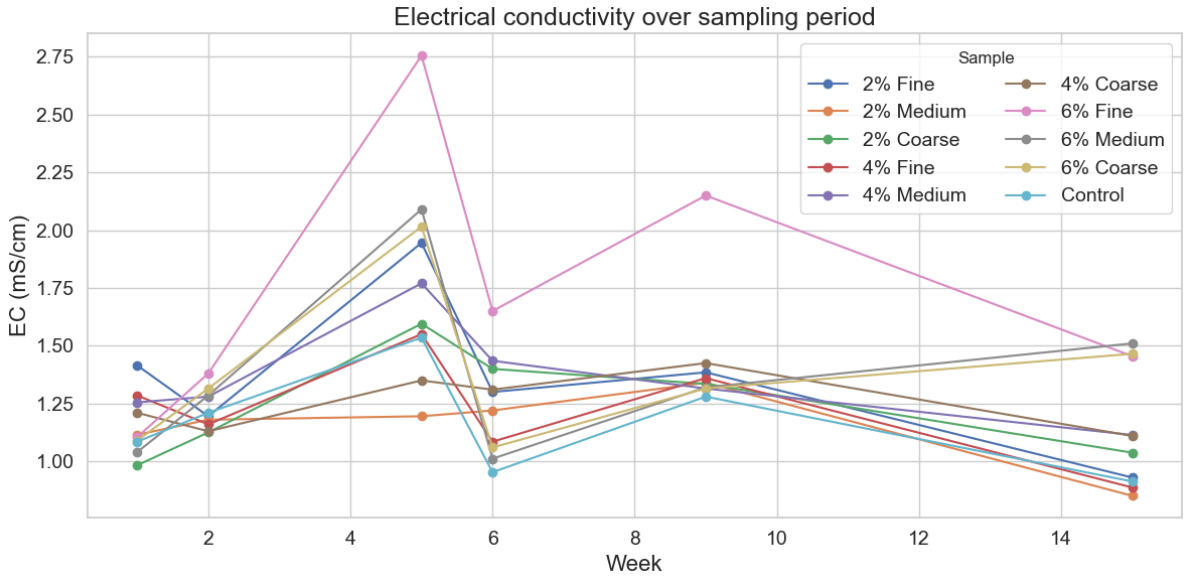

Figure 4.10: Development of electrical conductivity (EC) over 15 weeks of field ripening

Table 4.8: Average electrical conductivity for each application rate during the 15 week field ripening period

Experiment Week	1	2	5	6	9	15
2% Average	1.17	1.17	1.58	1.31	1.35	0.94
4% Average	1.25	1.19	1.56	1.28	1.37	1.11
6% Average	1.08	1.33	2.29	1.24	1.60	1.41
Control	1.09	1.21	1.54	0.95	1.28	0.91

4.4.3. Elemental composition (C, N, S)

Total organic and inorganic carbon content

Total carbon is comprised of inorganic and organic carbon. An increase of the total carbon content of the amended samples can be observed in between week 1 and 15, and it appears to be driven by an increase in the total organic carbon content (see Figure 4.11). The total carbon content of the control sample decreased from 3.375% DW to 3.340% DW from the start to the end of the ripening experiment.

The total inorganic carbon of the sediment-biochar mixtures appears to have decreased over the course of the ripening experiment 4.12b. In week 1, the amended samples had an average total inorganic

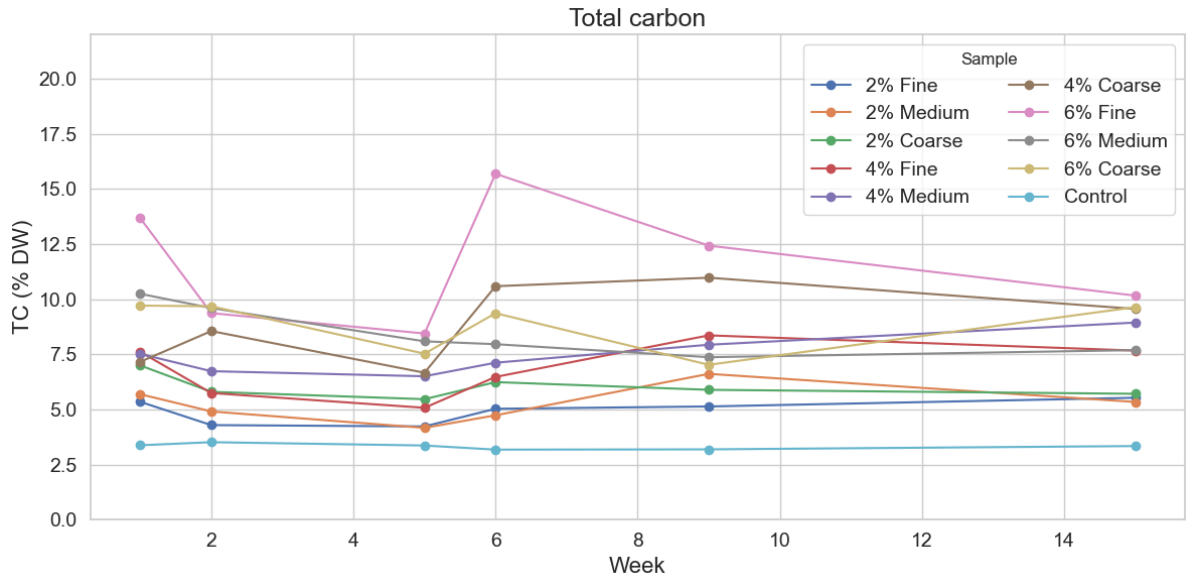

Figure 4.11: Total carbon content

carbon content in the range of 0.727-0.949% DW, and the control had a value of 0.870 % DW. These values then decreased until week 15, to 0.490-0.906% DW and 0.792 for the amended and control samples, which represents an average decrease of 9% and 6% respectively. The relative inorganic carbon content of the amended samples appears to increase over the course of the field ripening period, as it made up 6-20% of the total carbon at the start of the experiment, against 19-28% at the end of the 15 week ripening period. In comparison, the inorganic carbon content of the control sample remained started with 25% and ended with 24% TIC/TC.

The evolution of the total organic carbon content of the samples over 15 weeks of ripening can be viewed in Figure 4.12a. The TOC values in week 1 amended samples have a high spread compared to the following weeks as they range from 4.2 to 12% DW. From week 1 to week 5 or 6 depending on the sample, the TOC content of the amended samples and the control decreased on average by 30% and 6% respectively (excluding 4%-coarse). Week 6 is when the highest increases in total organic carbon were measured, most significantly in the 6%-fine, 4%-coarse and 4%-fine samples which increased on average by 96%, 66% and 48% respectively compared to the previous week. After this increase, the values appear to stabilize until week 15. The total organic carbon content of the control sample remained relatively constant throughout the 15 weeks of experiment, fluctuating from 2.28 to 2.72% DW.

The final TOC content of the samples with biochar measured in week 15 seems to increase with an increasing biochar application rate ($p < 0.05$) (details available in Appendix C). A median increase of 84%, 216% and 249% in TOC compared to the control can be observed in the 2%, 4% and 6% biochar application rates respectively. However, the application rate does not seem to be correlated to the TOC content ($p > 0.05$).

Total sulfur content

The evolution of the total sulfur content of the experimental variants throughout the ripening period can be viewed in Figure 4.12d. A decreasing trend can be observed in most samples, with an average decrease of 5% and 22% for the amended and the control samples respectively between the start and end of the ripening. The amended samples had a sulfur content in week 1 ranging from 0.306-0.442% DW which reduced to 0.331-0.391% DW in week 15. In comparison, the control sample also had a high initial sulfur content of 0.426% DW, which decreased to 0.350% DW in week 15.

Total nitrogen content

The total nitrogen content appears to generally decrease from the start of the analysis to week 5 or 6 depending on the sample, with the exception of sample 6%-fine. After this decrease, no clear trend

could be established among all samples as their nitrogen content seems to fluctuate until week 15. The initial total sulfur content of the samples lied in the range 0.28-0.32% DW, which is very close to the final range of 0.27-0.32% DW. Excluding the 4%-fine sample, total nitrogen appears to decrease with increasing biochar particle size. The effect of biochar application rate on nitrogen content, however, remains unclear.

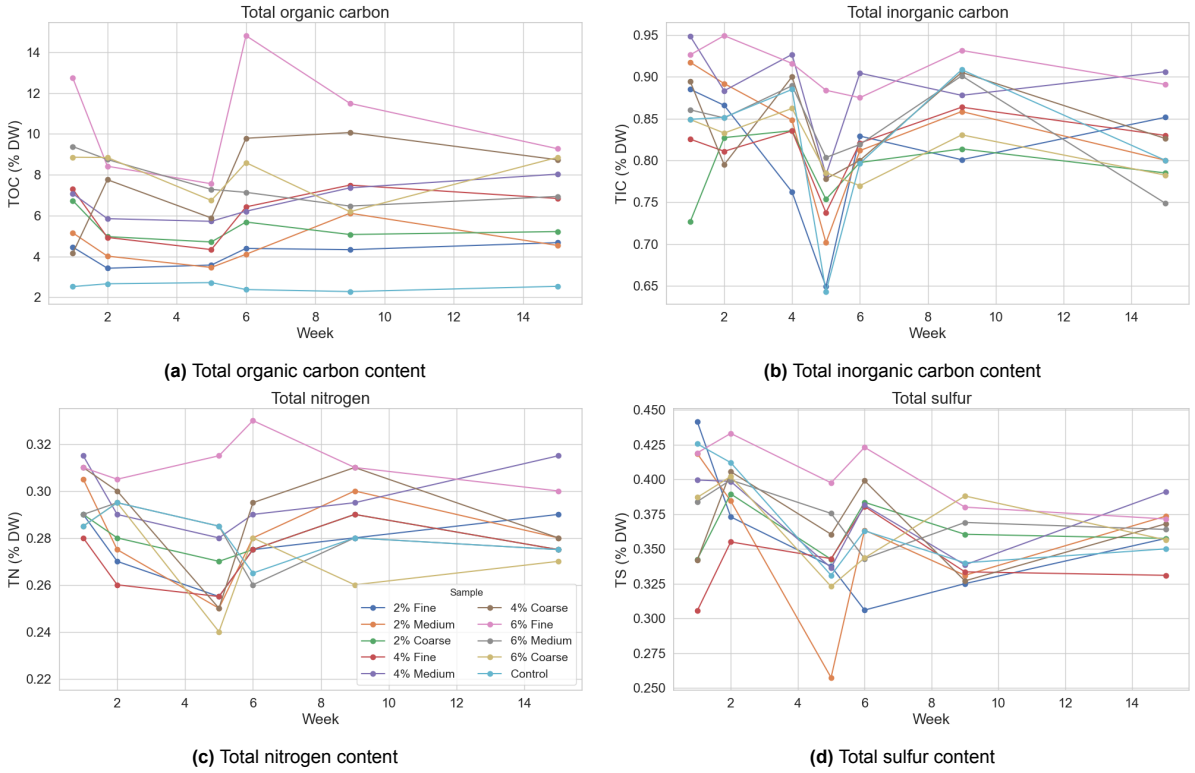

(a) Total organic carbon content

(b) Total inorganic carbon content

(c) Total nitrogen content

(d) Total sulfur content

Figure 4.12: Elemental composition of the experimental variants over 15 weeks of field ripening

4.5. Biological properties

4.5.1. Teabag index

The results of the teabag index (TBI) can be summarized with the analysis of the stabilization factor S and the decomposition rate k (also available in Appendix B.3). The evolution of the stabilization factor, which indicates the inhibiting effect of the sample on the decomposition of the organic matter, over the course of the ripening period can be observed in Figure 4.13. The S values generally decreased in the first 6 weeks, before increasing again until week 15 and surpassing the original values. In this initial phase, the stabilization factor both the amended and control samples stay within a close range, from 0.43-0.49, 0.36-0.41 and 0.34-0.40 in weeks 1, 4 and 6 respectively. In the second phase, the control sample displayed a higher S value than the amended samples. In the final measurement, at week 15, the control sample has a stabilization factor of 0.53 and the amended samples were 9-20% lower than the control. The biggest reduction in the S values at week 15 can be observed in the 6%-medium sample.

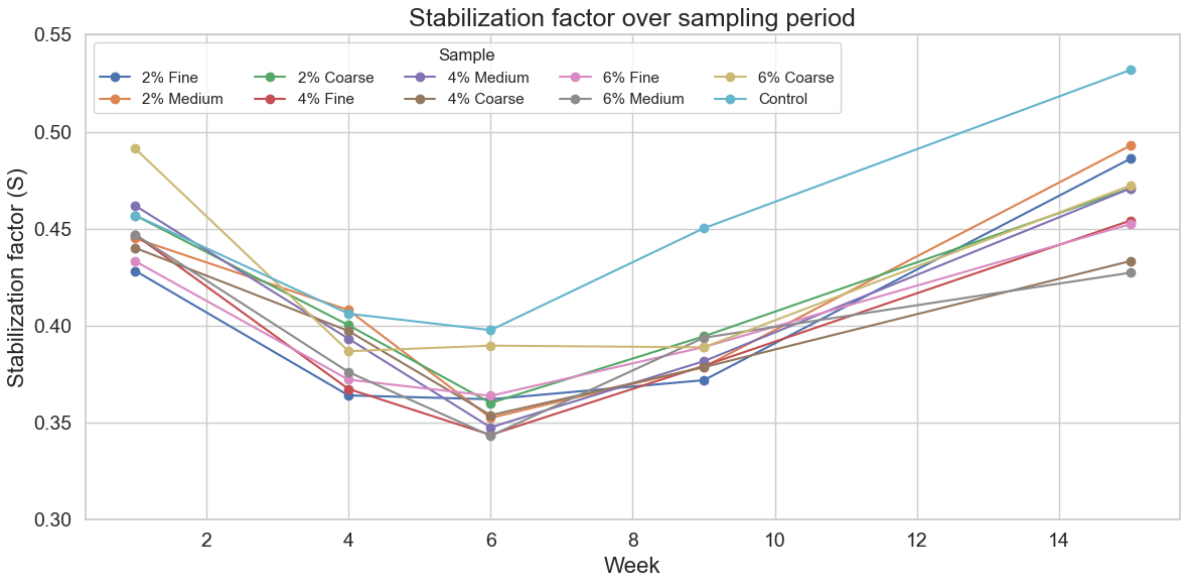

Figure 4.13: Stabilization factor of samples during 15 weeks of field ripening

The decomposition rate of the tea appears to be decreasing as the sediments ripen. In week 6, the values seem to increase out of line with the decreasing trend. In week 15, the decomposition rate of the amended samples are 23-62% higher than the control sample with decomposition rate of 0.0159. The biggest increase in decomposition rate is found in the 2%-coarse sample. A strong correlation between increasing application rate and decreasing decomposition can be observed in the last measurement ($p < 0.05$) (details available in Appendix C).

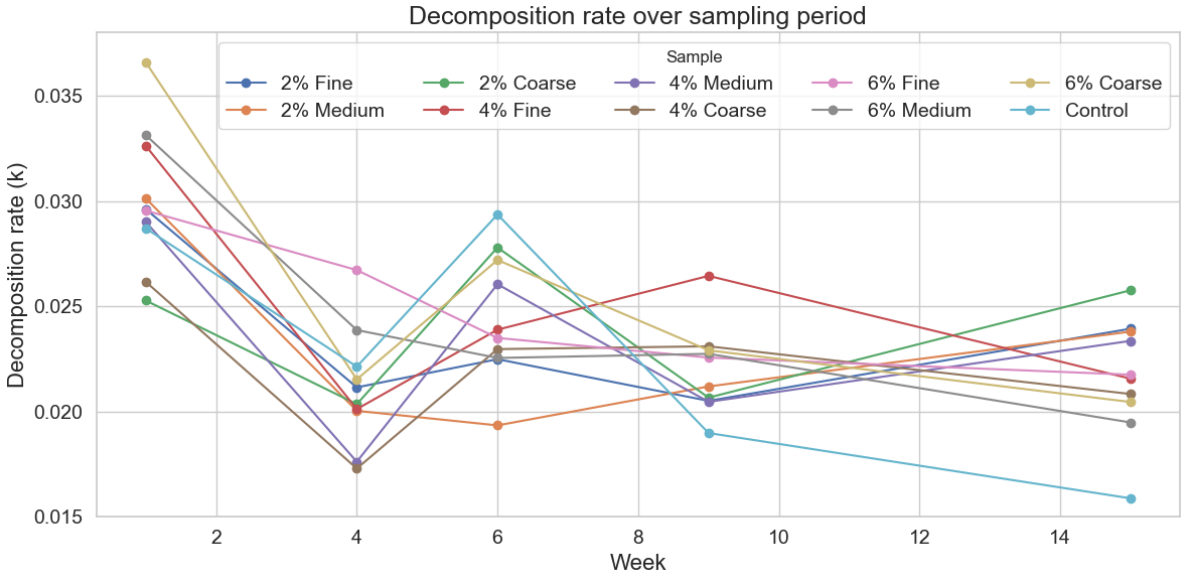

Figure 4.14: Decomposition rate of samples during 15 weeks of field ripening

4.5.2. Laboratory respiration

The measurement of the respiration of the original METHA material and experiment samples taken in week 1, 2 and 5 can be observed in Figure 4.15. The cumulated carbon release was calculated for each sample of the course of 86, 99, 80 and 63 days, in mg C/ g DW. The curve fitting parameters are available in Appendix A, Figure B.1.

The original METHA material reaches a maximum of 0.94 mg C/g DW after 86 days of incubation. The week 1 samples reach values ranging from 0.58 mg C/g DW (2%-medium) to 0.98 mg C/g DW (4%-medium) after 99 days of incubation. The week 2 samples attain from 0.79 mg C/g DW (4%-fine) to 0.92 mg C/g DW (6%-fine) after 80 days. Finally, the week 5 samples release up 0.29-0.43 mg C/g DW after 63 days.

Fitting an exponential decay function to the respiration data points enabled the estimation of the cumulative carbon efflux on day 32 for the samples collected in weeks 1, 2, and 5 to compare them to the week 9 and 15 measurement, as shown in Figure 4.16.

A significant drop in the carbon efflux can be observed between samples collected before and after week 5, from 0.42-0.52 mg C/g DW to 0.08-0.25 mg C/g DW. Two sample batches were collected in this first phase, in week 1 and week 2. The cumulative carbon release of the week 1 amended samples on day 32 ranged from 0.42 to 0.55 mg C/g DW and the control sample reached a value of 0.45 mg C/g DW. In comparison to the control, some amended samples presented a reduced carbon efflux (2%-fine, 2%-medium, 2%-coarse, 4%-fine) whilst the rest of the sampled showed either the same or higher values. The week 2 amended samples all released less carbon than the control after 32 days. Whilst the control released 0.52 mg C/g DW, the amended samples released between 0.42-0.50 mg C/g DW, which represents up to up to a 20% decrease.

In the second phase, samples collected in week 5, 9 and 15 can be compared. The control sample from week 5 of the experiment displays a significantly lower cumulative release than in previous weeks after 32 days as it reaches 0.22 mg C/g DW. In this sampling batch, all the samples with biochar released less carbon than the control, resulting in a 2%- 23% reduction with the biggest reduction found in the 6%-coarse sample. In the week 9 sampling batch, the carbon efflux of the amended samples lies in a reduced range compared to the week 5, from 0.08 to 0.19 mg C/g DW. On day 32 of the analysis, the control sample released 0.24 mg C/g DW and all the amended samples released lower amounts of carbon resulting in a 23-68% reduction. The result of the week 15 respiration analysis show a similar amount of carbon released by the control sample on day 32 compared to the week 9 samples, reaching 0.25 mg C/g DW. As observed in previous weeks, the amended samples display a lower carbon efflux than the control, ranging from 0.17 to 0.22 mg C/g DW. This amounts to a 14-32% reduction of the cumulative carbon released in amended samples.

In summary, the week 1 and week 2 samples show generally higher cumulative carbon release values compared to the samples collected in week 5 or later. In the first phase, some of the amended samples released more carbon than the control, which could be attributed to an initial priming effect of the biochar addition. However, samples collected later in the course of the field ripening experiment generally release less carbon than the control, though this reduction fluctuates from week to week from as little as 2% in the week 5 6%-fine sample, to 68% in the week 9 4%-coarse sample.

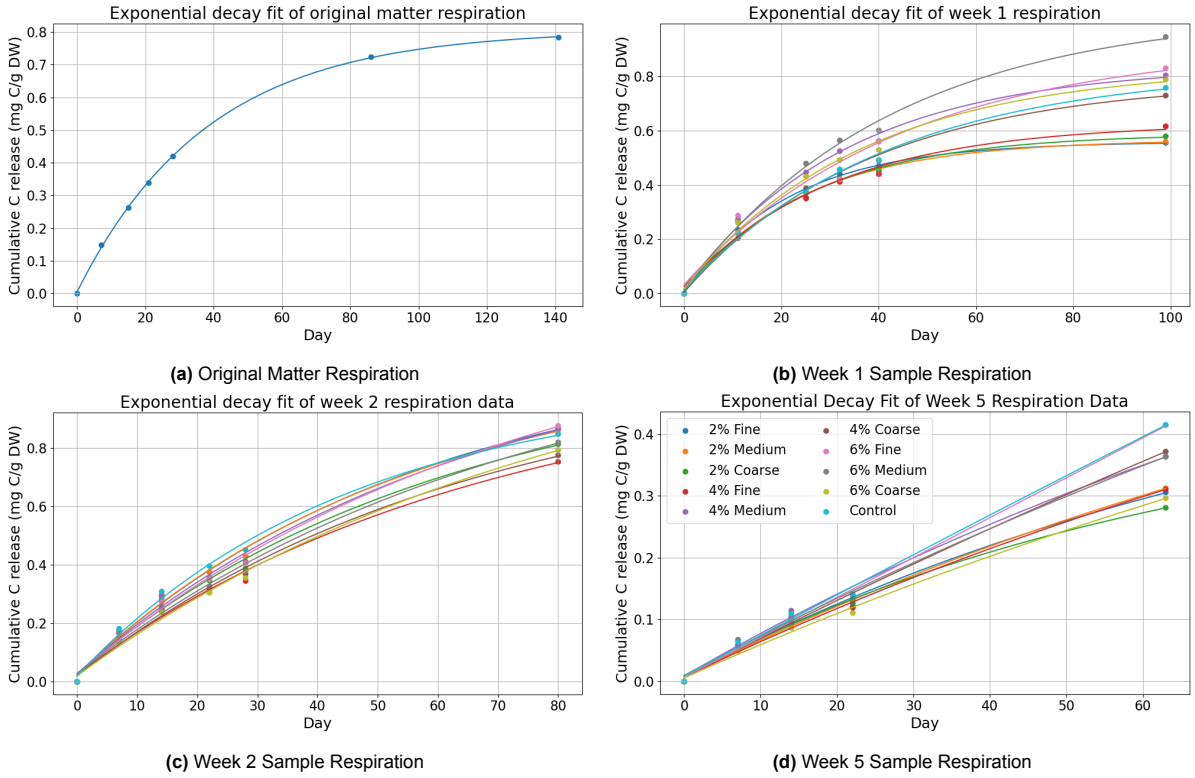

(a) Original Matter Respiration

(b) Week 1 Sample Respiration

(c) Week 2 Sample Respiration

(d) Week 5 Sample Respiration

Figure 4.15: Cumulative respiratory carbon release fitted to exponential decay function

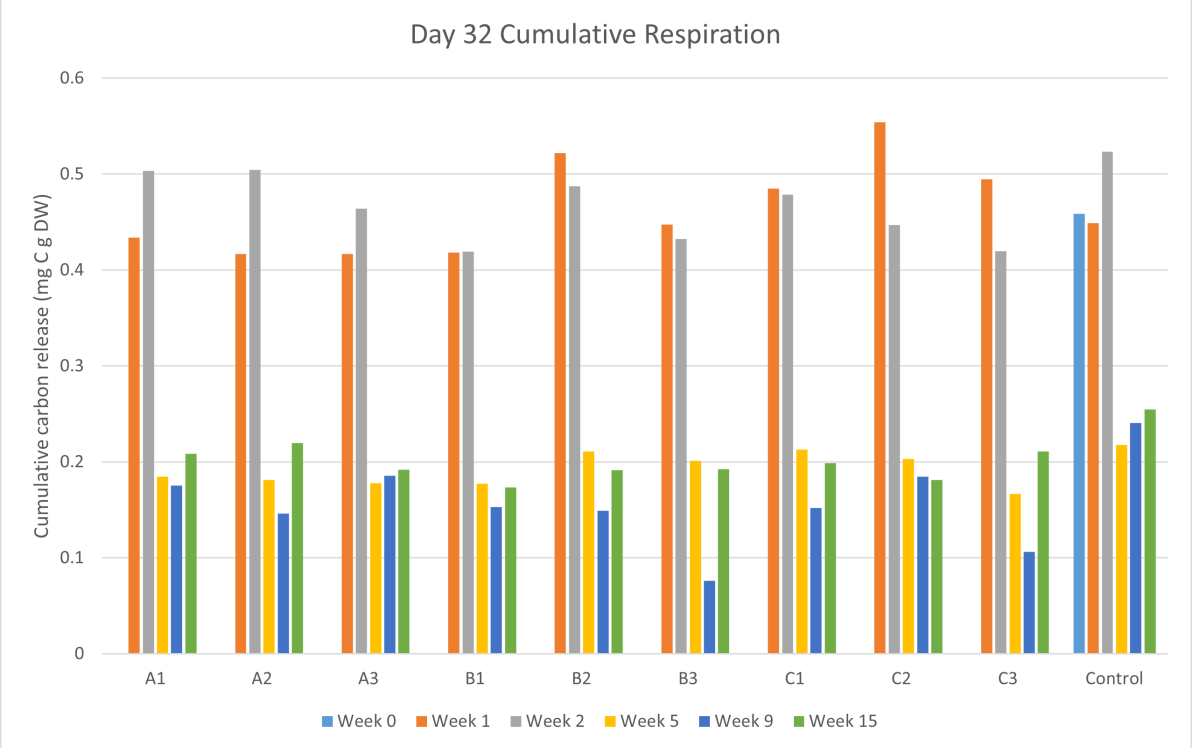

Figure 4.16: Respiration Rates in Week 1, 2, 5, 9 and 15 Samples on Day 32 (A1: 2%-fine, A2: 2%-medium, A3: 2%-coarse, B1: 4%-fine, B2: 4%-medium, B3: 4%-coarse, C1: 6%-fine, C2: 6%-medium, C3: 6%-coarse, Control)

4.5.3. Field respiration

The respiration of the samples was also measured in the field using CO_2 analyzers. The evolution of the daily cumulative carbon release from week 6 to week 15 are shown in Figure 4.17. The respiration flux appears to increase over the course of these 9 weeks, with a significant surge in week 6 across all samples.

The observation of the difference in the respiration rates of the amended samples compared to the control sample allows a better understanding of the impact of biochar application (see Appendix B.2). In week 6, the amended values ranged from 0.144-0.177 mg C/g DW/day and the control had a respiration rate of 0.160 mg C/g DW/day. All amended samples displayed a lower respiration rate with the exception of the 6%-fine sample, which was 11% higher than the control. In week 9, samples 2%-medium and 6%-fine both show an increase in their respiration rates relative to the control, of 4% and 22% respectively. This trend of the 6%-fine sample having a higher respiration rate than the control appears again in week 10. In week 12, the field respiration measurements show a significant decrease relative to the control reaching up to 22% in samples 4%-medium to 6%-coarse. In this week, the respiration rates increase significantly, reaching an average of 0.29 mg C/g DW/day for the amended samples and 0.31 mg C/g DW/day for the control. Finally, in week 15, there appears to be a linear increase decrease in the respiration rate with an increasing application rate and particle size, with the exception of sample 4%-fine which displays a higher reduction than the other samples amended at 4%.

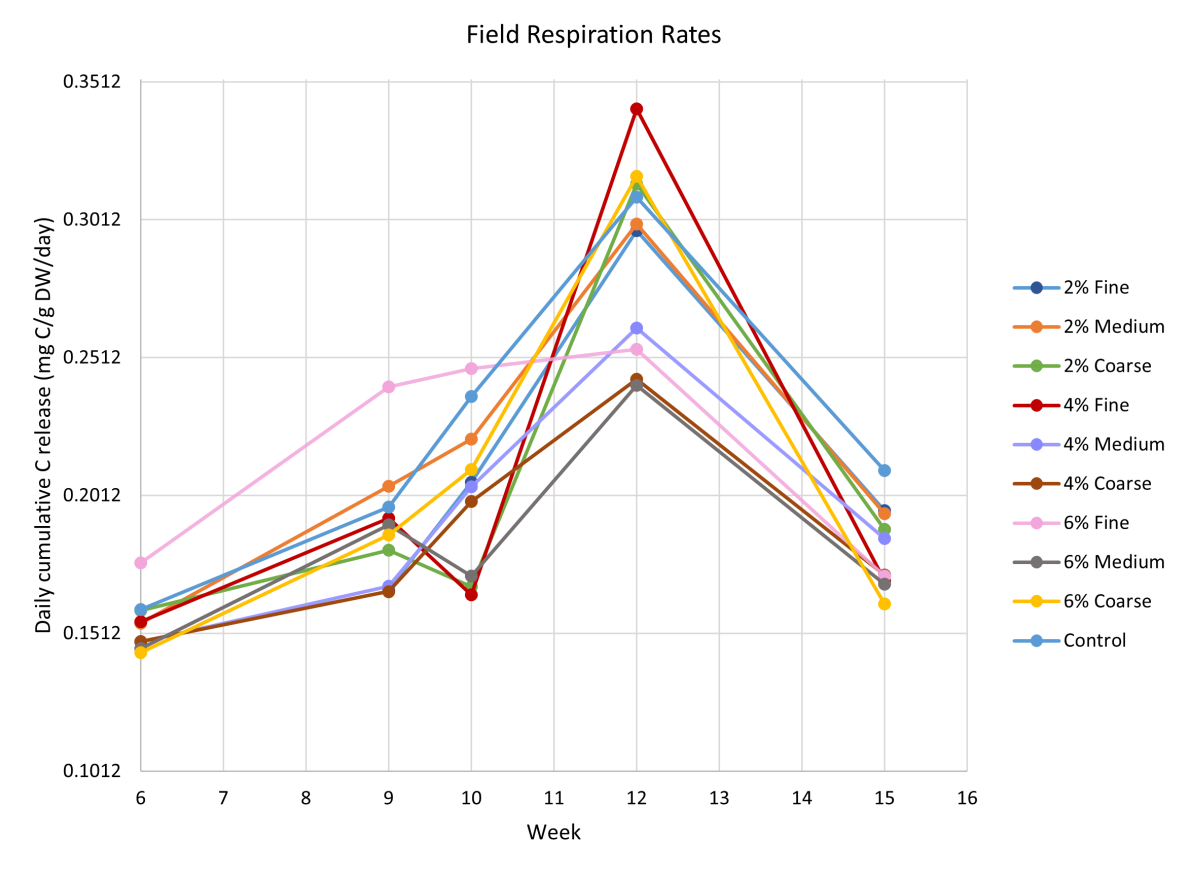

Figure 4.17: Field respiration measured from Week 6 to 15 of the ripening experiment

5

Discussion

5.1. Development of physical properties during ripening of biochar-sediment mixtures

The changes in the moisture content, water holding capacity, shrinkage potential and structure of sediment mixes varying in biochar application rate and particle size were assessed over the course of a 15 week ripening period. The results showed that biochar amendment could increase the moisture content and water holding capacity of the material, whilst reducing the shrinkage potential and accelerating soil structure formation.

5.1.1. Phase 1 - Initial drying: moisture loss, structural rearrangement and shrinkage reduction

In the first six weeks of the field ripening period, the lack of precipitation led to the loss of a majority of the moisture in all sediment samples as the water held in the sediment pores gradually evaporated. As a result, the moisture content and the water holding capacity of the samples dropped. This observation is in line with multiple investigations on the effect of ripening on sediment physical properties, which commonly identified the collapse of large pores and a reduction in the total pore volume of sediments after desiccation [128, 99, 58]. However, these decreases both in moisture content and water holding capacity were less significant in the samples amended with increasing biochar amounts. Whilst the previously water-filled sediment pores drained and collapsed, the biochar pores remained intact and maintained the water holding capacity of the amended samples. Previous studies have demonstrated that the internal porosity introduced following the addition of biochar consistently results in significant water holding capacity increases [94, 67, 8]. However, biochar pyrolysis temperature is an important factor in achieving these results, as higher temperatures (> 400°C) have been linked to reduced biochar hydrophobicity due to the volatilization of aliphatic and aromatic compounds which normally repel water molecules [79, 43, 80]. The high gasification temperature of the Bio Energy Netherlands biochar of 750°C makes this material ideal for increasing the water holding capacity of the ripening sediments. The outcome of this drying process is the oxygenation of the material, as air can finally enter the sediment pores which has compounding effects not only on the physical properties of sediments, but also on their chemical and biological properties [128, 92].

During this period, the shrinkage potential of the material reduced significantly, from an average corrected oven-dried COLE value of 14.46% to 7.66% in the amended samples and from 20.35% to 11.65% for the control. At the start of the ripening experiment, the plate-shaped clay crystals driving swell-shrink behavior were surrounded by water and when the moisture content of the material dropped, this layer of water was lost and the clay platelets grew closer together, resulting in an irreversible volume loss and primary shrinkage [10, 89] . These observations are closely linked to water holding capacity, which dictates the volume available for swelling [10, 97].

5.1.2. Phase 2 - Wetting-drying cycles: aggregate formation and physical stabilization

This initial period of desiccation was followed by three wetting-drying cycles. The combination of intense precipitation events and rising temperatures resulted in successive moisture content increases and decreases. A linear relation between increasing biochar application rate and an increasing sample moisture content ($p < 0.05$) was established with the week 15 measurements. However, the biochar particle size could not be correlated to any trends on the resulting moisture content.

In parallel to these moisture content fluctuations, the water holding capacity of the samples remained relatively stable until the end of the ripening period at 15 weeks. This suggests that a significant part of the structural changes that may occur over the course of the physical ripening process had already taken place by week 5. The biochar amended sampled resulted in a 33-72% increase in WHC compared to the control in the final measurement in week 15. No statistically significant relation could be established between biochar application rate nor particle size and sediment water holding capacity. However, it is clear that biochar amendment increases overall WHC. This observation is further confirmed by the high WHC of the biochar (see Table 4.1), which reached up to 612% in the fine fraction, which amounts to approximately 5 times more than the original sediment WHC. Several studies investigating the impact of biochar application on soil physical properties confirmed this increase in the water holding capacity owed to high internal porosity of biochar and the presence of hydroxyl and carboxyl hydrophilic functional groups on their surfaces [72, 90, 4].

The subsequent wetting–drying cycles, combined with weekly turning, disrupted the initial platy structure of the sediment and promoted the formation of smaller, more stable aggregates. Similar aggregate restructuring under repeated wetting–drying has been reported in ripening and shrink–swell studies where drying induces increased soil water tension, leading to the collapse of micropores and the development of larger surface-connected pores at aggregate boundaries [89, 128, 92, 58]. This effect was more pronounced in biochar-amended samples, particularly at higher application rates and with coarser particle sizes. This observation is consistent with the water holding capacity and shrinkage results, which show a faster physical stabilization in this sample group.

The COLE of the samples continued to decrease until week 15, and it was observed that several of the amended samples reached a stable state as soon as week 9. In between week 1 and 15, the corrected oven-dried COLE of the control sample decreased by 76%, from 20.35% to 4.91%. These observations are in line with previous scientific studies conducted on sediments of the same origin, which observed COLE values in the range 5% to 13% in unripe METHA sediments, which decreased by 20-80% after ripening [89]. The corrected oven-dried COLE of the amended samples at the end of the experiment ranged from 2.23% to 5.38%, which represents up to a 55% decrease relative to the control sample. This decrease was most significant in all coarse biochar amendments, and in the 6% biochar amendments. A correlation between increasing biochar particle size on decreasing COLE values was identified as statistically significant ($p < 0.05$), however the correlation with application rate could not be confirmed with this analysis. The importance of repeated wetting drying cycles in the reduction of shrinkage is well documented in scientific literature, as they cause unstable structure to break down and rearrange, thus accelerating the stabilization of soil structure [89, 97, 77, 101].

The shrinkage reduction observed in the amended samples could be explained by the non-plastic property of the biochar, which experiences no significant change in volume with an increased water content [75]. Thus, as an increasing ratio of this non-expandable material is added relative to the shrinkage prone clay, the overall shrink-swell behavior of the material can be reduced. Furthermore, the addition of biochar may have altered soil particle transitions as evidenced by Lu, Gu, Shen, Wang, Zhang, Tang, and Shi [75] in a study where biochar was added to soil in different particle size fractions (<0.25 mm, 0.25-1 mm, 1-2 mm) and application rates (1, 3, 5, 10%). This study observed loosening contacts between biochar particles and soil with increased biochar particle size. As a result, biochar particles positioned in between soil particles increase their repulsive forces, reducing the shrinkage of the soil. [147] hypothesized that this COLE reduction may be attributed to the biochar particles covering the clay mineral phase surfaces and occupy the pore space in between soil particles, resulting in reduced shrinkage.

The significant reduction of the shrinkage of samples amended with coarse biochar may be explained

by a change in the tensile stress propagation in the COLE rods obtained from the mold method. Coarse biochar particles increase the heterogeneity of sediment matrix compared to finer particles that can be more evenly mixed. This heterogeneity may have disrupted the transfer of stress within the COLE rod, resulting the localized concentration of tensile forces around the coarse biochar particles and reducing overall shrinkage.

The effect of an increasing biochar particle size on shrinkage behavior in the values obtained from the syringe method appears to contradict the results from the mold method. These results showed decreasing shrinkage with increasing application rate and decreasing particle size. This difference could be explained by the larger syringe opening used for the samples amended with coarse biochar, which slowed down the drying process and may have altered shrinkage behavior. The COLE only takes into consideration linear shrinkage, however an increased sample diameter causes additional shrinkage in all directions which may explain the higher COLE values observed [18].

The air-dried and oven-dried COLE results from the syringe method can be compared to the results of the values to the values determined from stockpile 5 (SP-5) of the large scale S2S ripening project, whose management was considered the closest to the strategy of this project, with 4 annual turnings and the removal of vegetation [84]. After 106 days of ripening in the stockpile, the sediments reached air-dried and oven-dried COLE values of 16.9% and 17.1%. This represents an 91% and 88% increase compared to the control. The difference in sediment management, including the turning frequency and stockpile size, could explain this significant

5.1.3. Methodological Limitations: measurement constraints and environmental influences

Adaptation of the COLE preparation method

There are several methodological limitations that may have hindered the COLE analysis. Some data points are missing in the first 5 measurements as the initial syringe method failed on samples with a 6% application rate and samples amended with coarse biochar particles. These issues were progressively solved, first by increasing the syringe opening diameter from 10 mm to 12 mm, which enabled the testing of the 6%-fine and 6%-medium samples. Then the linear shrinkage molds were used an alternative method to the standard syringe for the samples amended with coarse biochar particles (2%-coarse, 4%-coarse, 6%-coarse). From week 4 onward, a full set of measurements could be made, but some corrections had to be implemented in order to compare the data. The corrections were based on values obtained from the final samplings, where all samples were tested with both methods. In order to apply the syringe method to the samples amended with the coarse fraction, a syringe with a 20 mm opening was used. The results revealed that the linear shrinkage molds result in higher COLE values than the syringe method. This could be explained by the bigger size and surface area of the molds, which are 14 cm long with a 2.5 cm diameter, compared to the rods with a 6 cm length and 12-20 mm radius. Whilst the COLE calculation is related to the length of the rod or mold, it is not related to its diameter, which could result in some differences.

Two different COLE datasets were obtained from each test, one corresponding to the air-dried COLE and the other to the oven-dried COLE. When comparing the results from the two methods discussed above, the correction factor calculated for the air-dried COLE had a broad range, from 2.39 for the control sample to 6.06 for the 2%-fine sample. In contrast, the correction factors for the oven-dried COLE values only ranged from 1.70 (2%-medium) to 2.87 (2%-fine). This smaller range in correction factor values for the oven-dried samples was preferred to continue the analysis and compare results from both methods as it would indicate a more consistent change in the results. The high spread of the correction factors for the air-dried COLE may instead indicate a possible limitation of this experiment as discussed in Section 5.1.3.

Effect of relative humidity on air-dried COLE measurements

Fluctuations in the relative humidity of the room may have influenced the air-dried length of the COLE rods. However, in the absence of a complete dataset of the room relative humidity, the relationship between the room and outdoor relative humidity first had to be characterized. The two datasets can be visualized in Appendix E, Figure E.1, along with their correlation in Figure E.2a which shows a stronger correlation until June 15th which may be explained by a change in the atmospheric control of the

building. Thus, the missing room relative humidity values could be estimated from the linear regression parameters of the data until that date, available in E.1. Finally the room relative humidity could be plotted along with the air-dried COLE values in E.3.The relative humidity of the room lied approximately in the range of 39-56%. This could mean that the values measured in a more humid room may under-estimate shrinkage compared to the rest of the measurements. This may have been the case for the week 15 measurement, which were made at the highest relative humidity of all measurements, at 56%. This observation reinforces the advantage of using the oven-dried COLE values for a long term analysis with measurements spread out over different humidity conditions, as they eliminate the uncertainty associated with the fluctuations in room relative humidity.

5.2. Sulfur oxidation and indicators of chemical ripening

One of the most important process that takes place in chemical ripening is the aerobic oxidation of reduced sulfur (e.g., FeS, FeS□) into sulfate SO_4^{2-} that can then leach out of the material [98, 130]. This chemical reaction results in a decrease of the pH due to the release of positively charged hydrogen ions and a loss of the total sulfur content (TS) . Over the course of the ripening experiment, a small overall reduction of the total sulfur content of some samples was observed. The amended samples had initially lower sulfur contents, in the range of 0.306-0.442%TS, and lost on average 5% TS, whilst the control sample had a starting total sulfur content of 0.426 which dropped by 22% after 15 weeks of ripening. The effect of biochar application rate and particle size could not be clearly identified due small magnitude of the changes and the scale of the analysis, which only took two samples of 25 mg each. This result is in accordance with other findings, as Vermeulen, Van Dijk, and Grotenhuis [129] identified a loss of 23-80% of the total sulfur in the first 7 days of sediment ripening. The loss of total sulfur, albeit small in some samples, demonstrates the onset of chemical ripening in the sediments.

This decrease in total sulfur content was expected to result in a pH drop, due to the oxidation of reduced sulfur compounds producing sulfuric acid [130, 37]. However, the opposite was observed: in amended samples, pH rose from a mean of 7.38 to 7.73, while the control sample's pH increased from 7.19 to 7.64. Across all samples, pH increased during the ripening period, with a greater rise in biochar-amended treatments. The positive correlation between biochar application rate and pH was statistically significant ($p < 0.05$), whereas particle size showed no clear effect. Similar trends have been reported in previous studies, where increased soil pH was attributed to the high alkalinity, buffering capacity, and functional group composition of biochar [131, 119, 100]. Biochar contains exchangeable base cations such as Ca^{2+}, Mg^{2+}, K^{+} and Na^{2+}□, which dissolve and enhance buffering capacity [121], while abundant carbonates, hydroxyl, and phenolic functional groups consume protons and further raise pH [68].

In addition to altering pH, sulfur oxidation was expect to increase electrical conductivity through the oxidization of compounds and dissolution of salts into the pore water, releasing ions [128]. The ionic concentration of a solution is proportional to its electrical conductivity (EC), so an increase in EC can be linked to greater dissolution of ions and is an indicator of ongoing chemical ripening reactions [96]. Several studies have established a correlation between the chemical reactivity of sediments and their electrical conductivity, and have identified a proportional relation between EC and SO_4^{2-} concentrations, as higher concentrations of this ion results in an increase of the electrical conductivity [14, 13, 142].

In this study, EC did not show a consistent increase or decrease over the full ripening period, but it provided useful insights into in-situ processes and the influence of weather. The EC readings increased drastically from week 1 to week 5, from a mean of 1.155 to 1.807 mS/cm in the amended samples and from 1.085 to 1.535 mS/cm in the control sample, coinciding with a prolonged dry period marked by steadily decreasing moisture contents. In this period, a significant share of the sediment pore water evaporated and there was no leaching in the absence of precipitation. These conditions resulted in an increasing salt concentration in the pore water, which was detected with the increasing electrical conductivity values. This could indicate that the products of chemical ripening reactions such as the sulfur oxidation have been accumulating in the samples before leaching at the next rain event. The EC values increased again in week 9, point at which the sediments have been drying since week 8 as indicated by the decreased moisture content. Finally, between week 9 and week 15, the electrical conductivity of some samples increases (4%-medium, 6%-medium and coarse), whilst the rest decreased. This could be due to the heavy successive precipitation events that occurred in this period, which removed the leaching ions. In the samples with an increasing electrical conductivity, it is possible that

the sulfur reduction rate was higher than the rate at which the rain could remove the ionic product, thus increasing the total EC. No significant difference could be observed in the electrical conductivity of the amended samples compared to the control, as the results of both stayed within the same range through the ripening period. Accounts on the effect of biochar on soil electrical conductivity vary, with some studies observing increased electrical conductivity due to the addition of soluble salts [11, 114], whilst others could not establish a link due to the variability of biochar composition in leachable ions (Ca^{2+}, Mg^{2+}, K^{+}, Na^{2+})[1].

5.3. Effect of biochar on microbial activity

5.3.1. Phase 1 - Fast microbial degradation of labile organic carbon and biochar priming effect

In the first six weeks of the experiment, the stabilization factor decreased across all samples, and the amended samples had generally lower stabilization values. This general decrease indicates that a growing fraction of the litter is being degraded into CO_2 rather than being mineralized in this period. This could be explained by the drop in moisture content of the sample during this period, which led to sediment pores drying up and enabled air to enter the material which in turn facilitated the growth of the aerobic microbial community responsible for the degradation of organic matter [130].

Furthermore, this relative decrease of the stabilization factor in samples with biochar compared to the control could reveal a positive priming effect as the respiration process appears to be enhanced in those samples. This could be due to the creation of environments favorable to the development of microbial communities with the addition of biochar which provides them with the necessary substrates and habitats in their extensive pore structure [66, 5]. Simultaneously with this decreasing stabilization, the decomposition rate was decreasing until week 6 where a sharp increase could be observed, but no significant difference could be established between the control and the amended samples. This decreasing trend shows that the labile fraction is broken down at slower rates as ripening progresses which could indicate that the fraction of the easily degradable material is diminishing with time, leaving the more recalcitrant material to be broken down by the microorganisms.

The total nitrogen and organic carbon content of each experimental variant evolved over time, reflecting microbial dynamics consistent with the teabag index results. The microbial community relies on nutrients, most importantly nitrogen, to fuel its activity, decomposing organic matter into CO_2 [107]. Nearly all samples (except 6%-fine) showed a decrease in their total nitrogen content until week 5 or 6 of 13% on average for the amended samples and 8% for the control.

This drop could be explained by the reduction of nitrate to N_2 or N_2O as gases through the process of denitrification. This process has been proven to be enhanced in biochar amended soils due to the maintenance of moist conditions favorable to denitrifying bacteria and the increased soil pH [140, 44]. However, this hypothesis is uncertain as denitrification is conducted by anaerobic microbes [135], and the sediments were drying when this total nitrogen loss was measured.

It is also possible that nitrogen mineralization, which consists in the microbial conversion of nitrogen from organic to inorganic forms [61], may have been enhanced during this period of high microbial activity, resulting in some of the nitrogen content being lost as a gas.

At the same time, the total organic carbon content decreased by 30% on average and 6% in the amended samples (excluding 4%-coarse) and the control sample respectively. This observation corroborates the possibility of a positive priming effect following biochar addition, which may have stimulated the microbial decomposition of organic matter, thus increasing nitrogen mineralization and organic carbon respiration. These findings align with multiple studies reporting positive priming effects of biochar on microbial decomposer communities resulting in a drop in nitrogen and organic carbon content [17, 146, 76]. However, it is important to note that several studies also observed negative priming effects [25, 53, 55], which are often attributed to differences in biochar feedstock and production methods, which may have introduced additional labile carbon due to their incomplete pyrolysis [7, 132].

A significant decrease in cumulative respiratory carbon (C) release across all samples was observed between week 1 and week 5, amounting to a reduction of approximately 59% in the amended samples and 52% in the control. These values were measured in a controlled environment, with a moisture

content adjusted to 60% of the water holding capacity and a stable temperature of 20°C, which means they do not fully represent field respiration values. However, the pronounced decrease between week 1 and 5 indicates that a large fraction of the labile organic carbon has been broken down in this period. A study of the kinetics of organic matter mineralization in ripening sediments supports these findings with the identification of a first phase, lasting until 14 to 28 days, during which the easily degradable organic matter was rapidly mineralized at a rate 100 to 1000 times faster than the more recalcitrant fraction Vermeulen, Van Gool, Dorleijn, Joziasse, Bruning, Rulkens, and Grotenhuis [130]. This observation corroborates the hypothesis that between the start of the experiment and week 5, a large fraction of the labile fraction was broken down to release CO_2. Following this phase, mineralization slowed due to the predominance of more recalcitrant organic matter, resulting in reduced respiratory C release, consistent with findings from other studies on soil organic matter decomposition [61, 7].

5.3.2. Phase 2 - Shift in microbial decomposer community for the degradation of recalcitrant organic compounds

After six weeks of drying, the stabilization factors appeared to increase across all samples, and this increase was more significant in the control sample. This suggests that as a growing fraction of the labile material has already been degraded, the remaining material is becoming increasingly recalcitrant [56]. In parallel, the decomposition rate continued to decrease, but this decrease was more significant in the control sample. This can be interpreted as a slowing down of the microbial degradation of the control sample after the degradation of a large part of the labile litter[78]. In the last week of the field ripening experiment, the application of biochar resulted in a decrease of the stabilization factor reaching up to 20% relative to the control, and an increase of the decomposition rate up to 62% higher than the control. A linear correlation was established between increasing biochar application rate and increasing decomposition rate ($p < 0.05$). This would indicate that the microbial community in those samples is capable of actively breaking down organic material that the microbial community in the control sample cannot, and is doing so at a faster rate. This finding can be supported by several investigations which observed an enhanced microbial activity in biochar-amended soils, as the material supports microbial community development by increasing nutrient availability, habitats, water holding capacity and pH buffering [71, 40, 103, 54].

Following this phase of high microbial activity, a subsequent average 9% and 6% increase of the total nitrogen content in the amended and control samples respectively could be measured in weeks 6 and 9. After this increase, the total nitrogen contents stabilized until the end of the ripening experiment in week 15. In the same period, the TOC of the amended samples increased in weeks 5 or 6 by an average of 25% (excluding 6%-medium), and then stabilized around this new level. Meanwhile, the control sample's TOC content remained stable. This could be explained by a change in microbial community and substrate availability. At the start of the ripening period, the results of the biochemical analyses support the hypothesis that microorganisms rapidly degraded organic carbon and consumed nitrogen to support biomass growth and enzyme production [61]. Once this labile pool was depleted, the microbial community shifted towards populations adapted to the degradation of more recalcitrant carbon, which generally increases the nitrogen demand [107]. This could be explained by the higher energy microbial energy demand for the degradation of recalcitrant C, which stimulates nitrogen immobilization and fixation from the atmosphere and precipitation, thus increasing total nitrogen [12, 6].

The total inorganic carbon content of the amended samples and the control decreased by 9% and 6% respectively over the course of the ripening period. Inorganic carbon is found in carbonates, which can be produced by microbial respiration when the CO_2 released precipitates with pore water [62]. The carbonates can then be mobilized during rain events, resulting in a loss of TIC by leaching [33].

The increase and stabilization of the total organic carbon content observed only in the amended samples may reflect the stabilization of organic matter on biochar surfaces, which can protect organic carbon from further microbial degradation [132, 7]. Furthermore, biochar's porous structure and high surface area can adsorb dissolved organic carbon from precipitation increasing the measured TC [83]. It is also possible that some bacteria, such as cyanobacteria, present in the sediments prosper in the moist conditions maintained in the amended samples and contribute to carbon fixation [64]. These dynamics indicate a transition from a microbial community dominated by rapid decomposition of easily available substrates to one focused on slower turnover and organic matter stabilization. The respiration

analysis of samples collected in week 9 and 15 shows that biochar addition results in a decrease of the respiratory carbon released relative to the control of 23-68% and 14-32% respectively. These results suggest that biochar addition may have accelerated the degradation of organic carbon in the first five weeks of the experiment, resulting in a decrease of the respiration rate in the long term as this material is still being processed in the control.

The cumulated respiratory C release values of the experiment after 105 days of ripening can be compared to stockpile 5 (SP-5) of the S2S ripening project which used the same METHA material [84]. This comparison revealed that significantly lower respiratory C release values were reached much sooner in this experiment than in the S2S SP-5 samples. The cumulative C release of the amended and control samples were respectively 61-69% and 55% lower than the SP-5 values around the same time (105 days of ripening). This difference could be explained by the significantly larger amounts of material in the stockpile and the less frequent turning which may reduce the aeration of the material and slow down the ripening process. The final values obtained from this experiment are closer to the S2S values obtained after 636 days of ripening (or 1 year and 9 months), of 0.239 mg C/g DW. This implies that the stabilization of the METHA sediments is taking place much faster in this experiment than in stockpiles, even without biochar amendment.

Field respiration measurements taken in weeks 6, 9, 10, 12 and 15 enabled a more nuanced interpretation of the laboratory respiration measurements, as they reflect the effect of additional parameters such as water content and temperature. As the ripening progressed, the difference between the amended samples and the control sample grew. Progressively, the respiration rate in an increasing number of samples was lower than the control, from three experimental variants in week 10, to all nine variants in week 15. This could be the long term result of the priming effect of biochar observed in the first five weeks of ripening, which may have stabilized the organic matter faster, resulting in a quicker reduction of respiration rates. These findings were observed in several studies, proving the beneficial impact of biochar amendment sediment ripening [116, 91].

External weather conditions may have affected the respiration measurements. The highest overall field respiration rates measured occurred in week 12, which coincides with the highest sample moisture contents. This observation was corroborated by several studies assessing the impact of soil moisture on soil respiration, revealing an increase in microbial activity with soil moisture [22, 26, 148]. Thus, the influence of biochar on sediment moisture content can be linked to an increased microbial activity and possibly an acceleration of the biological ripening.

The measurement method constitutes a possible limitation for these observations. In weeks 6 and 15, only one analyzer was used on all the samples. However, in weeks 9, 10 and 12 two additional analyzers were used to reduce the test time and measure the respiration of multiple samples at the same time. In those weeks, the respiration of the control sample was measured with each measurement tool in order to correct any offset from the different probes. The difference between the additional analyzers and the reference analyzer was within the range of -10% to 13%.

Based on the field measurements of the daily cumulative C release of the samples, an estimation can be made for the maximum possible TOC lost over the course of the ripening period. Using the average respiration rate of the control across all field measurements, which amounts to 0.223 mg C/g DW/day, the TOC lost over 15 weeks of ripening would be approximately 2.34% DW. This exceeds the TOC loss calculated from the elemental analysis, of only 6% in the first 6 weeks. This significant difference could indicate some limitations of theses analyses. It is possible that the representativeness of the small sample size used in the elemental analysis was insufficient. Additionally, the field respiration measurements were taken after turning as the samples had to be transferred to a smaller closed bucket, which may have overestimated respiration rates.

6

Conclusions and Outlook

In the Netherlands and in the world, the need for more sustainable construction materials is growing. At the same time, a large amount of sediments is dredged each year mainly for waterway maintenance, but without any secondary use for the newly extracted material. This sparked the idea to transform dredged sediments into a usable construction material using biochar, a material already used in many soil remediation projects for its highly advantageous properties. This projects aimed to evaluate the impact of biochar amendment on the biophysicochemical sediment ripening processes with a focus on the biochar application rate and particle size. To answer this question, sediments amended at different biochar application rates (2, 4 and 6%) and particle size (<2 mm, 2-5 mm, >5 mm) were ripened outside over 15 weeks. Samples were regularly collected to conduct a physical, chemical and biological analysis of the ripening sediments.

The amendment of biochar enhanced the physical ripening of the METHA sediments by increasing moisture retention, reducing shrinkage potential, and accelerating structure formation. The porous structure and high specific surface area of the material contributed to maintaining pore space even after the material had consolidated. Furthermore, the non-expandable property of biochar combined with the effect of large biochar particles on tensile stress distribution in sediment COLE rods significantly reduced the shrinkage capacity of the material. In applications such as dikes, the amended material would therefore be more suitable than unamended sediments as shrinkage is a major threat to the structural integrity of dikes. The improvement in sediment moisture content of the amended samples also contributed to an accelerated structure stabilization of the initially dense and platy material into smaller aerated aggregates. A faster physical stabilization would contribute to making dredged sediments more competitive with primary raw material by reducing processing duration. The results of the physical analyses indicate that a higher biochar application rate and particle size is most beneficial to the structural properties of the ripened sediments.

The high buffering capacity of biochar appears to have benefited microbial degradation of organic matter by maintaining a high pH that is optimal for their activity, thus balancing out the release of acidifying compounds from this process. This chemical stability, supported by the high functional group and mineral content of biochar, is important in dike construction. It ensures that the dredged material will maintain a stable behavior in the face of events such as flooding and salt intrusion. Additionally, the occurrence of sulfur oxidation was confirmed with the measurement of loss of sulfur content and a fluctuation in electrical conductivity, however no conclusion could be drawn about level of completion of this reaction.

The biological analyses indicate that biochar addition promoted a positive priming effect in sediment biological ripening. During the first six weeks, a significant proportion of organic carbon was released via microbial respiration, accelerating the degradation of labile carbon early in the ripening period. In the long term, this led to faster stabilization of organic matter—an important benefit for dike construction, where biologically unstable sediments can compromise structural integrity through microbial CO_2 release and associated physical and chemical changes. A 6% biochar application rate significantly

reduced long-term respiration, while particle size showed no notable effect. Notably, the respiration of the control sample reached levels comparable to those from the large-scale S2S METHA ripening project in just 105 days, compared to 636 days in the stockpiles, underscoring the value of an optimized ripening strategy. Smaller stockpiles and more frequent turning could play a decisive role in further shortening ripening duration.

These findings highlight the potential of biochar in the transformation of the undervalued material that is dredged sediments into a circular construction material. The benefits of this application go beyond the enhancement of sediment ripening by also creating material properties desirable for dike construction. Thus, the adoption of this amendment could contribute to reaching national sustainability goals and meeting the demand for dike construction materials in a changing climate.

6.1. Outlook

Further work in the optimization of biochar application rate and particle size could help tailor the final material to specific mechanical or physical requirements. Additionally, higher application rates and different particle sizes could be investigated to identify the thresholds beyond which biochar no longer yields significant improvement.

The experiment was limited both in duration and scale and additional studies over a longer ripening period and a bigger sediment volume could help to identify whether the observed benefits can be replicated under full-scale application conditions.

A logical continuation of this work would be to assess the effect of the biochar amendment of the mechanical and hydraulic properties of the ripened material to confirm its suitability for dike construction. This could include analyses relevant to the permeability of the material, its resistance to erosion and its leaching behavior such as the Proctor compaction test, tensile strength measurement, crack formation and propagation analysis, and hydraulic conductivity. The influence of biochar on the leaching behavior could be particularly relevant for dredged sediments that do not currently meet the required contaminant thresholds and positive results could potentially open opportunities for the beneficial reuse of dredged material from more diverse origins in flood protection infrastructure

References

[1] I. S. Abujabhah, R. Doyle, S. A. Bound, and J. P. Bowman. “The effect of biochar loading rates on soil fertility, soil biomass, potential nitrification, and soil community metabolic profiles in three different soils”. In: *Journal of Soils and Sediments* 16 (2016), pp. 2211–2222. DOI: 10.1007/s11368-016-1420-5.

[2] A. G. Alghamdi, A. Alkhasha, and H. M. Ibrahim. “Effect of biochar particle size on water retention and availability in a sandy loam soil”. In: *Journal of Saudi Chemical Society* 24.12 (2020), pp. 1042–1050. DOI: 10.1016/j.jscs.2020.10.003.

[3] K. D. Alotaibi and J. J. Schoenau. “Application of two bioenergy byproducts with contrasting carbon availability to a prairie soil: Three-year crop response and changes in soil biological and chemical properties”. In: *Agronomy* 6.1 (2016), p. 13. DOI: 10.3390/agronomy6010013.

[4] M. C. Andrenelli, A. Maienza, L. Genesio, F. Miglietta, S. Pellegrini, F. P. Vaccari, and N. Vignozzi. “Field application of pelletized biochar: Short term effect on the hydrological properties of a silty clay loam soil”. In: *Agricultural Water Management* 163 (2016), pp. 190–196.

[5] Y. M. Awad, S. S. Lee, Y. S. Ok, and Y. Kuzyakov. “Effects of biochar and polyacrylamide on decomposition of soil organic matter and ^{14}C-labeled alfalfa residues”. In: *Journal of Soils and Sediments* 17.3 (2017), pp. 611–620.

[6] J. Belnap. “Nitrogen fixation in biological soil crusts from southeast Utah, USA”. In: *Biology and Fertility of Soils* 35.2 (2002), pp. 128–135. DOI: 10.1007/s00374-002-0452-x.

[7] E. Blagodatskaya and Y. Kuzyakov. “Mechanisms of real and apparent priming effects and their dependence on soil microbial biomass and community structure: critical review”. In: *Biology and Fertility of Soils* 45.2 (2008), pp. 115–131. DOI: 10.1007/s00374-008-0334-y.

[8] H. Blanco-Canqui. “Biochar and soil physical properties”. In: *Soil Science Society of America Journal* 81.4 (2017), pp. 687–711. DOI: 10.2136/sssaj2017.01.0017.

[9] J. Brils, P. de Boer, J. Mulder, and E. de Boer. “Reuse of dredged material as a way to tackle societal challenges”. In: *Journal of Soils and Sediments* 14 (2014), pp. 1638–1641.

[10] J. J. B. Bronswijk and J. J. Evers-Vermeer. “Shrinkage of Dutch clay soil aggregates”. In: *Netherlands Journal of Agricultural Science* 38.2 (1990), pp. 175–194.

[11] L. D. Burrell, F. Zehetner, N. Rampazzo, B. Wimmer, and G. Soja. “Long-term effects of biochar on soil physical properties”. In: *Geoderma* 282 (2016), pp. 96–102. DOI: 10.1016/j.geoderma.2016.06.023.

[12] Y. Cao, Z. He, T. Zhu, and F. Zhao. “Organic-C quality as a key driver of microbial nitrogen immobilization in soil: A meta-analysis”. In: *Geoderma* 383 (2021), p. 114784. DOI: 10.1016/j.geoderma.2020.114784.

[13] V. Cappuyns and R. Swennen. “Sediment characterization during oxidation and ripening and evaluation of its potential reuse”. In: *Environmental Technology* 30.8 (2009), pp. 785–797. DOI: 10.1080/09593330902957610.

[14] V. Cappuyns, R. Swennen, and A. Devivier. “Influence of ripening on pH stat leaching behaviour of heavy metals from dredged sediments”. In: *Journal of Environmental Monitoring* 6.9 (2004), pp. 774–781. DOI: 10.1039/B404323D.

[15] CEDA. *Sustainable Management of the Beneficial Use of Sediments. Information Paper*. Online. 2019. URL: https://dredging.org/media/ceda/org/documents/ceda/2019-05-bus-ip.pdf.

[16] CEDA Working Group on Beneficial Use of Sediments. *Case Study: Project METHA-Plant – Large Scale Sediment Treatment*. http://sednet.org/download/H-Detzner.pdf. Contact: Heinz-Dieter Detzner, Hamburg Port Authority. Hamburg, Germany, 1993–ongoing.

[17] P. Cely, A. M. Tarquis, J. Paz-Ferreiro, A. Méndez, and G. Gascó. “Factors driving the carbon mineralization priming effect in a sandy loam soil amended with different types of biochar”. In: *Solid Earth* 5.1 (2014), pp. 585–594. DOI: 10.5194/se-5-585-2014.

[18] A. Chen, X. Zhang, X. Shi, S. Zhao, and J. Chen. “Study on the dry shrinkage characteristics and size effect of swell-shrink characteristic soil”. In: *PLOS ONE* 19.8 (2024), e0307679. DOI: 10.1371/journal.pone.0307679.

[19] K. Chen, J. Peng, J. Li, Q. Yang, X. Zhan, N. Liu, and X. Han. “Stabilization of soil aggregate and organic matter under the application of three organic resources and biochar-based compound fertilizer”. In: *Journal of Soils and Sediments* 20 (2020), pp. 3633–3643. DOI: 10.1007/s11368-020-02730-6.

[20] X. Chen, L. Liu, Q. Yang, H. Xu, G. Shen, and Q. Chen. “Optimizing Biochar Application Rates to improve soil properties and crop growth in saline–alkali soil”. In: 16.6 (2024).

[21] M. Cronin, A. Judd, S. Blake, and J. Lonsdale. “Assessment of Data on the Management of Wastes or Other Matter (Dredged Material) 2008 - 2020”. In: *The 2023 Quality Status Report for the North-East Atlantic*. London: OSPAR Commission, 2023. URL: https://oap.ospar.org/en/ospar-assessments/quality-status-reports/qsr-2023/otherassessments/dredged-material.

[22] J. Curiel Yuste, D. D. Baldocchi, A. Gershenson, A. Goldstein, L. Misson, and S. Wong. “Microbial soil respiration and its dependency on carbon inputs, soil temperature and moisture”. In: *Global Change Biology* 13.9 (2007), pp. 2018–2035. DOI: 10.1111/j.1365-2486.2007.01415.x.

[23] M. Cybulak, Z. Sokołowska, P. Boguta, and A. Tomczyk. “Influence of pH and grain size on physicochemical properties of biochar and released humic substances”. In: *Fuel* 240 (2019), pp. 334–338.

[24] A. Daebeler, E. Petrová, E. Kinz, S. Grausenburger, H. Berthold, T. Sandén, and R. Angel. “Pairing litter decomposition with microbial community structures using the Tea Bag Index (TBI)”. In: *Soil* 8.1 (2022), pp. 163–176. DOI: 10.5194/soil-8-163-2022.

[25] D. N. Dempster, D. B. Gleeson, Z. R. Solaiman, D. L. Jones, and D. V. Murphy. “Decreased soil microbial biomass and nitrogen mineralisation with Eucalyptus biochar addition to a coarse textured soil”. In: *Plant and Soil* 354 (2012), pp. 311–324. DOI: 10.1007/s11104-011-1067-5.

[26] Q. Deng, D. Hui, G. Chu, X. Han, and Q. Zhang. “Rain-induced changes in soil CO2 flux and microbial community composition in a tropical forest of China”. In: *Scientific Reports* 7.1 (2017), p. 5539. DOI: 10.1038/s41598-017-05972-4.

[27] EcoShape – Building with Nature. *Clay Ripening Pilot Research Reports Available: Kleirijperij*. Technical report / Project news. Accessed July 2025. EcoShape – Building with Nature, Nov. 2023. URL: https://www.ecoshape.org/en/kleirijperij-pilot-research-reports-available/.

[28] European Biochar Foundation. *Guidelines of the European Biochar Certificate - Version 10.4 E*. Updated on 20th December 2024. European Biochar Foundation. 2024. URL: https://www.european-biochar.org/en/download.

[29] European Dredging Association. *Dredged Material & Environmental Regulation in EU*. EuDA Ems paper, 14. 2005.

[30] S. Fang, L. Zhao, G. Rong, B. Chen, X. Xu, H. Qiu, and X. Cao. “Converting coastal silt into subgrade soil with biochar as reinforcing agent, CO_2 adsorbent, and carbon sequestrating material”. In: *Journal of Environmental Management* 344 (2023), p. 118394.

[31] D. Feng, S. Wang, Y. Zhang, Y. Zhao, S. Sun, G. Chang, and Y. Qin. “Review of carbon fixation evaluation and emission reduction effectiveness for biochar in China”. In: *Energy & Fuels* 34.9 (2020), pp. 10583–10606. DOI: 10.1021/acs.energyfuels.0c01312.

[32] G. Fu, X. Qiu, X. Xu, W. Zhang, F. Zang, and C. Zhao. “The role of biochar particle size and application rate in promoting the hydraulic and physical properties of sandy desert soil”. In: *Catena* 207 (2021), p. 105607. DOI: 10.1016/j.catena.2021.105607.

[33] T. M. Gallagher and D. O. Breecker. “The obscuring effects of calcite dissolution and formation on quantifying soil respiration”. In: *Global Biogeochemical Cycles* 34.12 (2020), e2020GB006584. DOI: 10.1029/2020GB006584.

[34] A. Garg, I. Wani, H. Zhu, and V. Kushvaha. “Exploring efficiency of biochar in enhancing water retention in soils with varying grain size distributions using ANN technique”. In: *Acta Geotechnica* 17.4 (2022), pp. 1315–1326.

[35] J. Gebert, C. Chassagne, and R.N.J. Comans. *Project Title: Sediment to Soil (S2S)*. Research project application submitted to the Netherlands Organization for Scientific Research (NWO). Unpublished research proposal. 2024.

[36] J. Gebert and A. Groengroeft. “Long-term hydraulic behaviour and soil ripening processes in a dike constructed from dredged material”. In: *Journal of Soils and Sediments* 20 (2020), pp. 1793–1805. DOI: 10.1007/s11368-020-02591-1.

[37] J. J. Germida and H. H. Janzen. “Factors affecting the oxidation of elemental sulfur in soils”. In: *Fertilizer Research* 35.1 (1993), pp. 101–114. DOI: 10.1007/BF00750227.

[38] L. Githinji. “Effect of biochar application rate on soil physical and hydraulic properties of a sandy loam”. In: *Archives of Agronomy and Soil Science* 60.4 (2014), pp. 457–470.

[39] E. D. Goldberg. *Black carbon in the environment: properties and distribution*. Wiley-Interscience, 1985.

[40] J. D. Gomez, K. Denef, C. E. Stewart, J. Zheng, and M. F. Cotrufo. “Biochar addition rate influences soil microbial abundance and activity in temperate soils”. In: *European Journal of Soil Science* 65.1 (2014), pp. 28–39. DOI: 10.1111/ejss.12082.

[41] Government of the Netherlands. *A Circular Economy in the Netherlands by 2050*. Technical report. Accessed July 2025. Government□wide Programme for a Circular Economy, 2017. URL: https://circulareconomy.europa.eu/platform/sites/default/files/17037circulaireeconomie_en.pdf.

[42] Government of the Netherlands. *Eighth Netherlands National Communication and Fifth Biennial Report under the United Nations Framework Convention on Climate Change*. Published under the United Nations Framework Convention on Climate Change (UNFCCC). Mar. 2023. URL: https://english.rvo.nl/sites/default/files/2023-08/Eight%20Netherlands%20National%20Communication%20-%20Chapter%206%20-%20March%202023.pdf.

[43] M. Gray, M. G. Johnson, M. I. Dragila, and M. Kleber. “Water uptake in biochars: The roles of porosity and hydrophobicity”. In: *Biomass and Bioenergy* 61 (2014), pp. 196–205. DOI: 10.1016/j.biombioe.2013.12.010.

[44] L. He, J. Shan, X. Zhao, S. Wang, and X. Yan. “Variable responses of nitrification and denitrification in a paddy soil to long-term biochar amendment and short-term biochar addition”. In: *Chemosphere* 234 (Nov. 2019), pp. 558–567. DOI: 10.1016/j.chemosphere.2019.06.038.

[45] J. Hunt, M. DuPonte, D. Sato, and A. Kawabata. “The basics of biochar: A natural soil amendment”. In: *Soil and Crop Management* 30.7 (2010), pp. 1–6.

[46] IPCC. “Summary for Policymakers”. In: *Climate Change 2023: Synthesis Report. Contribution of Working Groups I, II and III to the Sixth Assessment Report of the Intergovernmental Panel on Climate Change*. Ed. by Core Writing Team, H. Lee, and J. Romero. Geneva, Switzerland: IPCC, 2023, pp. 1–34. DOI: 10.59327/IPCC/AR6-9789291691647.001.

[47] J. A. Ippolito, L. Cui, C. Kammann, N. Wrage-Mönnig, J. M. Estavillo, T. Fuertes-Mendizabal, and N. Borchard. “Feedstock choice, pyrolysis temperature and type influence biochar characteristics: a comprehensive meta-data analysis review”. In: *Biochar* 2 (2020), pp. 421–438. DOI: 10.1007/s42773-020-00067-x.

[48] N.M. Jaafar, P.L. Clode, and L.K. Abbott. “Soil microbial responses to biochars varying in particle size, surface and pore properties”. In: *Pedosphere* 25.5 (2015), pp. 770–780.

[49] B. H. Janssen. “A simple method for calculating decomposition and accumulation of ‘young’ soil organic matter”. In: *Biological Processes and Soil Fertility*. Elsevier, 1984, pp. 297–304.

[50] S. de Jesus Duarte, B. Glaser, and C. E. Pellegrino Cerri. “Effect of biochar particle size on physical, hydrological and chemical properties of loamy and sandy tropical soils”. In: *Agronomy* 9.4 (2019), p. 165. DOI: 10.3390/agronomy9040165.

[51] M. Ji, X. Wang, M. Usman, F. Liu, Y. Dan, L. Zhou, and W. Sang. “Effects of different feedstocks-based biochar on soil remediation: A review”. In: *Environmental Pollution* 294 (2022), p. 118655. DOI: 10.1016/j.envpol.2021.118655.

[52] S. H. Jien, C. C. Wang, C. H. Lee, and T. Y. Lee. “Stabilization of organic matter by biochar application in compost-amended soils with contrasting pH values and textures”. In: *Sustainability* 7.10 (2015), pp. 13317–13333. DOI: 10.3390/su71013317.

[53] D. L. Jones, D. V. Murphy, M. Khalid, W. Ahmad, G. Edwards-Jones, and T. H. DeLuca. “Short-term biochar-induced increase in soil CO_2 release is both biotically and abiotically mediated”. In: *Soil Biology and Biochemistry* 43.8 (2011), pp. 1723–1731. DOI: 10.1016/j.soilbio.2011.04.018.

[54] K. Karhu, T. Mattila, I. Bergström, and K. Regina. “Biochar addition to agricultural soil increased CH_4 uptake and water holding capacity–Results from a short-term pilot field study”. In: *Agriculture, Ecosystems & Environment* 140.1-2 (2011), pp. 309–313. DOI: 10.1016/j.agee.2010.12.005.

[55] A. Keith, Balwant Singh, S., and Bhupinder Pal. “Interactive priming of biochar and labile organic matter mineralization in a smectite-rich soil”. In: *Environmental Science & Technology* 45.22 (2011), pp. 9611–9618. DOI: 10.1021/es202186j.

[56] J. A. Keuskamp, B. J. Dingemans, T. Lehtinen, J. M. Sarneel, and M. M. Hefting. “Tea Bag Index: a novel approach to collect uniform decomposition data across ecosystems”. In: *Methods in Ecology and Evolution* 4.11 (2013), pp. 1070–1075.

[57] C. A. Kirkby, A. E. Richardson, L. J. Wade, J. B. Passioura, G. D. Batten, C. Blanchard, and J. A. Kirkegaard. “Nutrient availability limits carbon sequestration in arable soils”. In: *Soil Biology and Biochemistry* 68 (2014), pp. 402–409. DOI: 10.1016/j.soilbio.2013.10.022.

[58] J. Kodikara, S.L. Barbour, and D.G. Fredlund. “Changes in clay structure and behaviour due to wetting and drying”. In: *Proceedings 8th Australia New Zealand Conference on Geomechanics: Consolidating Knowledge*. Vol. 179. Australian Geomechanics Society, Feb. 1999.

[59] T. A. J. Kuhlbusch and P. J. Crutzen. “Toward a global estimate of black carbon in residues of vegetation fires representing a sink of atmospheric CO2 and a source of O2”. In: *Global Biogeochemical Cycles* 9.4 (1995), pp. 491–501. DOI: 10.1029/95GB02755.

[60] K. G. I. D. Kumari, P. Moldrup, M. Paradelo, L. Elsgaard, H. Hauggaard-Nielsen, and L. W. de Jonge. “Effects of biochar on air and water permeability and colloid and phosphorus leaching in soils from a natural calcium carbonate gradient”. In: *Geoderma* 221–222 (2014), pp. 51–58. DOI: 10.1016/j.geoderma.2014.01.005.

[61] Y. Kuzyakov, J. K. Friedel, and K. Stahr. “Review of mechanisms and quantification of priming effects”. In: *Soil Biology and Biochemistry* 32.11-12 (2000), pp. 1485–1498. DOI: 10.1016/S0038-0717(00)00084-5.

[62] Y. Kuzyakov, E. Shevtzova, and K. Pustovoytov. “Carbonate re-crystallization in soil revealed by ^{14}C labeling: Experiment, model and significance for paleo-environmental reconstructions”. In: *Geoderma* 131.1-2 (2006), pp. 45–58. DOI: 10.1016/j.geoderma.2005.03.002.

[63] M. D. Lafrenz, R. A. Bean, and D. Uthman. “Soil ripening following dam removal”. In: *Physical Geography* 34.2 (2013), pp. 124–135.

[64] O. L. Lange. “Photosynthesis of soil-crust biota as dependent on environmental factors”. In: *Biological Soil Crusts: Structure, Function, and Management*. Berlin, Heidelberg: Springer Berlin Heidelberg, 2001, pp. 217–240.

[65] J. Lehmann. “Bio energy in the black”. In: *Frontiers in Ecology and the Environment* 5.7 (Sept. 2007), pp. 381–387. DOI: 10.1890/1540-9295(2007)5[381:BITB]2.0.CO;2.

[66] J. Lehmann, M. C. Rillig, J. Thies, C. A. Masiello, W. C. Hockaday, and D. Crowley. “Biochar effects on soil biota–a review”. In: *Soil Biology and Biochemistry* 43.9 (2011), pp. 1812–1836. DOI: 10.1016/j.soilbio.2011.04.022.

[67] O. Lei and R. Zhang. “Effects of biochars derived from different feedstocks and pyrolysis temperatures on soil physical and hydraulic properties”. In: *Journal of Soils and Sediments* 13.9 (2013), pp. 1561–1572. DOI: 10.1007/s11368-013-0738-y.

[68] X. Li, Q. Shen, D. Zhang, X. Mei, W. Ran, Y. Xu, and G. Yu. “Functional groups determine biochar properties (pH and EC) as studied by two-dimensional ^{13}C NMR correlation spectroscopy”. In: *PLoS One* 8.6 (2013), e65949. DOI: 10.1371/journal.pone.0065949.

[69] C. Liang, G. Gascó, S. Fu, A. Méndez, and J. Paz-Ferreiro. “Biochar from pruning residues as a soil amendment: effects of pyrolysis temperature and particle size”. In: *Soil and Tillage Research* 164 (2016), pp. 3–10. DOI: 10.1016/j.still.2016.01.001.

[70] T. J. Lim, K. A. Spokas, G. Feyereisen, and J. M. Novak. “Predicting the impact of biochar additions on soil hydraulic properties”. In: *Chemosphere* 142 (2016), pp. 136–144.

[71] L. Ling, Y. Luo, B. Jiang, J. Lv, C. Meng, Y. Liao, and J. Xu. “Biochar induces mineralization of soil recalcitrant components by activation of biochar responsive bacteria groups”. In: *Soil Biology and Biochemistry* 172 (2022), p. 108778. DOI: 10.1016/j.soilbio.2022.108778.

[72] B. Liu, M. Liao, Y. Wan, X. He, and D. Wang. “Hydraulic characteristics and vegetation performance of the Yellow River sediment modified by biochar”. In: *Biogeotechnics* 2.2 (2024), p. 100070.

[73] X. Liu, J. Zheng, D. Zhang, K. Cheng, H. Zhou, A. Zhang, L. Li, X. Chen, S. Joseph, and G. Pan. “Biochar has no effect on soil respiration across Chinese agricultural soils”. In: *Science of the Total Environment* 554 (2016), pp. 259–265. DOI: 10.1016/j.scitotenv.2016.02.179.

[74] S. G. Lu, F. F. Sun, and Y. T. Zong. “Effect of rice husk biochar and coal fly ash on some physical properties of expansive clayey soil (Vertisol)”. In: *Catena* 114 (2014), pp. 37–44. DOI: 10.1016/j.catena.2013.10.005.

[75] Y. Lu, K. Gu, Z. Shen, X. Wang, Y. Zhang, C. S. Tang, and B. Shi. “Effects of biochar particle size and dosage on the desiccation cracking behavior of a silty clay”. In: *Science of the Total Environment* 837 (2022), p. 155788. DOI: 10.1016/j.scitotenv.2022.155788.

[76] Y. Luo, M. Durenkamp, M. De Nobili, Q. Lin, and P. C. Brookes. “Short term soil priming effects and the mineralisation of biochar following its incorporation to soils of different pH”. In: *Soil Biology and Biochemistry* 43.11 (2011), pp. 2304–2314. DOI: 10.1016/j.soilbio.2011.07.020.

[77] T. Ma, C. Wei, C. Yao, and P. Yi. “Microstructural evolution of expansive clay during drying–wetting cycle”. In: *Acta Geotechnica* 15.8 (2020), pp. 2355–2366. DOI: 10.1007/s11440-020-00917-0.

[78] E. MacDonald, M. E. Brummell, A. Bieniada, J. Elliot, A. Engering, T. L. Gauthier, and M. Strack. “Using the Tea Bag Index to characterize decomposition rates in restored peatlands”. In: *Boreal Environment Research*. Vol. 23. Suomen Ymparistokeskus, Aug. 2018, p. 221.

[79] J. Mao, K. Zhang, and B. Chen. “Linking hydrophobicity of biochar to the water repellency and water holding capacity of biochar-amended soil”. In: *Environmental Pollution* 253 (2019), pp. 779–789. DOI: 10.1016/j.envpol.2019.07.051.

[80] J. Marshall, R. Muhlack, B. J. Morton, L. Dunnigan, D. Chittleborough, and C. W. Kwong. “Pyrolysis temperature effects on biochar–water interactions and application for improved water holding capacity in vineyard soils”. In: *Soil Systems* 3.2 (2019), p. 27. DOI: 10.3390/soilsystems3020027.

[81] METHA-Plant. “Routine METHA material laboratory characterization”. Personal communication.

[82] R. O. Miller and D. E. Kissel. “Comparison of Soil pH Methods on Soils of North America”. In: *Soil Science Society of America Journal* 74.1 (2010), pp. 310–316. DOI: 10.2136/sssaj2008.0047. URL: https://acsess.onlinelibrary.wiley.com/doi/10.2136/sssaj2008.0047.

[83] A. Mukherjee and R. Lal. “Biochar impacts on soil physical properties and greenhouse gas emissions”. In: *Agronomy* 3.2 (2013), pp. 313–339.

[84] E. Nazeir. “S2S Ripening Analyses”. Personal dataset.

[85] Bio Energy Netherlands. “Characterization of the EBC certified production batch BA-NL-538-1-1”. Personal communication.

[86] J. M. Novak, W. J. Busscher, D. W. Watts, D. A. Laird, M. A. Ahmedna, and M. A. Niandou. “Short-term CO_2 mineralization after additions of biochar and switchgrass to a Typic Kandiudult”. In: *Geoderma* 154.3–4 (2010), pp. 281–288. DOI: 10.1016/j.geoderma.2009.10.014.

[87] M. Ogawa and Y. Okimori. “Pioneering works in biochar research, Japan”. In: *Soil Research* 48.7 (2010), pp. 489–500. DOI: 10.1071/SR10006.

[88] K. Oing. “Suitability of processed dredged material from the Hamburg harbor for dike construction”. Doctoral dissertation. Staats- und Universitätsbibliothek Hamburg Carl von Ossietzky, 2019.

[89] K. Oing, A. Gröngröft, and A. Eschenbach. “Ripening reduces the shrinkage of processed dredged material”. In: *Journal of Soils and Sediments* 20 (2020), pp. 571–583. DOI: 10.1007/s11368-019-02465-7.

[90] G. Ojeda, J. Patrício, S. Mattana, and A. J. Sobral. “Effects of biochar addition to estuarine sediments”. In: *Journal of Soils and Sediments* 16.10 (2016), pp. 2482–2491. DOI: 10.1007/s11368-016-1451-0.

[91] J. O. Olaniyan, T. O. Isimikalu, and B. A. Raji. “An investigation of the effect of biochar application rates on CO2 emissions in soils under upland rice production in southern Guinea Savannah of Nigeria”. In: *Heliyon* 6.11 (2020).

[92] B. R. Oliveira, M. P. Smit, L. A. van Paassen, T. C. Grotenhuis, and H. H. Rijnaarts. “Functional properties of soils formed from biochemical ripening of dredged sediments—subsidence mitigation in delta areas”. In: *Journal of Soils and Sediments* 17 (2017), pp. 286–298.

[93] Bruna R. F. Oliveira, Krisjan Van Laarhoven, Martijn P. J. Smit, et al. “Impact of compost and manure on the ripening of dredged sediments”. In: *Journal of Soils and Sediments* 17 (2017), pp. 567–577.

[94] M. O. Omondi, X. Xia, A. Nahayo, X. Liu, P. K. Korai, and G. Pan. “Quantification of biochar effects on soil hydrological properties using meta-analysis of literature data”. In: *Geoderma* 274 (2016), pp. 28–34.

[95] K. N. Palansooriya, J. T. F. Wong, Y. Hashimoto, L. Huang, J. Rinklebe, S. X. Chang, and Y. S. Ok. “Response of microbial communities to biochar-amended soils: a critical review”. In: *Biochar* 1 (2019), pp. 3–22. DOI: 10.1007/s42773-019-0009-2.

[96] M. Pansu and J. Gautheyrou. *Handbook of Soil Analysis: Mineralogical, Organic, and Inorganic Methods*. Heidelberg, Berlin, Germany: Springer-Verlag, 2006, p. 995. DOI: 10.1007/978-3-540-31211-6.

[97] X. Peng, R. Horn, and A. Smucker. “Pore shrinkage dependency of inorganic and organic soils on wetting and drying cycles”. In: *Soil Science Society of America Journal* 71.4 (2007), pp. 1095–1104. DOI: 10.2136/sssaj2006.0178.

[98] F. N. Ponnamperuma. “The chemistry of submerged soils”. In: *Advances in Agronomy* 24 (1972), pp. 29–96.

[99] L. J. Pons and I. S. Zonneveld. *Soil Ripening and Soil Classification: Initial Soil Formation of Alluvial Deposits with a Classification of the Resulting Soils*. Wageningen, Netherlands: International Institute for Land Reclamation and Improvement, 1965.

[100] T. J. Purakayastha, T. Bera, D. Bhaduri, B. Sarkar, S. Mandal, P. Wade, S. Kumari, S. Biswas, M. Menon, H. Pathak, and D. C. W. Tsang. “A review on biochar modulated soil condition improvements and nutrient dynamics concerning crop yields: Pathways to climate change mitigation and global food security”. In: *Chemosphere* 227 (2019), pp. 345–365. DOI: 10.1016/j.chemosphere.2019.03.170.

[101] Wei Qi, X. Zhang, Y. Wang, L. Chen, and H. Ma. “Experimental investigation on the impact of drying–wetting cycles on the shrink–swell behavior of clay loam in farmland”. In: *Agriculture* 12.2 (2022), p. 245.

[102] M. Qiu, L. Liu, Q. Ling, Y. Cai, S. Yu, S. Wang, and X. Wang. “Biochar for the removal of contaminants from soil and water: a review”. In: *Biochar* 4.1 (2022), p. 19. DOI: 10.1007/s42773-022-00150-5.

[103] R. S. Quilliam, H. C. Glanville, S. C. Wade, and D. L. Jones. “Life in the ‘charosphere’–Does biochar in agricultural soil provide a significant habitat for microorganisms?” In: *Soil Biology and Biochemistry* 65 (2013), pp. 287–293. DOI: 10.1016/j.soilbio.2013.06.004.

[104] A. Rehman, S. Nawaz, H. A. Alghamdi, S. Alrumman, W. Yan, and M. Z. Nawaz. “Effects of manure-based biochar on uptake of nutrients and water holding capacity of different types of soils”. In: *Case Studies in Chemical and Environmental Engineering* 2 (2020), p. 100036. DOI: 10.1016/j.cscee.2020.100036.

[105] K. Rijniersce. “Simulation model for soil ripening in the IJsselmeerpolders (in Dutch)”. PhD thesis. Wageningen, Netherlands: Wageningen Agricultural University, 1983.

[106] P. E. Rijtema, P. Groenendijk, and J. G. Kroes. *Environmental Impact of Land Use in Rural Regions: The Development, Validation and Application of Model Tools for Management and Policy Analysis*. London: Imperial College Press, 1999.

[107] G. P. Robertson and P. M. Groffman. “Nitrogen transformations”. In: *Soil Microbiology, Ecology and Biochemistry*. Ed. by Eldor A. Paul. Elsevier, 2024, pp. 407–438. DOI: 10.1016/B978-0-12-823414-9.00013-9.

[108] J. Rousk, D. N. Dempster, and D. L. Jones. “Transient biochar effects on decomposer microbial growth rates: evidence from two agricultural case-studies”. In: *European Journal of Soil Science* 64.6 (2013), pp. 770–776. DOI: 10.1111/ejss.12065.

[109] Royal Netherlands Meteorological Institute (KNMI). *KNMI Daily Weather Data (Daggegevens van het weer)*. https://daggegevens.knmi.nl/klimatologie/daggegevens. Accessed: 2025-07-12. 2024.

[110] F. Saathoff, S. Cantré, and Z. Sikora. *Application of dredged materials, coal combustion products and geosynthetics in dike construction. South Baltic Guideline*. South Baltic Guideline. n.d.

[111] R. J. Sánchez, D. E. Perrotti, and A. G. P. Fort. “Looking into the future ten years later: Big full containerships and their arrival to South American ports”. In: *Journal of Shipping and Trade* 6.1 (2021), p. 2. DOI: 10.1186/s41072-021-00081-1.

[112] H. P. Schmidt, T. Bucheli, C. Kammann, B. Glaser, S. Abiven, and J. Leifeld. *European biochar certificate – guidelines for a sustainable production of biochar*. European Biochar Foundation. Version 6.1, Arbaz, Switzerland. 2016.

[113] G. C. Sigua, J. M. Novak, D. W. Watts, K. B. Cantrell, P. D. Shumaker, A. A. Szögi, and M. G. Johnson. “Carbon mineralization in two ultisols amended with different sources and particle sizes of pyrolyzed biochar”. In: *Chemosphere* 103 (2014), pp. 313–321. DOI: 10.1016/j.chemosphere.2013.11.049.

[114] B. Singh, M. M. Dolk, Q. Shen, and M. Camps-Arbestain. “Biochar pH, electrical conductivity and liming potential”. In: *Biochar: A Guide to Analytical Methods*. CSIRO Publishing, 2017, p. 23.

[115] S. P. Singh, F. M. G. Tack, and M. G. Verloo. “Land disposal of heavy metal contaminated dredged sediments: a review of environmental aspects”. In: *Land Contamination & Reclamation* 6.3 (1998), pp. 149–158.

[116] J. L. Smith, H. P. Collins, and V. L. Bailey. “The effect of young biochar on soil respiration”. In: *Soil Biology and Biochemistry* 42.12 (2010), pp. 2345–2347. DOI: 10.1016/j.soilbio.2010.09.013.

[117] N. Snoeijink. “An Eco□efficiency analysis of conventional and living dikes”. Highlights material sourcing and transport environmental costs. MA thesis. University of Twente, 2024.

[118] K. A. Spokas, K. B. Cantrell, J. M. Novak, D. W. Archer, J. A. Ippolito, H. P. Collins, and K. A. Nichols. “Biochar: A synthesis of its agronomic impact beyond carbon sequestration”. In: *Journal of Environmental Quality* 41.4 (2012), pp. 973–989. DOI: 10.2134/jeq2011.0069.

[119] Z. Sun, Y. Hu, L. Shi, G. Li, Z. H. E. Pang, S. Liu, and B. Jia. “Effects of biochar on soil chemical properties: A global meta-analysis of agricultural soil”. In: *Plant, Soil and Environment* 68.6 (2022), pp. 272–289.

[120] N. Svensson, A. Norén, O. Modin, K. K. Fedje, S. Rauch, A. M. Strömvall, and Y. Andersson-Sköld. “Integrated cost and environmental impact assessment of management options for dredged sediment”. In: *Waste Management* 138 (2022), pp. 30–40. DOI: 10.1016/j.wasman.2021.11.024.

[121] Z. Tan, C. S. Lin, X. Ji, and T. J. Rainey. “Returning biochar to fields: A review”. In: *Applied Soil Ecology* 116 (2017), pp. 1–11. DOI: 10.1016/j.apsoil.2017.03.017.

[122] J. E. Thies and M. C. Rillig. “Characteristics of biochar: biological properties”. In: *Biochar for Environmental Management*. Ed. by J. Lehmann and S. Joseph. Routledge, 2012, pp. 117–138.

[123] A. Tomczyk, Z. Sokołowska, and P. Boguta. “Biochar physicochemical properties: pyrolysis temperature and feedstock kind effects”. In: *Reviews in Environmental Science and Bio/Technology* 19.1 (2020), pp. 191–215. DOI: 10.1007/s11157-020-09523-3.

[124] S. Tresch and A. Fliessbach. *Decomposition study using tea bags*. Unpublished study. 2016.

[125] USDA Natural Resources Conservation Service. *Soil Electrical Conductivity*. Accessed: 2025-05-30. 2012. URL: https://www.nrcs.usda.gov/sites/default/files/2022-10/Soil%20Electrical%20Conductivity.pdf.

[126] J. M. Van Loon-Steensma and P. Vellinga. “How “wide green dikes” were reintroduced in The Netherlands: a case study of the uptake of an innovative measure in long-term strategic delta planning”. In: *Journal of Environmental Planning and Management* 62.9 (2019), pp. 1525–1544. DOI: 10.1080/09640568.2018.1519041.

[127] M. VanKoningsveld, J. P. Mulder, M. J. Stive, L. VanDerValk, and A. W. VanDerWeck. “Living with sea-level rise and climate change: a case study of the Netherlands”. In: *Journal of Coastal Research* 24.2 (2008), pp. 367–379.

[128] J. Vermeulen, T. Grotenhuis, J. Joziasse, and W. Rulkens. “Ripening of clayey dredged sediments during temporary upland disposal: a bioremediation technique”. In: *Journal of Soils and Sediments* 3 (2003), pp. 49–59.

[129] J. Vermeulen, S. G. Van Dijk, and J. T. C. Grotenhuis. “Quantification of physical properties of dredged sediments during physical ripening”. In: *Geoderma* 129.3–4 (2005), pp. 147–166.

[130] J. Vermeulen, M. P. Van Gool, A. S. Dorleijn, J. Joziasse, H. Bruning, W. H. Rulkens, and J. T. C. Grotenhuis. “Biochemical ripening of dredged sediments. Part 1. Kinetics of biological organic matter mineralization and chemical sulfur oxidation”. In: *Environmental Toxicology and Chemistry* 26.12 (2007), pp. 2530–2539.

[131] V. Vijay, S. Shreedhar, K. Adlak, S. Payyanad, V. Sreedharan, G. Gopi, and P. V. Aravind. “Review of large-scale biochar field-trials for soil amendment and the observed influences on crop yield variations”. In: *Frontiers in Energy Research* 9 (2021), p. 710766.

[132] J. Wang, Z. Xiong, and Y. Kuzyakov. “Biochar stability in soil: meta analysis of decomposition and priming effects”. In: *GCB Bioenergy* 8.3 (2016), pp. 512–523. DOI: 10.1111/gcbb.12266.

[133] Z. Wang, Y. Li, S. X. Chang, J. Zhang, P. Jiang, G. Zhou, and Z. Shen. “Contrasting effects of bamboo leaf and its biochar on soil CO_2 efflux and labile organic carbon in an intensively managed Chinese chestnut plantation”. In: *Biology and Fertility of Soils* 50 (2014), pp. 1109–1119. DOI: 10.1007/s00374-014-0934-5.

[134] C. Wei, W. Gao, and B. Li. “Shrinkage characteristics of lime concretion black soil as affected by biochar amendment”. In: *Pedosphere* 28.5 (2018), pp. 713–725. DOI: 10.1016/S1002-0160(17)60445-6.

[135] N. Wrage, G. L. Velthof, M. L. van Beusichem, and O. Oenema. “Role of nitrifier denitrification in the production of nitrous oxide”. In: *Soil Biology and Biochemistry* 33 (2001), pp. 1723–1732.

[136] Y. Yang, S. Ye, C. Zhang, G. Zeng, X. Tan, B. Song, and Q. Chen. “Application of biochar for the remediation of polluted sediments”. In: *Journal of Hazardous Materials* 404 (2021), p. 124052. DOI: 10.1016/j.jhazmat.2020.124052.

[137] S. Yi, B. Witt, P. Chiu, M. Guo, and P. Imhoff. “The origin and reversible nature of poultry litter biochar hydrophobicity”. In: *Journal of Environmental Quality* 44.3 (2015), pp. 963–971. DOI: 10.2134/jeq2014.07.0303.

[138] C. Yip, P. D. Weyman, K. A. Wemmer, Y. Y. Yang, A. Chowdhury, B. A. Traag, and G. Fuenzalida-Meriz. “Quantification of soil inorganic carbon using sulfamic acid and gas chromatography”. In: *PLoS One* 20.5 (2025), e0320778. DOI: 10.1371/journal.pone.0320778.

[139] X. Zhang, H. Wang, L. He, K. Lu, A. Sarmah, J. Li, and H. Huang. “Using biochar for remediation of soils contaminated with heavy metals and organic pollutants”. In: *Environmental Science and Pollution Research* 20.12 (2013), pp. 8472–8483. DOI: 10.1007/s11356-013-1659-0.

[140] X. Zhang, Q. Zhou, L. Wang, B. Wan, and Q. Yang. “How Biochar Addition Affects Denitrification and the Microbial Electron Transport System (ETSA): A Meta-Analysis Based on a Global Scale”. In: *Agriculture* 14.12 (2024), p. 2320. DOI: 10.3390/agriculture14122320.

[141] Y. Zhang, J. Wang, and Y. Feng. “The effects of biochar addition on soil physicochemical properties: A review”. In: *Catena* 202 (2021), p. 105284. DOI: 10.1016/j.catena.2021.105284.

[142] C. Zhao, V. V. Gupta, F. Degryse, and M. J. McLaughlin. “Effects of pH and ionic strength on elemental sulphur oxidation in soil”. In: *Biology and Fertility of Soils* 53.2 (2017), pp. 247–256. DOI: 10.1007/s00374-016-1166-5.

[143] L. Zhao, X. Cao, O. Mašek, and A. Zimmerman. “Heterogeneity of biochar properties as a function of feedstock sources and production temperatures”. In: *Journal of Hazardous Materials* 256 (2013), pp. 1–9.

[144] X. Zhao, Y. Liu, L. Xie, X. Fu, L. Wang, M. T. Gao, and J. Hu. “Biochar promotes microbial CO_2 fixation by regulating feedback inhibition of metabolites”. In: *Bioresource Technology* 406 (2024), p. 130990. DOI: 10.1016/j.biortech.2024.130990.

[145] G. Zhou, X. Zhou, T. Zhang, Z. Du, Y. He, X. Wang, J. Wang, G. Han, C. Wang, and C. Xu. “Biochar increased soil respiration in temperate forests but had no effects in subtropical forests”. In: *Forest Ecology and Management* 405 (2017), pp. 339–349. DOI: 10.1016/j.foreco.2017.09.053.

[146] A. R. Zimmerman, B. Gao, and M.-Y. Ahn. “Positive and negative carbon mineralization priming effects among a variety of biochar-amended soils”. In: *Soil Biology and Biochemistry* 43 (2011), pp. 1169–1179. DOI: 10.1016/j.soilbio.2011.02.005.

[147] Y. Zong, D. Chen, and S. Lu. “Impact of biochars on swell–shrinkage behavior, mechanical strength, and surface cracking of clayey soil”. In: *Journal of Plant Nutrition and Soil Science* 177.6 (2014), pp. 920–926. DOI: 10.1002/jpln.201300455.

[148] H. Zu, Z. Deng, X. Liu, J. Luo, Y. Chen, M. Yi, and W. Yan. “Effects of biochar on soil respiration mediated by rainfall events: evidence from one-year field experiment in an urban forest”. In: *Ecological Processes* 14.1 (2025), p. 1. DOI: 10.1186/s13717-024-00571-z.

A

Methodology

A.1. Gas Chromatograph Operation

Outlined below is the GC operation procedure:

1. Check the pressure of the helium gas tank, which should be around 30 bar, and the pressure of the gas running through the GC, slightly above 5 bar;
2. Turn on the GC and the computer;
3. Select the ”BIOMUD_LOW_20240124(THE BEST).met” method, which is appropriate for samples within a 0-14% range of CO_2 or CH_4;
4. Let the GC equilibrate by running it with lab air and the calibration gases if necessary and verify that the values are within the expected range;
5. Proceed with respiration measurements by injecting approximately 1.5 mL of each sample.

A.2. Respiration Calculation

$$V_{CO_2} = V_{hs} \times [CO_2]_{corrected} \tag{A.1}$$

Where:

- V_{CO_2} — volume of gaseous CO_2 in the bottle,
- V_{hs} — headspace volume in the bottle (L),
- $[CO_2]_{\text{corrected}}$ — adjusted CO_2 content (%).

$$n_{CO_2} = \frac{P_{sample} \times V_{CO_2}}{R \times T} \tag{A.2}$$

Where:

- n_{CO_2}: amount of CO_2 in sample (mol),
- P_{sample}: pressure measured (Pa),
- R: gas constant 8.3144 (J/mol . K),
- T: temperature (K).

$$C_{gas} = \frac{n_{CO_2} \times MM_C \times 1000}{DM} \tag{A.3}$$

Where:

- C_{gas}: amount of gaseous carbon (mg C / g DW)
- MM_C: molar mass of carbon 12 (g/mol)

- DM: dry mass of sample (g)

$$PP_{CO_2} = P_{sample} \times [CO_2]_{corrected} \tag{A.4}$$

Where:

- PP_{CO_2}: Partial pressure of CO_2 (Pa).

$$Henry_{eff} = 1.82533e-10 \times exp^{-pH/-0.43293} + 3.94288e-4 \tag{A.5}$$

Where:

- $Henry_{eff}$: Effective Henry's coefficient.

$$Ca = PP_{CO_2} \times Henry_{eff} \tag{A.6}$$

Where:

- Ca: (mol/m^3),
- $Henry_{eff}$: Effective Henry's coefficient.

$$DIC = \frac{Ca \times MM_C \times V_w}{1000 \times DM} \tag{A.7}$$

Where:

- DIC: Dissolved inorganic carbon (mg C/ g DW),
- V_w: Volume of water (L).

$$C_{Total} = C_{gas} + DIC \tag{A.8}$$

Where:

- C_{Total}: Total carbon (mg C/ g DW).

A.3. Total Inorganic Carbon

$$V_{CO_2} = \frac{V_{bottle} \times [CO_2]_{corrected}/100}{1 - [CO_2]_{corrected}/100} \tag{A.9}$$

Where:

- V_{CO_2}: volume of gaseous CO_2 in the bottle (mL),
- V_{bottle}: bottle volume (mL),
- $[CO_2]_{corrected}$: adjusted CO_2 content (%).

$$C_{abs} = V_{CO_2} \times \frac{MM_C}{V_m} \tag{A.10}$$

Where:

- C_{abs}: absolute amount of released carbon (mg),
- MM_C: molar mass of carbon 12 (g/mol),
- V_m: molar volume of gas (22.41 m^3/mol).

$$C_{ant} = C_{abs} \times \frac{100}{DM} \tag{A.11}$$

Where:

- C_{ant}: concentration of released carbon (% DM).

$$mol_{CO_2} = V_{bottle} \times \frac{P_{sample}}{10 \times R \times T} \times [CO_2]_{corrected} \tag{A.12}$$

Where:

- mol_{CO_2}: carbon dioxide (mol),
- T: temperature (K),
- R: gas constant 8.3144 (J/mol . K),
- P_{sample}: pressure measured (hPa).

$$C = mol_{CO_2} \times \frac{MM_C}{1000} \tag{A.13}$$

Where:

- C: mass of carbon (mg).

$$TIC = C \times \frac{100}{DM} \tag{A.14}$$

Where:

- TIC: Total inorganic carbon (% DM).

B

Results

B.1. Respiration curve fitting

Week	Base_Sample	Label	A1	t1	y0	R2	y_32
0	OM	OM	-0.801	38.243	0.806	1.000	0.459
1	A1	2% Fine	-0.556	21.454	0.559	0.998	0.434
1	A2	2% Medium	-0.562	24.275	0.567	0.998	0.417
1	A3	2% Coarse	-0.582	26.299	0.589	0.997	0.417
1	B1	4% Fine	-0.602	30.261	0.628	0.977	0.418
1	B2	4% Medium	-0.825	33.574	0.840	0.995	0.522
1	B3	4% Coarse	-0.782	38.368	0.787	0.998	0.447
1	C1	6% Fine	-0.887	44.868	0.920	0.975	0.485
1	C2	6% Medium	-1.028	42.951	1.042	0.996	0.554
1	C3	6% Coarse	-0.817	36.498	0.835	0.993	0.495
1	Control	Control	-0.819	42.017	0.831	0.996	0.449
2	A1	2% Fine	-1.109	56.518	1.133	0.994	0.504
2	A2	2% Medium	-1.088	54.961	1.112	0.993	0.504
2	A3	2% Coarse	-1.076	61.443	1.104	0.990	0.464
2	B1	4% Fine	-1.047	67.594	1.071	0.991	0.419
2	B2	4% Medium	-1.175	64.371	1.202	0.992	0.487
2	B3	4% Coarse	-1.068	65.335	1.086	0.995	0.432
2	C1	6% Fine	-1.268	72.249	1.293	0.994	0.479
2	C2	6% Medium	-1.196	73.927	1.223	0.993	0.447
2	C3	6% Coarse	-1.246	82.720	1.266	0.995	0.419
2	Control	Control	-0.995	45.364	1.015	0.995	0.523
5	A1	2% Fine	-0.584	88.116	0.591	0.995	0.184
5	A2	2% Medium	-0.756	122.074	0.763	0.995	0.181
5	A3	2% Coarse	-0.445	65.825	0.451	0.994	0.178
5	B1	4% Fine	-0.853	143.374	0.860	0.996	0.177
5	B2	4% Medium	-0.887	123.677	0.896	0.994	0.211
5	B3	4% Coarse	-2.055	323.225	2.062	0.996	0.201
5	C1	6% Fine	-1503.034	233339.140	1503.041	0.995	0.213
5	C2	6% Medium	-1.304	199.381	1.314	0.994	0.203
5	C3	6% Coarse	-0.930	168.589	0.936	0.996	0.166
5	Control	Control	-7.020	1058.593	7.028	0.996	0.218

Table B.1: Respiration Curve Fitting Parameters

B.2. Field Respiration

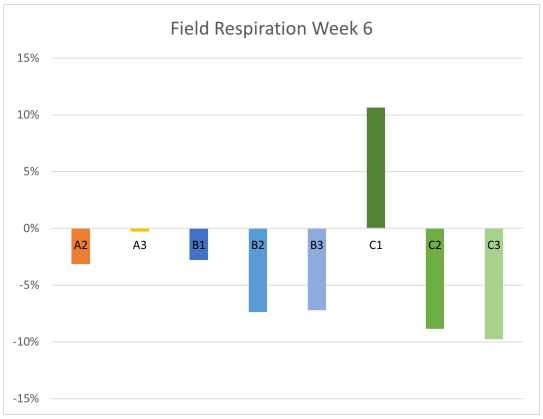

(a) Field Respiration Week 6

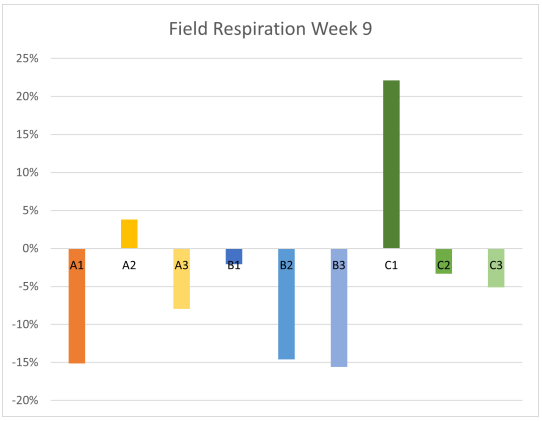

(b) Field Respiration Week 9

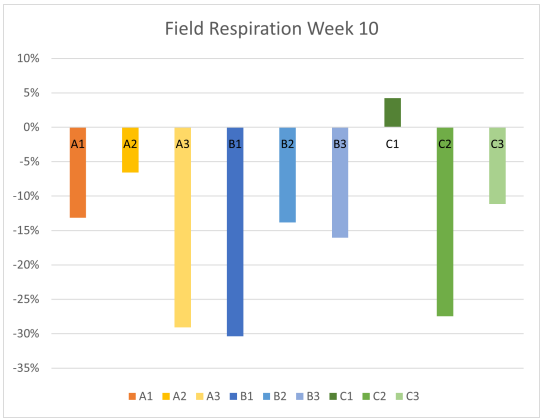

(c) Field Respiration Week 10

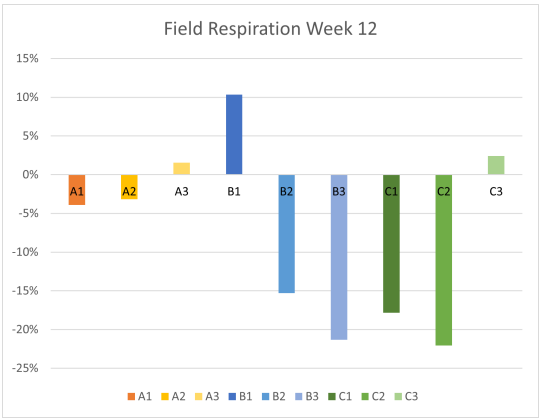

(d) Field Respiration Week 12

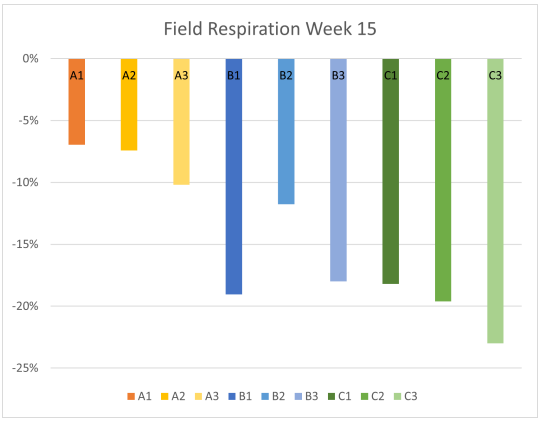

(e) Field Respiration Week 15

Figure B.1: Respiration rate in field relative to control for Weeks 6, 9, 10, 12 and 15 (A1: 2%-fine, A2: 2%-medium, A3: 2%-coarse, B1: 4%-fine, B2: 4%-medium, B3: 4%-coarse, C1: 6%-fine, C2: 6%-medium, C3: 6%-coarse, Control)

B.3. Teabag Index Results

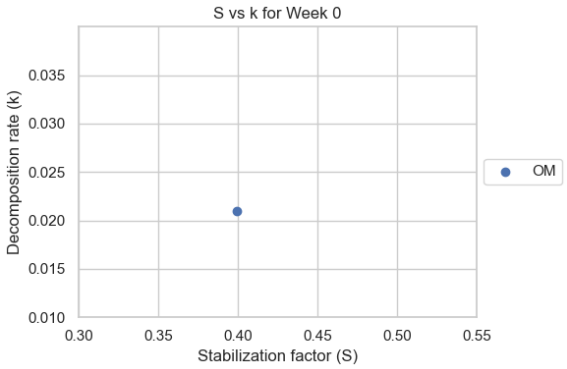

(a) S and k values of Week 1 Samples on Day 38

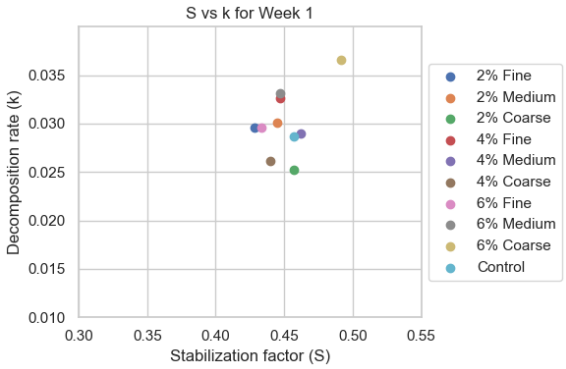

(b) S and k values of Week 1 Samples

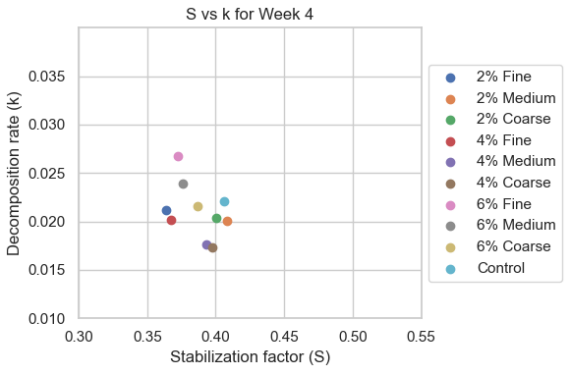

(c) S and k values of Week 4 Samples

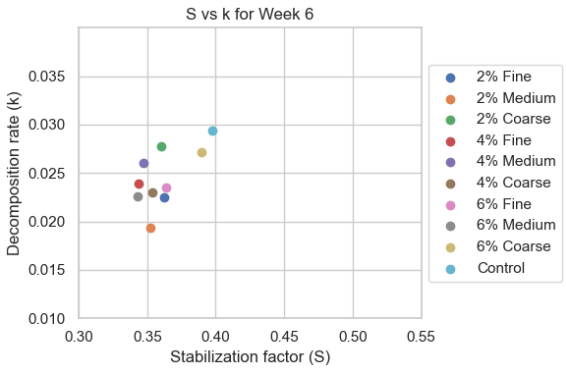

(d) S and k values of Week 6 Samples

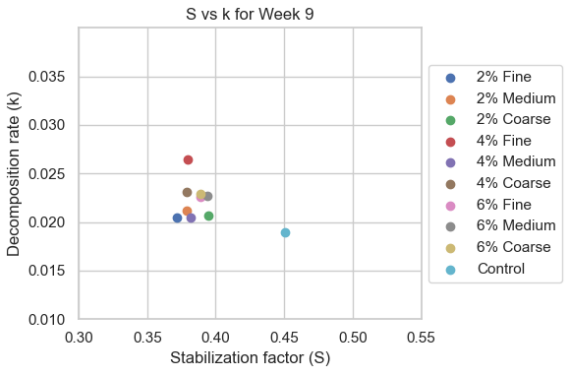

(e) S and k values of Week 9 Samples

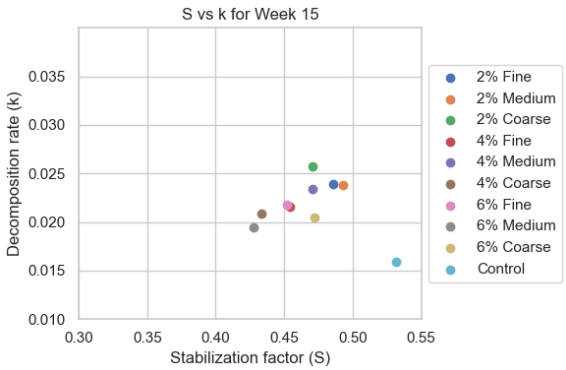

(f) S and k values of Week 15 Samples

Figure B.2: Stabilization Factor and Decomposition Rate Values of Week 1, 4, 6, 9, and 15 Samples

B.4. Elemental Analysis

[H]

Sample	N [%]	C [%]	H [%]	S [%]	C/N ratio	C/H ratio	N Factor	C Factor	H Factor	S Factor	TIC [%]	TOC [%]
A1	0.29	5.65	0.644	0.444	19.3381	8.7727	1.0193	0.9715	1.0034	1.1709	0.885014	4.459986
A1	0.29	5.04	0.648	0.439	17.3347	7.7869	1.0193	0.9715	1.0034	1.1709		
A2	0.31	5.72	0.643	0.455	18.5989	8.9043	1.0169	0.9372	1.0532	1.0873	0.91735	5.15765
A2	0.3	5.66	0.643	0.382	18.683	8.8081	1.0169	0.9372	1.0532	1.0873		
A3	0.29	6.92	0.599	0.306	24.2808	11.5525	1.0169	0.9372	1.0532	1.0873	0.72687	6.73813
A3	0.29	7.07	0.614	0.379	24.1402	11.5077	1.0169	0.9372	1.0532	1.0873		
B1	0.28	7.55	0.586	0.323	27.0941	12.8756	1.0169	0.9372	1.0532	1.0873	0.825503	7.304497
B1	0.28	7.68	0.597	0.288	27.4781	12.8589	1.0169	0.9372	1.0532	1.0873		
B2	0.32	7.59	0.672	0.437	23.8837	11.2968	1.0169	0.9372	1.0532	1.0873	0.948532	7.076468
B2	0.31	7.45	0.662	0.362	24.1456	11.2634	1.0169	0.9372	1.0532	1.0873		
B3	0.32	7.46	0.703	0.361	23.6024	10.6146	1.0145	0.9332	1.0637	1.048	0.894437	4.155563
B3	0.3	6.86	0.657	0.323	23.109	10.4472	1.0145	0.9332	1.0637	1.048		
C1	0.31	13.61	0.751	0.426	43.6146	18.1295	1.0193	0.9715	1.0034	1.1709	0.926251	12.74875
C1	0.31	13.74	0.766	0.412	44.3907	17.9475	1.0193	0.9715	1.0034	1.1709		
C2	0.29	10.31	0.683	0.386	35.556	15.1081	1.0193	0.9715	1.0034	1.1709	0.860508	9.384492
C2	0.29	10.18	0.683	0.382	35.35	14.9179	1.0193	0.9715	1.0034	1.1709		
C3	0.29	9.88	0.66	0.388	34.4508	14.9807	1.0193	0.9715	1.0034	1.1709	0.84902	8.86098
C3	0.28	9.54	0.641	0.386	34.2729	14.8733	1.0193	0.9715	1.0034	1.1709		
Control	0.29	3.38	0.602	0.428	11.7493	5.6122	1.0193	0.9715	1.0034	1.1709	0.84916	2.52584
Control	0.28	3.37	0.606	0.423	11.9108	5.5693	1.0193	0.9715	1.0034	1.1709		

Table B.2: Week 1 CHNS Results

Sample	N [%]	C [%]	H [%]	S [%]	C/N ratio	C/H ratio	N Factor	C Factor	H Factor	S Factor	TIC [%]	TOC [%]
A1	0.26	4.14	0.555	0.353	15.8377	7.4557	1.0193	0.9715	1.0034	1.1709	0.865929	3.424071
A1	0.28	4.44	0.603	0.393	16.0743	7.3706	1.0193	0.9715	1.0034	1.1709		
A2	0.27	4.87	0.606	0.371	17.7728	8.0427	1.0193	0.9715	1.0034	1.1709	0.891929	4.018071
A2	0.28	4.95	0.605	0.398	17.8145	8.1887	1.0193	0.9715	1.0034	1.1709		
A3	0.27	5.77	0.624	0.375	21.0576	9.2441	1.0193	0.9715	1.0034	1.1709	0.827338	4.972662
A3	0.29	5.83	0.629	0.404	20.2517	9.2719	1.0193	0.9715	1.0034	1.1709		
B1	0.27	6.02	0.596	0.363	22.6607	10.1043	1.0193	0.9715	1.0034	1.1709	0.810978	4.934022
B1	0.25	5.47	0.56	0.347	21.4645	9.7743	1.0193	0.9715	1.0034	1.1709		
B2	0.29	6.85	0.657	0.398	23.6911	10.4218	1.0193	0.9715	1.0034	1.1709	0.883317	5.851683
B2	0.29	6.62	0.632	0.399	23.1	10.4712	1.0193	0.9715	1.0034	1.1709		
B3	0.3	8.69	0.707	0.414	28.8704	12.292	1.0193	0.9715	1.0034	1.1709	0.794996	7.760004
B3	0.3	8.42	0.697	0.397	28.4931	12.0845	1.0193	0.9715	1.0034	1.1709		
C1	0.31	9.51	0.734	0.43	30.2201	12.9632	1.0193	0.9715	1.0034	1.1709	0.949206	8.420794
C1	0.3	9.23	0.727	0.436	30.3302	12.6822	1.0193	0.9715	1.0034	1.1709		
C2	0.29	9.45	0.697	0.386	32.4687	13.5546	1.0193	0.9715	1.0034	1.1709	0.850872	8.749128
C2	0.3	9.75	0.718	0.413	32.7382	13.5792	1.0193	0.9715	1.0034	1.1709		
C3	0.29	9.73	0.698	0.401	33.1661	13.9455	1.0193	0.9715	1.0034	1.1709	0.832789	8.847211
C3	0.3	9.63	0.716	0.403	31.8552	13.4504	1.0193	0.9715	1.0034	1.1709		
Control	0.29	3.43	0.621	0.396	11.9712	5.5232	1.0193	0.9715	1.0034	1.1709	0.851485	2.663515
Control	0.3	3.6	0.659	0.428	12.061	5.4639	1.0193	0.9715	1.0034	1.1709		

Table B.3: Week 2 CHNS Results

Sample	N [%]	C [%]	H [%]	S [%]	C/N ratio	C/H ratio	N Factor	C Factor	H Factor	S Factor	TIC [%]	TOC [%]
A1	0.25	4.02	0.556	0.32	15.8201	7.2331	1.0293	0.95	1.0292	1.1801	0.649184	3.580816
A1	0.26	4.44	0.574	0.355	17.2921	7.7383	1.0293	0.95	1.0292	1.1801		
A2	0.25	3.89	0.545	0.227	15.8566	7.1327	1.0293	0.95	1.0292	1.1801	0.701724	3.463276
A2	0.25	4.44	0.571	0.288	17.6489	7.7827	1.0293	0.95	1.0292	1.1801		
A3	0.28	5.46	0.626	0.391	19.7952	8.7265	1.0293	0.95	1.0292	1.1801	0.753668	4.711332
A3	0.26	5.47	0.601	0.294	21.163	9.103	1.0293	0.95	1.0292	1.1801		
B1	0.26	5.02	0.566	0.336	19.6328	8.8735	1.0195	0.9625	0.9703	1.1397	0.737677	4.337323
B1	0.25	5.13	0.55	0.35	20.9173	9.327	1.0195	0.9625	0.9703	1.1397		
B2	0.28	6.82	0.641	0.313	24.5766	10.6474	1.0195	0.9625	0.9703	1.1397	0.782923	5.722077
B2	0.28	6.19	0.633	0.36	22.3906	9.7785	1.0195	0.9625	0.9703	1.1397		
B3	0.24	6.34	0.542	0.354	26.6846	11.6896	1.0195	0.9625	0.9703	1.1397	0.778049	5.886951
B3	0.26	6.99	0.598	0.367	27.2163	11.6797	1.0195	0.9625	0.9703	1.1397		
C1	0.32	8.72	0.748	0.39	27.5772	11.6603	1.0195	0.9625	0.9703	1.1397	0.883912	7.561088
C1	0.31	8.17	0.728	0.405	26.517	11.2245	1.0195	0.9625	0.9703	1.1397		
C2	0.28	8.13	0.663	0.369	29.188	12.2633	1.0195	0.9625	0.9703	1.1397	0.803561	7.286439
C2	0.29	8.05	0.675	0.382	28.2137	11.9258	1.0195	0.9625	0.9703	1.1397		
C3	0.25	7.93	0.584	0.333	32.0101	13.5873	1.0195	0.9625	0.9703	1.1397	0.785456	6.744544
C3	0.23	7.13	0.534	0.313	31.1988	13.3356	1.0195	0.9625	0.9703	1.1397		
Control	0.29	3.37	0.604	0.344	11.5764	5.577	1.0195	0.9625	0.9703	1.1397	0.643299	2.721701
Control	0.28	3.36	0.593	0.318	11.942	5.6674	1.0195	0.9625	0.9703	1.1397		

Table B.4: Week 5 CHNS Results

Sample	N [%]	C [%]	H [%]	S [%]	C/N ratio	C/H ratio	N Factor	C Factor	H Factor	S Factor	TIC [%]	TOC [%]
A1	0.27	4.93	0.614	0.31	18.2764	8.0304	1.0195	0.9625	0.9703	1.1397	0.82917	4.39583
A1	0.28	5.13	0.637	0.302	18.065	8.0535	1.0195	0.9625	0.9703	1.1397		
A2	0.28	4.81	0.633	0.355	16.9245	7.5985	1.0195	0.9625	0.9703	1.1397	0.81183	4.10817
A2	0.28	4.66	0.619	0.372	16.738	7.5216	1.0195	0.9625	0.9703	1.1397		
A3	0.27	6.13	0.634	0.383	22.4797	9.6667	1.0195	0.9625	0.9703	1.1397	0.797595	5.687405
A3	0.28	6.35	0.654	0.384	22.8984	9.7213	1.0195	0.9625	0.9703	1.1397		
B1	2.73	8.8	0.051	1.429	3.2166	174.072	1.0195	0.9625	0.9703	1.1397	0.820954	6.429046
B1	0.28	6.74	0.635	0.385	24.069	10.6132	1.0193	0.9715	1.0034	1.1709		
B2	0.29	7.06	0.758	0.356	23.9606	9.3126	1.0293	0.95	1.0292	1.1801	0.90439	6.21561
B2	0.29	7.18	0.727	0.407	24.4959	9.8679	1.0293	0.95	1.0292	1.1801		
B3	0.29	10.67	0.783	0.39	36.2878	13.6258	1.0293	0.95	1.0292	1.1801	0.800139	9.789861
B3	0.3	10.51	0.766	0.408	35.4827	13.7234	1.0293	0.95	1.0292	1.1801		
C1	0.33	15.65	0.923	0.428	46.9399	16.9563	1.0293	0.95	1.0292	1.1801	0.875081	14.81492
C1	0.33	15.73	0.932	0.418	47.5468	16.8704	1.0293	0.95	1.0292	1.1801		
C2	0.26	7.81	0.669	0.309	29.5494	11.6739	1.0293	0.95	1.0292	1.1801	0.819139	7.140861
C2	0.26	8.11	0.668	0.377	30.5905	12.1346	1.0293	0.95	1.0292	1.1801		
C3	0.28	9.47	0.715	0.302	34.3456	13.2573	1.0293	0.95	1.0292	1.1801	0.769852	8.595148
C3	0.28	9.26	0.703	0.385	33.5388	13.174	1.0293	0.95	1.0292	1.1801		
Control	0.27	3.19	0.566	0.384	11.832	5.6319	1.0193	0.9715	1.0034	1.1709	0.796635	2.380865
Control	0.26	3.13	0.567	0.37	12.0219	5.5216	1.0193	0.9715	1.0034	1.1709		

Table B.5: Week 6 CHNS Results

Sample	N [%]	C [%]	H [%]	S [%]	C/N ratio	C/H ratio	N Factor	C Factor	H Factor	S Factor	TIC [%]	TOC [%]
A1	0.28	5.1	0.605	0.328	18.4065	8.4205	1.0145	0.9332	1.0637	1.048	0.800896	4.334104
A1	0.28	5.17	0.614	0.322	18.2622	8.4197	1.0145	0.9332	1.0637	1.048		
A2	0.3	6.57	0.67	0.311	22.0384	9.795	1.0145	0.9332	1.0637	1.048	0.495253	6.119747
A2	0.3	6.66	0.657	0.351	22.3036	10.1461	1.0145	0.9332	1.0637	1.048		
A3	0.28	5.81	0.63	0.349	20.4088	9.2362	1.0145	0.9332	1.0637	1.048	0.813857	5.076143
A3	0.3	5.97	0.656	0.372	20.1305	9.1068	1.0145	0.9332	1.0637	1.048		
B1	0.29	8.22	0.633	0.336	28.5814	12.9827	1.0145	0.9332	1.0637	1.048	0.863675	7.496325
B1	0.29	8.5	0.652	0.331	29.4321	13.0484	1.0145	0.9332	1.0637	1.048		
B2	0.29	7.83	0.65	0.325	26.7583	12.0523	1.0145	0.9332	1.0637	1.048	0.877868	7.362132
B2	0.3	8.04	0.671	0.352	27.0991	11.9773	1.0145	0.9332	1.0637	1.048		
B3	0.27	8.72	0.632	0.393	32.0999	13.78	1.0193	0.9715	1.0034	1.1709	0.905334	10.06967
B3	0.27	8.37	0.628	0.402	31.3631	13.3326	1.0193	0.9715	1.0034	1.1709		
C1	0.31	12.48	0.812	0.419	39.7115	15.3641	1.0293	0.95	1.0292	1.1801	0.931492	11.49851
C1	0.31	12.38	0.829	0.341	40.3393	14.9328	1.0293	0.95	1.0292	1.1801		
C2	0.28	7.4	0.689	0.42	26.0641	10.7367	1.0293	0.95	1.0292	1.1801	0.90115	6.46885
C2	0.28	7.34	0.682	0.318	26.3334	10.7586	1.0293	0.95	1.0292	1.1801		
C3	0.27	7.33	0.661	0.424	26.9887	11.1013	1.0293	0.95	1.0292	1.1801	0.830586	6.194414
C3	0.25	6.72	0.622	0.352	26.38	10.8117	1.0293	0.95	1.0292	1.1801		
Control	0.27	3.17	0.594	0.339	11.6456	5.3376	1.0145	0.9332	1.0637	1.048	0.908494	2.281506
Control	0.29	3.21	0.621	0.341	11.1676	5.1654	1.0145	0.9332	1.0637	1.048		

Table B.6: Week 9 CHNS Results

Sample	N [%]	C [%]	H [%]	S [%]	C/N ratio	C/H ratio	N Factor	C Factor	H Factor	S Factor	TIC [%]	TOC [%]
A1	0.29	5.18	0.716	0.349	17.6135	7.2266	1.0193	0.9715	1.0034	1.1709	0.851567	4.678433
A1	0.29	5.88	0.71	0.366	19.9993	8.2825	1.0193	0.9715	1.0034	1.1709		
A2	0.28	5.52	0.66	0.361	19.8927	8.3557	1.0193	0.9715	1.0034	1.1709	0.800323	4.539677
A2	0.28	5.16	0.646	0.386	18.3294	7.9832	1.0193	0.9715	1.0034	1.1709		
A3	0.27	5.51	0.632	0.36	20.2838	8.7104	1.0193	0.9715	1.0034	1.1709	0.489787	5.220213
A3	0.28	5.91	0.654	0.355	21.4545	9.0325	1.0193	0.9715	1.0034	1.1709		
B1	0.28	7.97	0.712	0.338	28.5462	11.1937	1.0193	0.9715	1.0034	1.1709	0.829953	6.840047
B1	0.27	7.37	0.645	0.324	27.6436	11.4247	1.0193	0.9715	1.0034	1.1709		
B2	0.31	10.01	0.784	0.37	32.0349	12.778	1.0193	0.9715	1.0034	1.1709	0.906135	8.033865
B2	0.32	7.87	0.764	0.412	24.6987	10.3031	1.0193	0.9715	1.0034	1.1709		
B3	0.29	10.53	0.708	0.379	36.5088	14.8727	1.0193	0.9715	1.0034	1.1709	0.82628	8.73372
B3	0.27	8.59	0.668	0.357	32.1589	12.8645	1.0193	0.9715	1.0034	1.1709		
C1	0.3	9.84	0.737	0.358	33.2107	13.3479	1.0193	0.9715	1.0034	1.1709	0.890927	9.274073
C1	0.3	10.49	0.758	0.385	34.5706	13.8418	1.0193	0.9715	1.0034	1.1709		
C2	0.27	7.68	0.655	0.375	27.9416	11.7154	1.0193	0.9715	1.0034	1.1709	0.748882	6.941118
C2	0.28	7.7	0.659	0.353	27.6687	11.689	1.0193	0.9715	1.0034	1.1709		
C3	0.27	9.77	0.67	0.353	35.5842	14.5794	1.0193	0.9715	1.0034	1.1709	0.782498	8.857502
C3	0.27	9.51	0.649	0.36	35.0325	14.6419	1.0193	0.9715	1.0034	1.1709		
Control	0.27	3.3	0.607	0.33	12.0122	5.4367	1.0193	0.9715	1.0034	1.1709	0.800181	2.539819
Control	0.28	3.38	0.615	0.37	11.924	5.4998	1.0193	0.9715	1.0034	1.1709		

Table B.7: Week 15 CHNS Results

C

Statistical Analysis

The statistical analysis of the parameters which presented significant correlations (p <0.05) to application rate or particle size is presented in this document. The equations of the fits are shown in C.3, which have the form $y = A \times Rate + B \times Size + p$. In this equation, $Rate$ takes a value of 2-4% and $Size$ ranges from -1 to 0 (where -1: fine, 0: medium, 1: coarse).

Parameter	Moisture content	COLE (mould)	pH	EC	TOC	k
Std. Dev.	0.0248	0.6297	0.051	0.1294	1.14	0.0017
Mean	0.1536	3.9	7.73	1.15	7.01	0.0217
C.V.	16.13	16.16	0.66	11.22	16.26	7.68
R^2	0.5316	0.7532	0.8451	0.7849	0.7144	0.7618
Adjusted R^2	0.3754	0.6709	0.7935	0.7133	0.6192	0.6824
Predicted R^2	-0.0631	0.3593	0.5816	0.6049	0.4323	0.3865
Adeq Precision	4.5803	8.3252	10.0728	8.4199	6.4045	7.0023

Table C.1: Fit statistics of the statistically significant week 15 system responses calculated with Stat.Ease

Parameter	Moisture content	COLE (mould)	pH	EC	TOC	k
Application rate p-value	0.0463	0.0661	**0.0015**	**0.0045**	**0.0089**	**0.0049**
Particle size p-value	0.4901	**0.0108**	0.152	0.1764	0.4971	0.5614

Table C.2: P-values of the application rate and particle size of the week 15 responses calculated with Stat.Ease (p <0.05 in **bold**)

Parameter	Moisture content	COLE (mould)	pH	EC	TOC	k
Intercept (p)	0.102942	5.04889	7.50111	0.685667	3.46839	0.027568
Rate coefficient (A)	0.012666	-0.288333	0.057083	0.116792	0.886198	-0.001474
Size coefficient (B)	-0.007435	-0.936667	0.034167	0.080917	0.33648	-0.000418

Table C.3: Equations of the statistically significant week 15 system responses calculated with Stat.Ease

D

Field Photos

Presented in this document are the photos taken of each experimental variant over the course of the 15 week field ripening period. The images were all scaled to the length of a ruler.

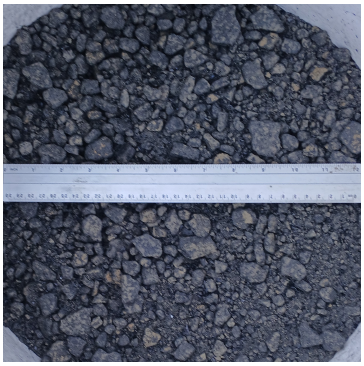

(a) A1: 2% Fine

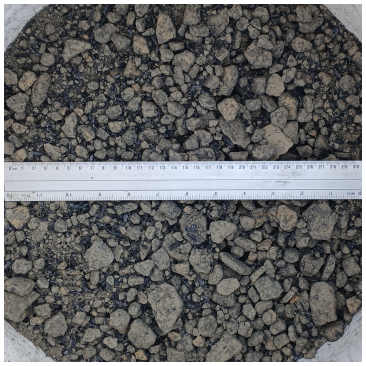

(b) A2: 2% Medium

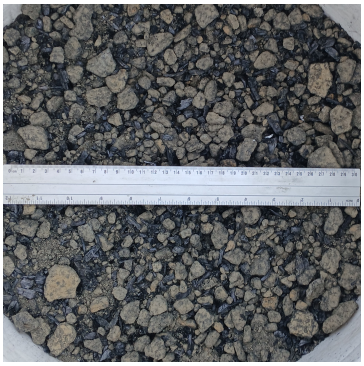

(c) A3: 2% Coarse

(d) B1: 4% Fine

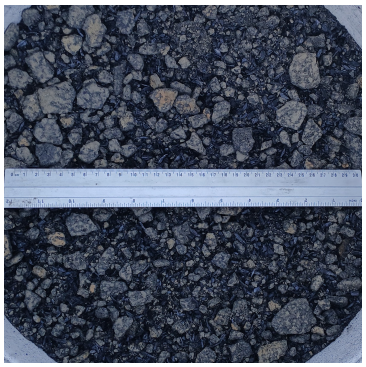

(e) B2: 4% Medium

(f) B3: 4% Coarse

(g) C1: 6% Fine

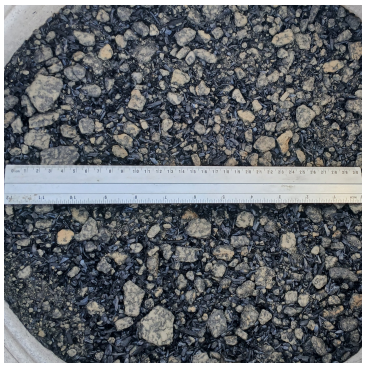

(h) C2: 6% Medium

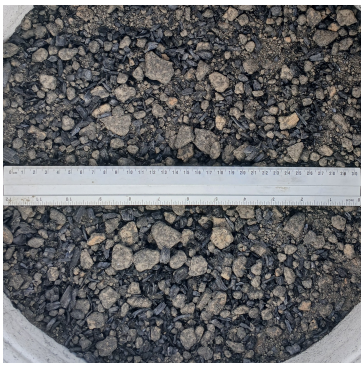

(i) C3: 6% Coarse

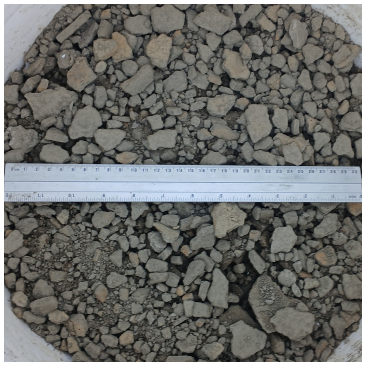

(j) Control

Figure D.1: Week 1

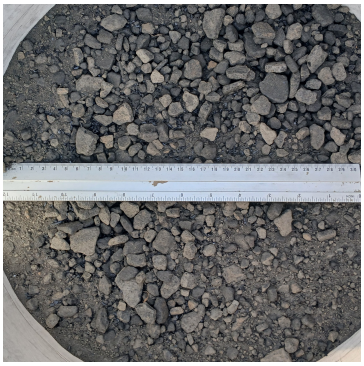

(a) A1: 2% Fine

(b) A2: 2% Medium

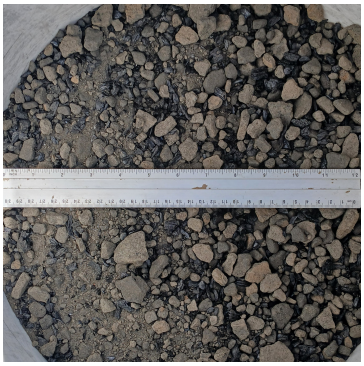

(c) A3: 2% Coarse

(d) B1: 4% Fine

(e) B2: 4% Medium

(f) B3: 4% Coarse

(g) C1: 6% Fine

(h) C2: 6% Medium

(i) C3: 6% Coarse

(j) Control

Figure D.2: Week 5

(a) A1: 2% Fine

(b) A2: 2% Medium

(c) A3: 2% Coarse

(d) B1: 4% Fine

(e) B2: 4% Medium

(f) B3: 4% Coarse

(g) C1: 6% Fine

(h) C2: 6% Medium

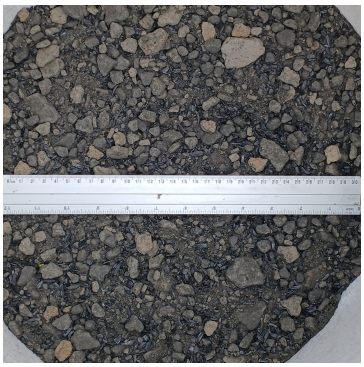

(i) C3: 6% Coarse

(j) Control

Figure D.3: Week 9

(a) A1: 2% Fine

(b) A2: 2% Medium

(c) A3: 2% Coarse

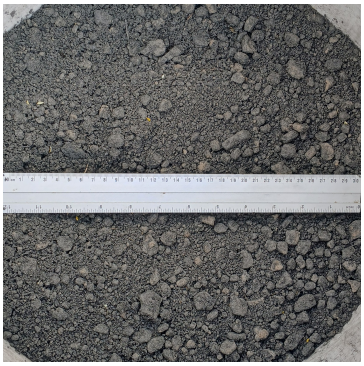

(d) B1: 4% Fine

(e) B2: 4% Medium

(f) B3: 4% Coarse

(g) C1: 6% Fine

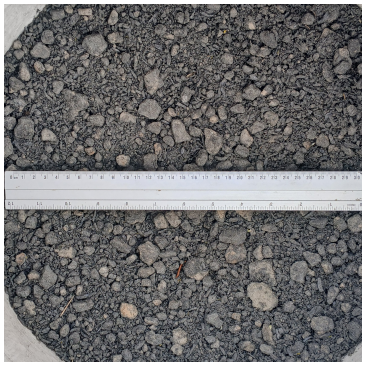

(h) C2: 6% Medium

(i) C3: 6% Coarse

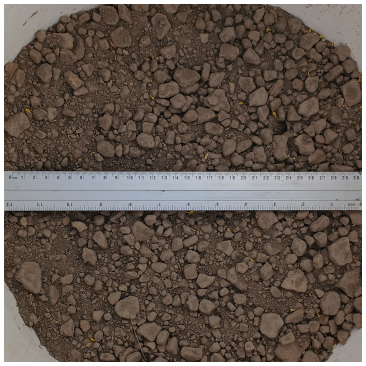

(j) Control

Figure D.4: Week 15

E

Relative Humidity

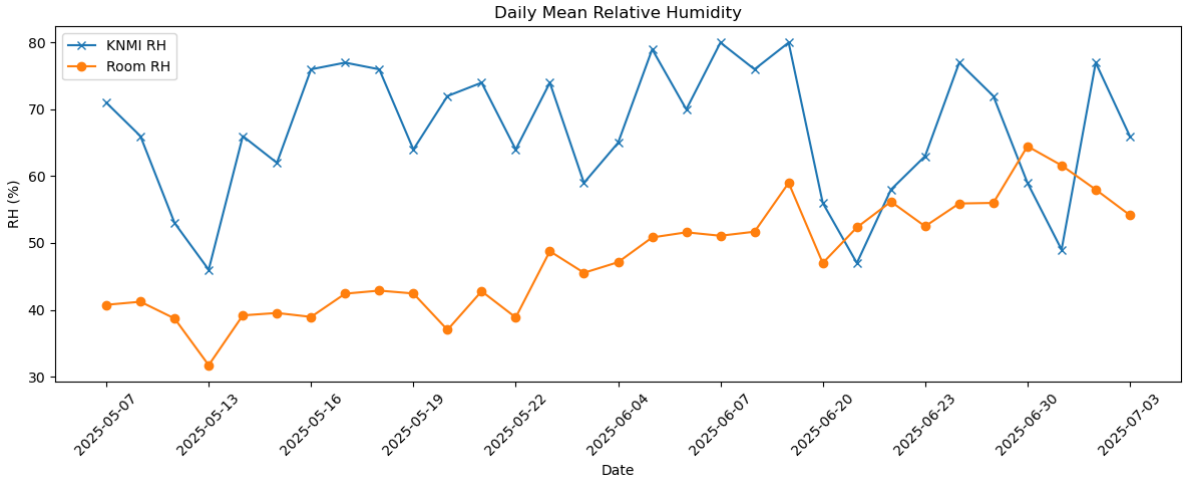

Figure E.1: Daily mean relative humidity measured in laboratory (”Room RH”) and outdoor (”KNMI RH”)

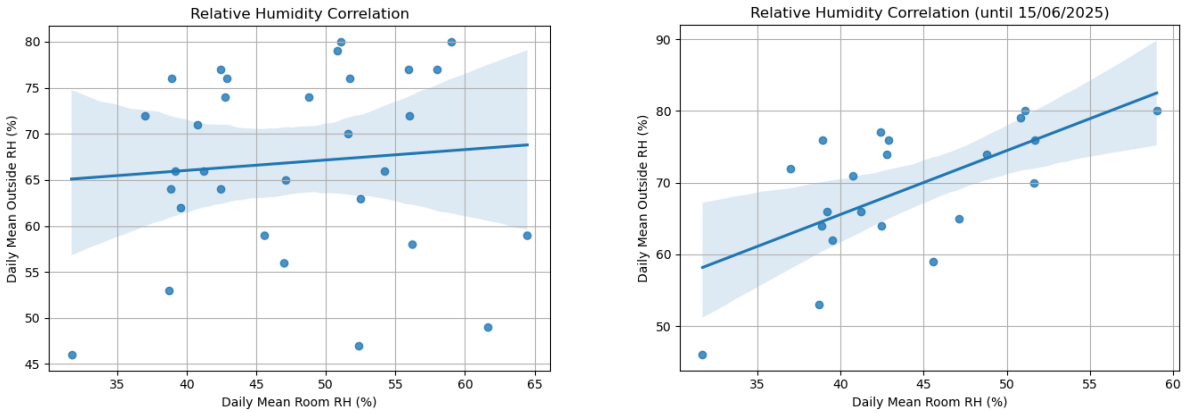

(a) Relative humidity correlation of full dataset

(b) Relative humidity correlation until 15/06

Figure E.2: Linear regression fit of room and outside relative humidity

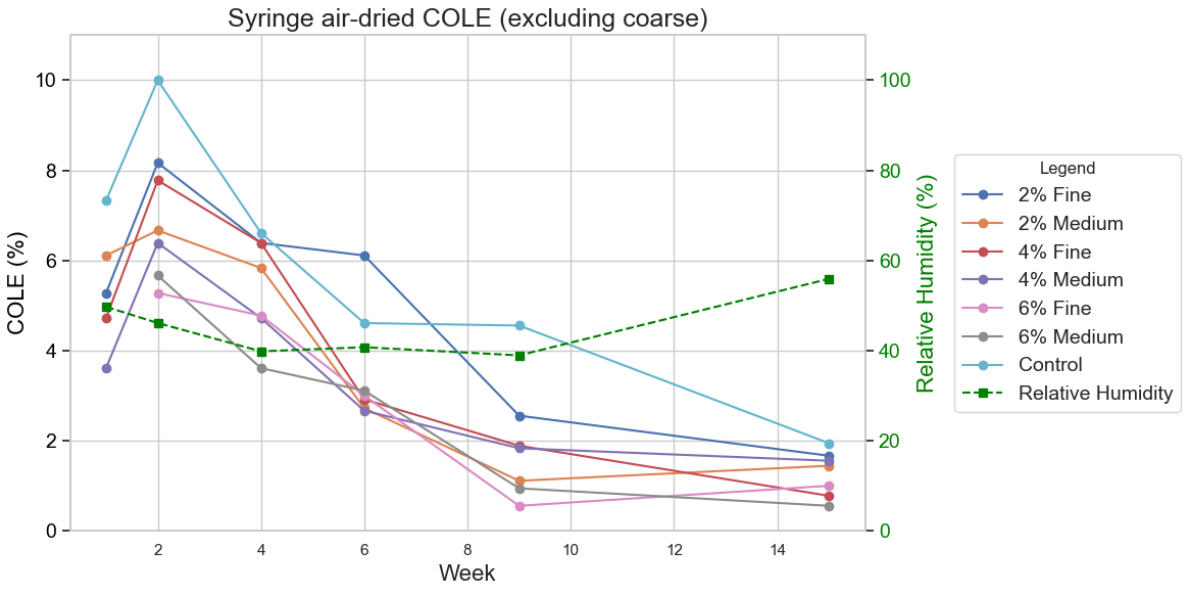

Figure E.3: Air dried syringe COLE and room relative humidity

Parameter	Correlation of full dataset	Correlation until 15/06
Pearson's Correlation Coefficient	0.093	0.633
Linear Fit Slope	0.113	0.892
Linear Fit Intercept	61.510	29.882
Linear Fit R^2	0.009	0.401

Table E.1: Room and outside relative humidity linear regression parameters